ADSORPTION FROM BINARY SOLUTIONS OF POLAR n-DECYL DERIVATIVES AND HEPTANE ONTO ALUMINA

by

Katherine M. Phillips

Thesis submitted to the Faculty of the

Virginia Polytechnic Institute and State University

in partial fulfillment of the requirements for the degree of

MASTER OF SCIENCE

in

Chemistry

APPROVED:

_____

Dr. J. P. Wightman

_____ _____

Dr. H. O. Finklea Dr. H. M. Bell

July, 1984

Blacksburg, Virginia

ABSTRACT

ADSORPTION FROM BINARY SOLUTIONS OF POLAR n-DECYL DERIVATIVES AND HEPTANE ONTO ALUMINA
by

Katherine M. Phillips

Committee Chairman: James P. Wightman

Chemistry

The preferential adsorption of n-decanol, n-decylamine, n-decanoic acid, and ethyl octanoate from binary solutions with heptane onto alumina was studied. The net surface excess isotherms were measured and resolved into component isotherms. The heat of immersion of the alumina in n-decanol, ethyl octanoate, and n-decanoic acid solutions was measured. The heats of immersion support the resolved isotherms which indicate that the order of preferential adsorption is n-decanoic acid > n-decanol ≈ n-decylamine ≈ ethyl octanoate. However, adsorption equilibrium constants calculated for each system indicate that the order of preferential adsorption is ethyl octanoate > n-decanol > n-decylamine > n-decanoic acid. An explanation for the discrepancy is put forth. A theoretical model of surface heterogeneity is also applied to the data for the ethyl octanoate and n-decanol systems. The reasonable fit of the model in each case suggests that the alumina surface is heterogeneous.

ACKNOWLEDGEMENTS

The author wishes to express sincere gratitude to her research advisor, Dr. J.P. Wightman, a unique person and professor. His constant support, through encouragement, advice, patience, and understanding has been a key factor in the completion of this degree.

The author also thanks her parents for their support and generosity over the years. She also thanks her husband Bob for his love, patience, and flexibility, and also for typing the tables for this thesis.

The author also wishes to thank other people who have assisted in various ways with this research. Andy Mollick and the University Glass Shop personnel provided custom glass work and evacuated the calorimeter bulbs. Carolyn Harris and Dee Tastet helped with their initial work on the solution adsorption problem. Steve McCartney ran the ESCA spectra. The author is indebted to Professor W. Rudzinski of the Maria Curie-Sklodowska University for his explanations which were instrumental in the successful application of his model of surface heterogeneity.

Finally, the author wishes to thank the Alcoa Technical Center which financially supported this work. Dr. Karl Wefers served as technical liason.

TABLE OF CONTENTS

LIST OF TABLES

LIST OF FIGURES

Chapter I

INTRODUCTION

Adsorption from solution is an area of interest with applications to such processes as lubrication, chromatography, enhanced oil recovery, and adhesion. The past two decades have seen much progress in the area, yet some aspects are not yet well-characterized.

Early attempts at understanding solution adsorption focused on dilute solutions (1). As a result, the associated theory was closely related to that of the gas/solid interface. The Langmuir equation,

$$\theta_2 = Ka_2^b/(Ka_2^b+1) \qquad \text{<I-1>}$$

was used to relate the fraction of the surface covered by the solute, θ_2, to the solute activity in the bulk solution, a_2^b. Generally, θ_2 is plotted as a function of a_2^b. The equilibrium constant, K, arises from the equilibrium:

(adsorbed solvent)+(solute in bulk solution) $\rightleftarrows$

(adsorbed solute)+(solvent in bulk solution) <I-2>

According to equation <I-1>, as a_2^b approaches 0, the curve approaches a maximum slope equal to K. Furthermore, as a_2^b increases and $Ka_2^b >> 1$, θ_2 approaches 1, implying complete coverage of the surface by the solute. Figure 1 illustrates the Langmuir isotherm. Inherent in the Langmuir model are

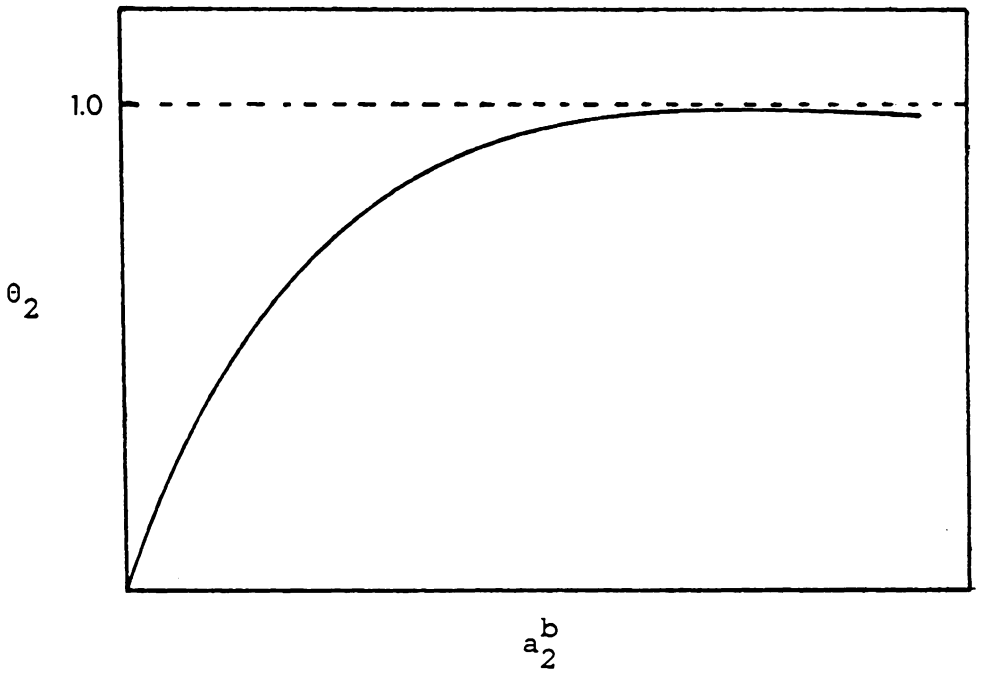

Figure 1: Langmuir adsorption isotherm

the assumptions of adsorbed phase ideality, monolayer coverage, surface homogeneity, and a dilute solution. Therefore, while limited systems are found to fit this model, many cases of interest do not conform to its assumptions, and furthermore most applications require information over the whole concentration range. As a result, a more general concept of solution adsorption is useful.

It has been convenient to view solution adsorption in terms of the surface excess of one component, typically that component which is preferentially adsorbed on the solid. If a solid is immersed in a solution of components 1 and 2 at a given concentration, adsorption of the molecules on the solid surface can cause a change in the solution concentration. Thus the surface phase would consist of components 1 and 2 in a different proportion than in the bulk phase. The surface excess of component 2 is defined as the amount of component 2 present in n moles of the surface phase minus the amount present in the same number of moles of the bulk solution. Experimentally the change in mole fraction of component 2, ΔX_2, upon equilibration with the solid is measured. The specific surface excess of component 2 is calculated as $n^{\circ}\Delta X_2/m$, where n° is the total number of moles of both components in the system and m is the mass of

the adsorbent. $n^{o}\Delta X_2/m$ plotted as a function of X_2 gives the surface excess (or adsorption) isotherm.

According to the definition of surface excess, its value may be negative if the two solution components compete for the surface. If $X_2^{final} > X_2^{initial}$ then $n^{o}\Delta X_2$ is negative. Schay (2) has classified adsorption isotherms into five types, as illustrated in Figure 2 . Kipling and Tester (3) and Elton (4) independently proposed a method to resolve the surface excess (net) adsorption isotherm into component isotherms. The resolved isotherms corresponding to each of the five net isotherms are shown in Figure 3 . As Figures 2 and 3 illustrate, the shape of the isotherm varies from system to system depending on the degree of preferential adsorption of one component.

Aspects of significance in the adsorption process are the surface orientation of the adsorbed molecules, multilayer formation, and surface heterogeneity. These are areas of research interest. Furthermore, in order to adequately characterize the adsorption process, provisions must be made for bulk and surface phase nonideality and also for precise concentration measurements over a range of temperature. Therefore, research has also focused on the determination of activity coefficients and on improving the precision of the experimental method. Everett and coworkers (5) have

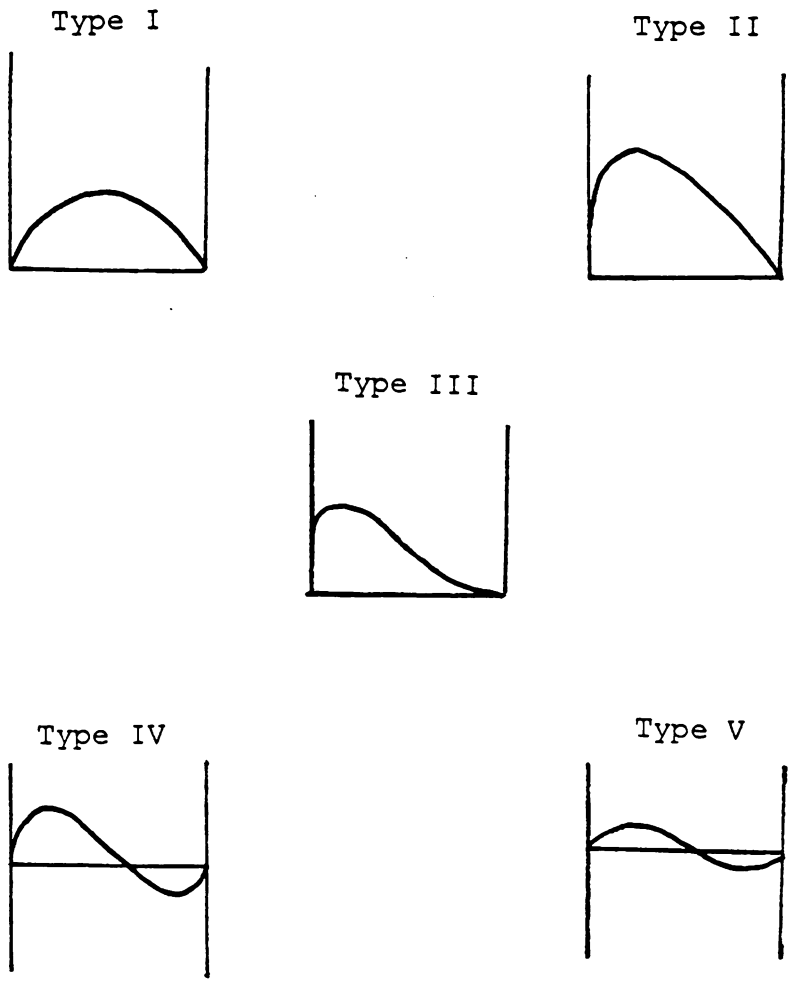

Figure 2: Classification of net isotherms

Plotted as $n^{\circ}\Delta X_2/m$ vs. X_2 (reference 2)

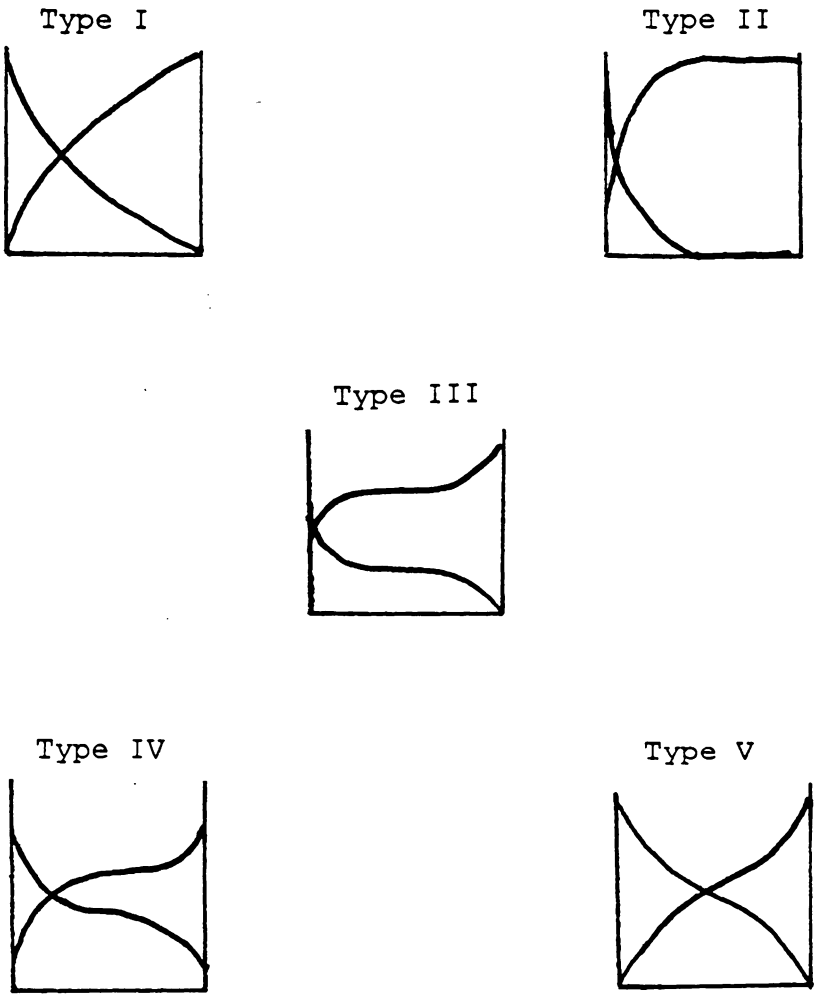

Figure 3: Five types of resolved isotherms Plotted as $n^{s}_{1,2}$ vs. X_2 (reference 2)

described a high precision flow apparatus for measuring concentration changes over a range of temperature.

The objective of this research was to characterize the adsorption from binary solution of a series of polar n-decyl derivatives in heptane onto alumina. The surface excess isotherms were determined and supported with calorimetric measurements. The results were analyzed to determine the adsorption equilibrium constant for each system. Additionally, the results were analyzed in terms of surface heterogeneity. Conclusions were drawn as to the appropriateness of each model in describing the systems studied, and a comparison was made between the adsorption of the various solutes.

Chapter II

LITERATURE REVIEW

An excellent text by Kipling (6) reviews the field of adsorption from nonelectrolyte solution prior to 1965. Everett (1,7,8,9) surveys the progress from 1970 to 1981 in a series of periodical reports. Therefore, this survey highlights relevant literature from 1965 to present. No work has been reported for adsorption on alumina from binary solutions of a series of polar n-decyl compounds in a nonpolar solvent. Also, few researchers have measured adsorption excess isotherms along with heats of immersion in the same solutions. Consequently, this review includes work pertinent to this research, encompassing both theory as well as specific studies on alumina or silica.

2.1 THEORY

Everett has developed (10) a thermodynamic treatment of adsorption from solution in which a "perfect" binary solution/solid system is described . The solution is pictured as a collection of plane lattices stacked parallel to the adsorbent surface. The concentration of both components is constant in each plane except in that plane which is adjacent to the solid surface. In this layer, the

so-called "adsorbed phase", the concentration of one component is enhanced, due to its preferential adsorption. The solid surface is a collection of identical adsorption sites. Only one molecule may occupy a given site and all sites are occupied. Both solution components are assumed to be approximately equal in size. Adsorption is assumed to be a phase exchange equilibrium (10) between the adsorbed layer (s) and the bulk solution (ℓ):

$$(B)^{s}+(A)^{\ell} \rightleftharpoons (B)^{\ell}+(A)^{s} \qquad \text{<II-1>}$$

and characterized by an equilibrium constant, K. Assuming ideal bulk and surface phases, K may be calculated from experimental isotherms using the equation:

$$X_B^{\ell}X_A^{\ell}/\{n^{o}\Delta X_A^{\ell}/m\} = (m/n^{s})\{X_A^{\ell}+1/(K-1)\} \qquad \text{<II-2>}$$

where X_A^{ℓ} and X_B^{ℓ} are the mole fractions of components A and B in the bulk solution, n^{s}/m is the specific monolayer capacity of the adsorbent, and $n^{o}\Delta X_A^{\ell}/m$ is the specific surface excess of component A. A linear plot of $X_B^{\ell}X_A^{\ell}/\{n^{o}\Delta X_A^{\ell}/m\}$ as a function of X_A^{ℓ} is obtained where the slope is equal to m/n^{s} and the intercept at $X_A^{\ell}=0$ is $m/\{n^{s}(K-1)\}$. Therefore, K is equal to (slope/intercept)+1.

Billet, Everett, and Wright (11) have related the equilibrium constant K to the heat of wetting (immersion), $\Delta_w H$. K is calculated from equation <II-2> and is related to $\Delta_w H$ by the equation:

$$\Delta_w H-(X_B^{\ell}\Delta H_B^{\circ}+X_A^{\ell}\Delta H_A^{\circ}) = \frac{X_A^{\ell}X_B^{\ell}}{X_B^{\ell}+1/(K-1)}\left[\Delta H_B^{\circ}-\Delta H_A^{\circ}\right] \qquad \text{<II-3>}$$

where ΔH° refers to the heat of wetting in the pure component and subscripts A and B refer to components A and B. All other quantities are experimentally accessible from calorimetric data. The left-hand side of equation <II-3> is plotted as a function of $X_B^{\ell}X_A^{\ell}/(X_B^{\ell}+1/(K-1))$. The slope of the best fit line should be equal to the experimental value of $\Delta H_B^{\circ}-\Delta H_A^{\circ}$. The model assumes an ideal solution, an ideal surface, and monolayer adsorption.

Furthermore, Everett (12) has combined calorimetric and adsorption data to determine surface area. For an ideal solution of equal size components, $\Delta_w H$ is related to $n_A^{s,o}$, the monolayer capacity, by the equation:

$$\Delta_w H-(X_B^{\ell}\Delta H_B^{\circ}+X_A^{\ell}\Delta H_A^{\circ}) = \frac{n^{\circ}\Delta X_A^{\ell}}{n_A^{s,o}}\ (\Delta H_A^{\circ}-\Delta H_B^{\circ}) \qquad \text{<II-4>}$$

A plot of the left-hand side of equation <II-4> as a function of $(n^{\circ}\Delta X_A^{\ell})(\Delta H_A^{\circ}-\Delta H_B^{\circ})$ should yield a linear plot with the reciprocal of the slope equal to $n_A^{s,o}$. The surface area is determined by multiplying $n_A^{s,o}$ by the cross-sectional area of the adsorbate.

Everett (12) has also considered nonideal adsorption systems. Equations for the activity coefficient of each

component in the adsorbed phase were developed. Again, a phase exchange equilibrium and equal-size molecules were assumed. Furthermore, it was assumed that bulk solution properties are known. The equilibrium constant K is now modified by the bulk solution activity coefficients, γ_A^ℓ and γ_B^ℓ:

$$\ln K = \int_0^1 \ln(X_B^s X_A^\ell \gamma_A^\ell / X_A^s X_B^\ell \gamma_B^\ell) dX_B^s \qquad \text{<II-5>}$$

and can be evaluated without knowledge of the surface activity coefficients, γ_A^s and γ_B^s. The surface activity coefficients can then be calculated from the equations:

$$\ln\gamma_A^s = X_B^s \ln \frac{X_B^s X_A^\ell \gamma_A^\ell}{X_A^s X_B^\ell \gamma_B^\ell} - \int_0^{X_B^s} \ln \frac{X_B^s X_A^\ell \gamma_A^\ell}{X_A^s X_B^\ell \gamma_B^\ell} dX_B^s \qquad \text{<II-6>}$$

$$\ln\gamma_B^s = X_A^s \ln \frac{X_A^s X_B^\ell \gamma_B^\ell}{X_B^s X_A^\ell \gamma_A^\ell} - \int_0^{X_A^s} \ln \frac{X_A^s X_B^\ell \gamma_B^\ell}{X_B^s X_A^\ell \gamma_A^\ell} dX_A^s \qquad \text{<II-7>}$$

again assuming that γ_A^ℓ and γ_B^ℓ are known. The Everett method of analysis will be considered in detail in the Results and Discussion section.

One aspect of solution adsorption not considered in detail by Everett is surface heterogeneity. Everett acknowledges that aside from bulk and surface phase nonideality the heterogeneity of the solid surface can play a major role in solution adsorption (12). Surface

heterogeneity, as related to adsorption from solution, refers to the variation in the energies of different adsorption sites on the solid surface. This heterogeneity may arise from the physical topography or chemical composition of the surface. The surface is no longer seen as a collection of discrete, equally spaced, equal-energy sites as described by Everett (10). Rather, two different types of heterogeneous surface are recognized and described by Tompkins (13) and named by Hill (14): (a) "patchwise" heterogeneous, consisting of patches of equal-energy sites with energy varying from patch to patch, and (b) "random" heterogeneous, consisting of sites of different energy distributed randomly over the surface. A review of the theory of adsorption on heterogeneous surfaces is given by House (15). Few researchers have considered this area, however.

Rudzinski et al. (16-21) have extensively studied the effect of surface heterogeneity on solution adsorption. Several aspects have been addressed, including surface excess isotherms, multilayer formation, and heats of immersion, as well as bulk and surface phase nonideality. Theoretical equations have been derived and applied to actual experimental data for systems previously analyzed with a homogeneous surface assumed. A review of the work by

Rudzinski and coworkers will illustrate the effect of considering surface heterogeneity in dealing with solution adsorption.

A method for quantitatively estimating the heterogeneity of a solid surface in binary solution adsorption was developed (16). The model is of a patchwise heterogeneous surface. Equations for the surface excess isotherm and energy distribution function were derived. The theoretical surface excess of component A, $n^{o}\Delta X_A$, as a function of its mole fraction in a solution of components A and B is given by:

$$n^{o}\Delta X_A = n_{\omega}^{-}(X_A^{c_A^{-}}-X_A)-n_{\omega}^{+}(X_A^{c_B^{+}}-X_A) \qquad \text{<II-8>}$$

where n_{ω}^{-}, n_{ω}^{+}, c_A^{-}, and c_B^{+} are parameters related to the surface energy distribution and used to fit the equation to experimental data. n_{ω}^{-} and n_{ω}^{+} are the total number of molecules adsorbed on the fractions of the surface where $\varepsilon<0$ and $\varepsilon>0$, respectively. ε is the difference in adsorption potential between components A and B, respectively. c_A^{-} and c_B^{+} are "heterogeneity parameters" for the fractions of the surface where $\varepsilon<0$ and $\varepsilon>0$, respectively. The normalized energy distribution function, $\chi(\varepsilon)$, is given by the equations:

$$\chi(\varepsilon) = (n_{\omega}^{-}/n_{\omega})\chi^{-}(\varepsilon,c_A^{-}) \text{ for } \varepsilon<0 \qquad \text{<II-9>}$$

and

$$\chi(\varepsilon) = (n_\omega^+/n_\omega)\chi^+(\varepsilon, c_B^+) \text{ for } \varepsilon>0 \qquad \text{<II-10>}$$

Equations <II-9> and <II-10> were applied to the data of Sircar and Meyers (22) for the system benzene/cyclohexane/silica gel. A homogeneous surface had been assumed by Sircar and Meyers in their analysis. The "best fit" of the theoretical surface excess isotherm, equation <II-8>, to the experimental data was found by varying the "heterogeneity parameters" c_A^- and c_B^+ and the quantities n_ω^- and n_ω^+. Introducing the concept of surface heterogeneity provided a better description of the experimental isotherm at low concentrations of benzene, as illustrated by Figure 4 . However, at high concentrations of benzene there was little difference between the fit of the equations for a homogeneous and for a heterogeneous surface. The conclusion is that at low concentrations of benzene only the patches of lowest adsorption energy are covered by benzene. The better fit of the Rudzinski model at low mole fraction supports the assumption that the part of the surface with the lowest adsorption energy is the most heterogeneous. It should be noted that the model assumes ideality of both the bulk and surface phases, short-ranged liquid/solid interaction potentials, and equal molar volumes of both components. Nevertheless, this earlier work

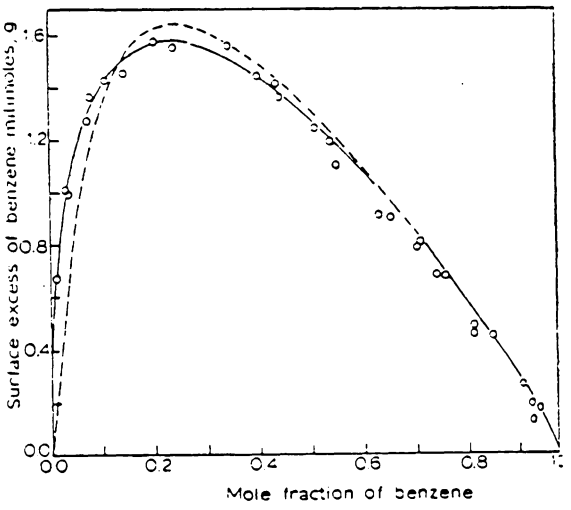

Figure 4: Fit of Rudzinski model for benzene/cyclohexane/silica gel

Circles=experimental data (22).
Solid line=theoretical curve (eqn. <II-8>)
Dashed line=theoretical curve of Sircar and Meyers
(reference 16)

indicates the significance of considering surface heterogeneity in interpreting adsorption data.

Oscik, Dabrowski, and Rudzinski (17) developed a more comprehensive method which addresses both surface heterogeneity and multilayer formation . In systems in which one component is preferentially adsorbed, investigations indicated that introducing the concept of multilayer formation in deriving the equation for the surface excess isotherm does not affect the height of the surface excess maximum, but strongly affects its position as a function of mole fraction. If the preferentially adsorbed component forms multilayers, then the surface excess maximum is shifted to a lower concentration. The converse is true if the second component tends to form multilayers.

Another important aspect to consider along with surface heterogeneity is bulk and surface phase nonideality. The combined effect of these conditions can significantly influence solution adsorption and can provide insight into interactions between adsorbed molecules (18). Oscik et al. (23) and Dabrowski et al. (24) studied the combined effect of surface heterogeneity and nonideality in the bulk and surface phases on the excess isotherm. Rudzinski et al. (18,20,21) extended the treatment and addressed the effect on both excess isotherms and heats of immersion. For the

system benzene/cyclohexane/silica gel, derived equations led to lower calculated surface activity coefficients for both components over the whole concentration range (18). This effect indirectly contributed to the fit of theoretical equations to experimental data for the surface excess isotherm and heat of immersion. Equations which account for both surface heterogeneity and nonideality of the bulk and surface phases were far superior to those for a homogeneous model when experimental and theoretical results were correlated. Furthermore, for binary solutions of equal-size molecules in which one component is preferentially adsorbed, increasing the degree of surface heterogeneity shifts the maximum of the surface excess isotherm to a higher concentration of the preferred adsorbate (20). It should be noted that the direction in which the surface excess isotherm is shifted as a function of concentration is opposite for surface heterogeneity and multilayer effects. Surface heterogeneity was also shown to have a large effect on the heat of immersion.

Most recently, Rudzinski et al. (21) developed generalized equations for the surface excess isotherm and heat of immersion of a heterogeneous solid surface in a binary solution whose components may have different cross-sectional areas. The treatment is appropriate for

systems which exhibit small departures from bulk solution ideality, a fairly ideal surface phase, and a small tendency to form multilayers. While these criteria exclude some of the factors previously considered (nonideality and multilayer formation), the authors note that a large number of systems meet these assumptions. The allowance for different cross-sectional molecular areas of the solution components renders the approach suitable to commonly encountered adsorption systems.

A novel method for determining the dependence of the heat of immersion on solution composition using the experimental surface excess isotherm was developed (21). Values of $n^{o}\Delta X_{A}$ are used to calculate theoretical heats of immersion which are then compared to the experimental values. First, the fraction of the surface area covered by the polar component (ϕ_{A}^{s}) is calculated, using the equation:

$$\phi_{A}^{s} = (n_{A}^{e}+n^{o}X_{A}r)/n^{o}(1-X_{A}+rX_{A}) \qquad \text{<II-11>}$$

where n^{o} is the monolayer capacity, r is the ratio of the cross-sectional molecular area of component A to that of component B, and X_{A} is the mole fraction of component A in the bulk solution. The specific surface excess of component A, n_{A}^{e}, and X_{A} are determined experimentally. The monolayer capacity is estimated from the surface excess isotherm, and r is estimated from reported values of

cross-sectional molecular areas. The model assumes a certain distribution in energy among the adsorption sites. For a Gaussian distribution, the following linear equation is derived from which a heterogeneity parameter, c, can be calculated:

$$\ln\{(1-\phi_A^s)/\phi_A^s\} = \frac{RT\ln(2^{r-1})-\varepsilon_o}{c} - \frac{RT}{c}\ln(X_A/X_B) \quad \text{<II-12>}$$

The mean energy value is ε_o, c is related to the spread of the energy distribution, R is 8314 mJ/mole^oK, and T is absolute temperature. Figure 5 illustrates two possible energy distribution functions. The left-hand side of equation <II-12> is plotted as a function of $\ln(X_A/X_B)$ and c is calculated from the slope of the linear plot. The heat of immersion, $\Delta_w H$, is related to ϕ_A^s according to the equation:

$$\Delta_w H = \Delta_w H_B + n^o \phi_A^s(\varepsilon_o-\lambda) - cn^o\{(1-\phi_A^s)\ln(1-\phi_A^s)+\phi_A^s\ln\phi_A^s\} \quad \text{<II-13>}$$

where $\Delta_w H_B$ is the heat of immersion in pure component B, and λ is a term related to the molecular partition functions for molecules A and B in the adsorbed state. The bracketed term in equation <II-13> goes to zero when $\phi_A^s=0$ or 1. Therefore, the first two terms describe the line connecting the points $(\phi_A^s=0, \Delta_w H_B)$ and $(\phi_A^s=1, \Delta_w H_A)$, the heat of immersion expected if the surface were homogeneous. The

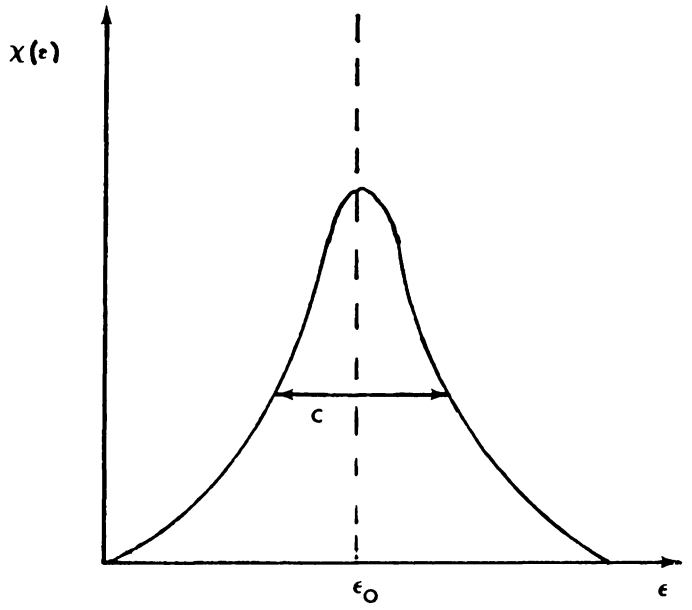

a. Gaussian energy distribution function

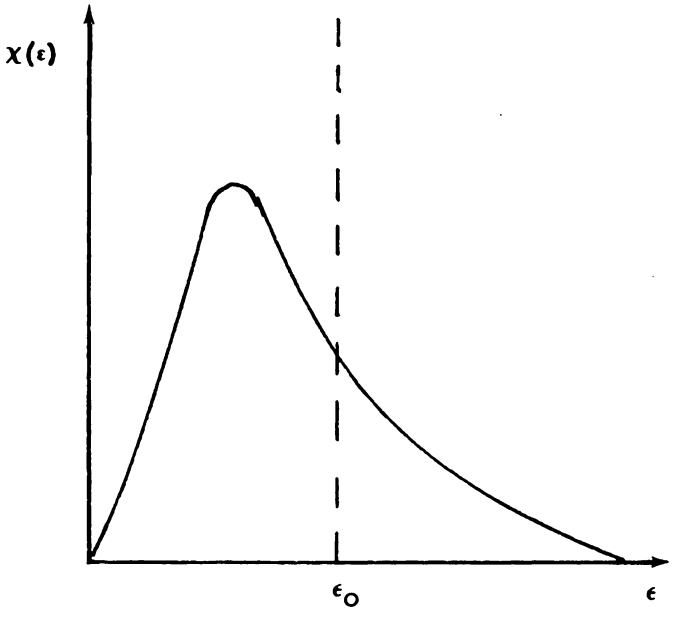

b. Right-hand widened Gaussian energy distribution function

Figure 5: Adsorption energy distribution functions

second term in equation <II-13> is the theoretical excess heat of immersion, $\Delta_w^T H$, due to surface heterogeneity and is calculated for each value of ϕ_A^s. The experimental heats of immersion can be plotted as a function of ϕ_A^s instead of X_A, to compare the theoretical and experimental values. If the model adequately describes the adsorption system the two curves should correspond. The application of this model will be considered in detail in the Results and Discussion section.

2.2 SIMILAR SYSTEMS

Jednacak-Biscan and Pravdic (25,26) studied the interaction of n-butylamine, n-butanol, and n-butyric acid in hexane solutions with porous borosilicate glass, using flow microcalorimetry. For mole fractions up to $5x10^{-3}$ of the polar component, heats of adsorption and the amount of solute adsorbed were measured. The values of the specific heats of adsorption were in the order $n\text{-}C_4NH_2$ > $n\text{-}C_4OH$ > $n\text{-}C_3COOH$, whereas the monolayer adsorbed amounts were in the order $n\text{-}C_4OH$ > $n\text{-}C_4NH_2$. The authors reported that data for $n\text{-}C_3COOH$ were irreproducible. Monolayer coverage was indicated by the shape of the isotherms, in which the heat of adsorption reached a maximum as a function of mole fraction. The authors concluded that these trends suggest a

heterogeneous surface and an effect of the Lewis base character of the adsorbate on the adsorptive interaction. Surface heterogeneity is suggested by the shift of the curve plateau, for all adsorbates, to a higher mole fraction for isotherms of adsorbed amount compared to heat of adsorption isotherms (25). A correlation was found between the relative basicity of the adsorbate (defined as $pK_A+1.74$) and its monolayer heat of adsorption, as well as between heat of adsorption and surface coverage. A model of a highly acidic surface was postulated (26), with adsorption sites having either Bronsted or Lewis acid character depending on whether or not the surface is hydrated. Either way it was assumed that the sites have a strong affinity for Lewis bases. The correlation of the heat of adsorption and coverage was explained by coverage of highly acidic sites first, followed by those that are progressively less acidic. n-Butylamine is a strong base and hence showed a higher ratio of heat to coverage than n-butanol. The alcohol was assumed to adsorb by hydrogen bonding. It should be noted that the measurements reported were made at relatively low mole fractions. The implication is that monolayer coverage occurs at concentrations less than $5x10^{-3}$ mole fraction solute, since all curves plateau before this point. Also, the flow microcalorimetric experiments are based on

replacement of hexane by the solute; the adsorbent was presoaked in hexane. This is in contrast to heat of wetting experiments in which the dry solid is immersed in the solution.

Armistead, Tyler, and Hockey (27,28) measured adsorption isotherms for a series of n-fatty acids in hexane and benzene solutions onto silica. The surface hydroxyl concentration of the adsorbent was well-characterized. Limiting coverage and the effect of the acid's hydrocarbon chain length were studied. Factors controlling preferential adsorption of the acid were investigated. The results indicated that adsorbed acid molecules are not oriented with their hydrocarbon chains parallel to the surface, contradicting the findings of Kipling and Wright (29). This conclusion was drawn because limiting adsorption was invariant with chain length for the C_{12}, C_{14}, and C_{18} acids in benzene. In hexane solutions, coverage was dependent on adsorbate chain length, decreasing with increasing carbon number. However, the observed ratios of adsorbent surface area to adsorbate molecule for the longer chain acids were too small to imply an orientation parallel to the surface. Furthermore, the ratio of limiting areas for longer chain to shorter chain acids was too small to fit this model. Heat of immersion data for the acids in benzene solution

supported the postulated noninteraction of the hydrocarbon chains with the adsorbent surface. The heat of immersion was found to increase linearly with surface concentration of acid, implying that the heat of adsorption is independent of surface coverage. Since fatty acid molecules can exist as polymorphic species in nonaqueous solution (30), it was concluded that the chain-length dependence of limiting adsorption and heat of immersion is due to exclusive adsorption of the monomeric species. Maximum adsorption occurs when the solution monomer concentration approaches a limiting value, rather than when adsorption sites are saturated. The selectivity of the monomer for the surface was explained by decreased preference of hydrogen bonded aggregates to hydrogen bond to surface sites. It was suggested that a similar effect may occur in adsorption of long chain alcohols and amines. This work indicates how bulk solution characteristics may affect the nature of preferential adsorption.

Adsorption of n-fatty acids has been used to determine adsorbent surface areas. For this application it is important to know the surface orientation of the admolecules. Rahman and Ghosh (31) used adsorption of stearic acid from benzene to find the specific surface areas of alumina powders. Possible surface orientations of the

acid molecules were proposed. If a perpendicular orientation was assumed, with each molecule being attached to the surface by its carboxyl group, an area of 18 $\mathring{A}^2$ per adsorbed molecule was calculated. Conversely, 100 $\mathring{A}^2$ per molecule was calculated when a parallel orientation was assumed. The authors found that the actual area per adsorbed molecule would be 60 $\mathring{A}^2$ in order for the calculated surface of the adsorbent to agree with the BET nitrogen value. It was concluded that the stearic acid molecules lie neither completely parallel nor completely perpendicular to the surface. Two orientations were postulated. Both models include attachment by the carboxyl group to the surface. The first model supposes all methylene units except the terminal six lie on the surface, with the "tail" extending into the bulk solution. The second model assumes that every sixth methylene unit is attached to the surface, creating a spiral arrangement. These results imply that care must be taken in assuming a specific orientation of a molecule on the adsorbent surface.

Borowko, Goworek, and Jaroniec (32) considered the combined effect of surface heterogeneity and the bulk phase association of one component on adsorption from binary solution. A theoretical model was developed and applied to experimental data for systems of sec-butanol and

tert-butanol, each in benzene and heptane solutions onto silica gel. Their results confirm a strong effect of bulk phase association on both the shape and maximum of the excess isotherm.

Surface heterogeneity was also considered by Oscik, Goworek, and Kusak (33) who studied the structure and thickness of the adsorbed phase in binary solutions of C_2 to C_5 n-aliphatic alcohols in benzene with silica gel. The theory developed by Oscik et al. (23) was applied; a test for monolayer coverage was proposed to determine the surface phase thickness. The best fit of theory to experimental data was found when a nonideal bulk phase was assumed. The surface layer capacity in this case was found to be much less than when an ideal bulk solution was assumed. Determination of the thickness of the adsorbed layer was based on a mass balance between the bulk liquid and the adsorbed phase. The surface excess,

$$n^{o}\Delta X_A/m = n_A^s(1-X_A)-n_B^sX_A \qquad \text{<II-14>}$$

was combined with the equation:

$$n_1^s/(t-n_{1,m}^s) + n_2^s/n_{2,m}^s = 1 \qquad \text{<II-15>}$$

to calculate the number of moles of each component (n_A^s, n_B^s) adsorbed per gram of solid. The number of moles of each component required to completely cover the surface of one gram of adsorbent are given by $n_{A,m}^s$ and $n_{B,m}^s$, and t

corresponds to the number of monomolecular surface layers. The method of McClellan and Harnsberger (34) was employed to calculate the cross-sectional area of an adsorbed alcohol molecule; the area of a benzene molecule was taken to be 41 $\mathring{A}^2$, assuming an orientation parallel to the surface. Calculations based on equations <II-14> and <II-15> were performed, inserting various values of t into equation <II-15>. The amount of alcohol adsorbed was plotted versus bulk mole fraction. According to the model, the minimum number of monomolecular surface layers is that value of t which yields a curve having a minimum greater that the maximum of the t=1 curve, as shown in Figure 6 for the system ethanol/benzene/silica gel. It was concluded that for bulk mole fractions of alcohol greater than 0.3 the minimum number of surface layers is 3, suggesting multilayer formation by both the alcohol and benzene. The results were explained by association of the alcohol molecules in the bulk solution at high concentrations. Similar surface layer thicknesses were reported for aliphatic alcohols in heptane solution on silica gel by Goworek, Jaroniec, and Czarniecki (35).

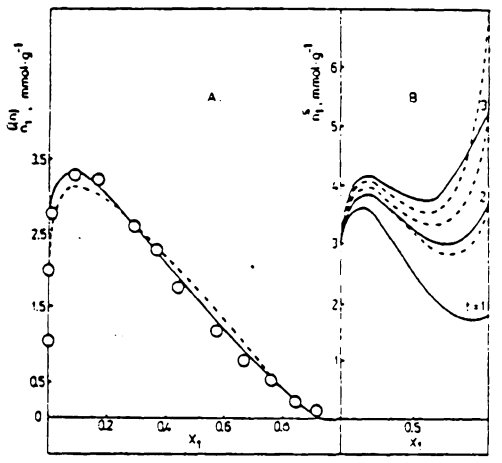

Figure 6: Plot to determine surface layer thickness system: ethanol/benzene/silica gel. n_1^s (mmole/g) plotted as a function of X_1 (plot B) according to equations <II-14> and <II-15> for various values of t. (——) multilayer adsorption of both components; (----) multilayer adsorption of ethanol and monolayer adsorption of benzene (reference 33).

Chapter III

EXPERIMENTAL METHODS

3.1 ADSORPTION MEASUREMENTS

n-Decylamine, n-decanoic acid, and ethyl octanoate (99+%, Aldrich Chemical Co.) were used as received. n-Decanol (99%, Aldrich Chemical Co.) and n-heptane (spectranalyzed, Fisher Scientific) were stored over Davison 4-A molecular sieve (Fisher Scientific). The adsorbent was a well-characterized wide-porous, pelletized amorphous alumina (referred to as H151) produced from alumina gel and received from Alcoa Technical Center. The reported nitrogen surface area was 338 m^2/g. Table 1 gives further characteristics of the alumina. A batch of the adsorbent was stored in a 50 ml glass bottle in a drying oven at 110°C until needed.

An attempt was made to exclude all trace water and contaminants from the adsorption system. All bottles and syringes were prepared by first soaking in a 6N nitric acid bath, followed by copious rinsing with water, then acetone, and finally with distilled deionized water. Syringe needles were sonicated in acetone, were then rinsed with distilled water and sonicated in distilled water for about 5 minutes. Excess water was shaken from the bottles, syringes, and needles which were all then dried in a Precision Thelco

TABLE 1

Characteristics of H151 alumina*

$\%Al_2O_3$	97.0
$\%SiO_2$	1.50
$\%Na_2O$	1.30
%CaO	.075
$\%B_2O_3$	.057
other trace oxides (<.05% each)	.069
primary pore size range	0 - 400 Å
% moisture to 110°C	.41
% moisture 110 - 250°C	1.43
% crushing strength	78.0

*From Alcoa Technical Center

model 16 gravity convection oven at 110°C for at least 2 hours or until needed. Stock solutions of n-decanol, n-decylamine, and ethyl octanoate in heptane were prepared gravimetrically as described below in 150 ml clear glass Hypo-vials (Pierce Chemical Co.). 5cc and 10cc Micromate glass syringes with Luer-lock tips fitted with 18 gauge stainless steel needles were used. The bottles were removed from the oven and capped immediately with Hycar septa and aluminum seals (Pierce Chemical Co.) and allowed to cool to room temperature. Syringes and needles were also removed from the oven and cooled to room temperature before use. A capped Hypo-vial was tared, then n-decanol, n-decylamine, or ethyl octanoate was added via syringe and weighed. The volume of heptane (V_H) required to yield the desired mole fraction of polar component (X_A) was calculated from the equation:

$$V_H = \{(1-X_A)M_H W_A\}/(M_A d_H X_A) \qquad \text{<III-1>}$$

where M is molecular weight, d is density, W is weight in grams, and the subscripts H and A refer to heptane and the polar component, respectively. Heptane was then added with a 10cc syringe and its weight was recorded. Mole fraction of A was calculated from the measured weights of A and heptane. Since n-decanoic acid is a solid at room temperature, the above procedure was modified. After a

bottle had cooled, it was uncapped and the desired amount of acid was added with a spatula to the tared bottle and weighed. The bottle was again capped and sealed, and heptane was weighed in as before. All solutions were shaken at least 2 hours at 250 rpm on a Labline automatic orbital table shaker.

The amount adsorbed was calculated from changes in solution concentration. In order to determine the solution concentration changes it was necessary to construct calibration curves for each system as follows. Thirteen prepared 15 ml Hypo-vials were removed from the oven, capped with Hycar septa and aluminum seals, and cooled to room temperature. 5 ml of the stock solution were carefully measured in a dried gastight Hamilton 5cc syringe with a Teflon coated plunger (American Scientific Products) and injected into each bottle. One bottle contained 10 to 15 ml solution to be used as a reference. Each calibration standard consisted of a microliter quantity of the polar component, carefully measured and added to the 5 ml stock solution using a dried 50 µl Hamilton microsyringe. n-Decanoic acid was added as a concentrated solution in heptane of known weight composition. Generally, 12 standards were prepared, 3 solutions each with 10 µl, 20 µl, 30 µl, and 40 µl additions of the solute (polar component).

Alumina samples were prepared at the same time as the calibration solutions. The bottle of alumina kept in the oven was removed, capped, sealed, and cooled to room temperature along with five 15 ml Hypo-vials. One or two pellets (0.2 to 0.4 g) were weighed into each vial then placed in the oven at 110°C for at least an additional 2 hours. For an experimental run the vials containing the adsorbent were removed from the oven, capped with Hycar septa, sealed with aluminum seals, and cooled to room temperature. 5 ml stock solution were carefully measured and added to each vial using a gastight Hamilton 5cc syringe with a Teflon coated plunger. Samples were then shaken along with the calibration standards and reference solution at 180 rpm on the orbital shaker for 2 hours.

Changes in solution concentration were determined by differential refractometry. A Waters Associates model R403 differential refractive index detector (DRID) connected to a Hewlett-Packard Moseley 680 stripchart recorder at 10 mV full-scale was used. The DRID was thermostatted at 29°C with a Haacke D1 circulating water bath. A Teflon tube was connected to the outlet tube from each detector cell and placed in a 250 ml waste flask. Detector inlet tubes were fitted with 1/16" stainless steel Swagelok unions with Teflon ferrules. To minimize evaporation, solutions were

injected into the detector in the following manner: About 5 ml of solution was first drawn into a 5cc gastight Hamilton syringe fitted with an 18 gauge stainless steel needle. Any air was ejected and the needle was wiped with a Kimwipe. The needle was then connected securely to the inlet tube via the airtight Swagelok union as shown in Figure 7 .

A typical experimental run consisted of the following series: 1 reference solution, 12 calibration standards, and 5 samples. The recorder was zeroed at 50% of full-scale. The DRID was zeroed by injecting the reference solution into both detector cells with the attenuation set at "zero test"; then, keeping both syringes in place, the attenuation was turned to 16x and the chart recorder pen was brought to 50% of full-scale using the detector optical zero knob. If the pen remained steady, more solution was pushed through the sample cell to assure that the pen would again return to zero. The attenuation was returned to zero test. Subsequently each calibration solution and each supernatant sample solution was injected one after another for analysis. Each solution was left in the detector with the syringe remaining in place until deflection on the chart recorder was constant for at least one minute. Then more solution was pushed through to see that deflection again returned to the same point. Attenuation was always set between 128x and 16x, at the highest position that kept the pen on scale.

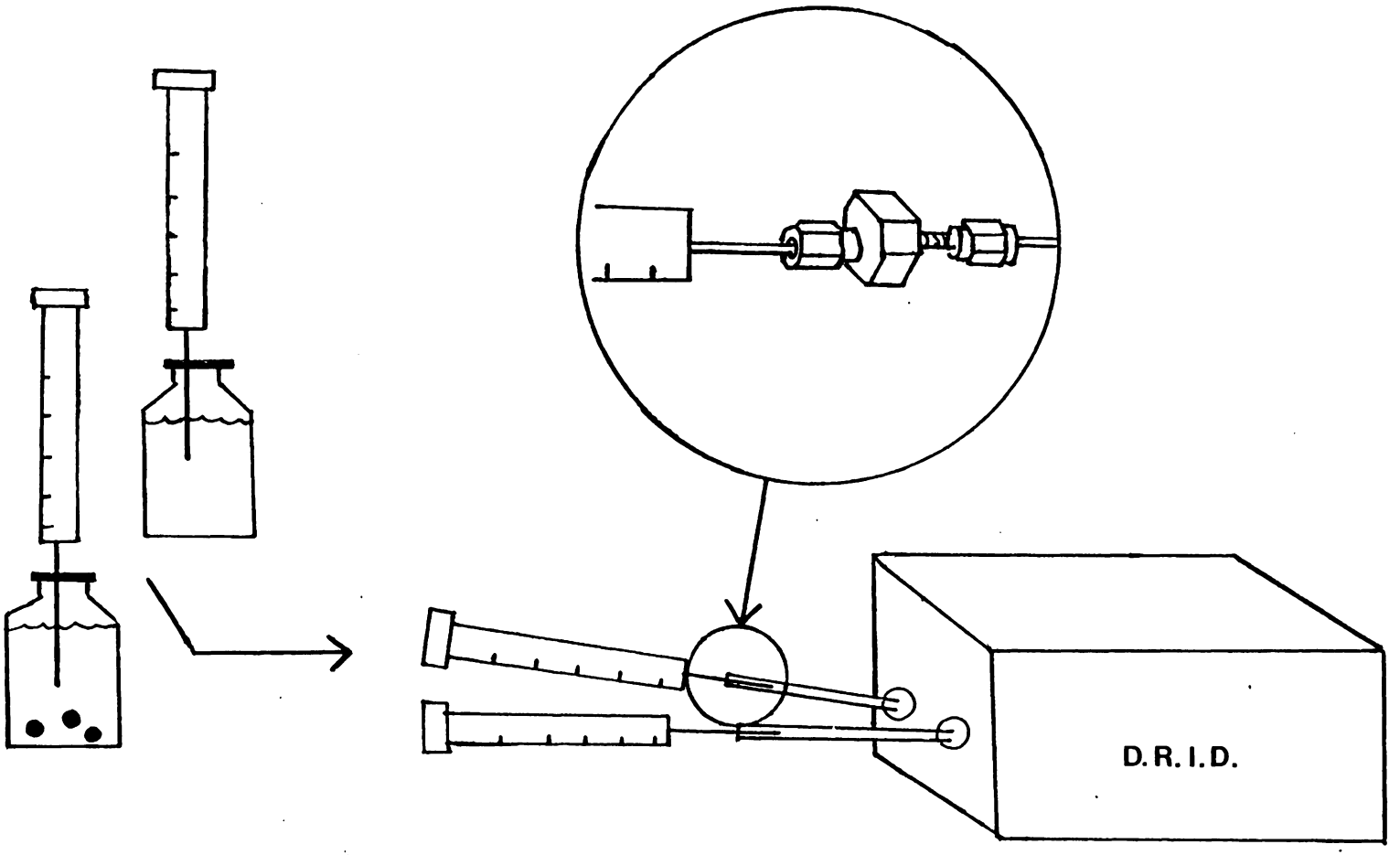

Figure 7: Schematic diagram of injection setup

To quantify adsorption, a calibration plot was made for each binary solution at the desired concentrations. All chart recorder deflections were converted to 16x units. For example, a sample or standard solution giving a deflection of 15 units at 32x would correspond to 30 units at 16x. From the calibration standards 16x units were plotted as a function of microliters of polar component added (µl concentrated solution for n-decanoic acid). The best straight line was drawn through the points based on a least squares regression. Representative calibration curves are shown in Figures 8 - 11 . An example data set is given in Appendix A. Good linear fits were obtained for every solution. The microliter change in concentration of a given sample supernatant solution was found from 16x units deflection by interpolation from the appropriate calibration plot.

3.2 MICROCALORIMETRY

Heats of immersion of H151 alumina in heptane solutions of n-decanol, ethyl octanoate, and n-decanoic acid were measured in a Calvet MS-70 microcalorimeter shown schematically in Figure 12 . Due to the corrosive nature of n-decanoic acid it was not possible to measure heats of immersion at greater than 0.15 mole fraction. For the same

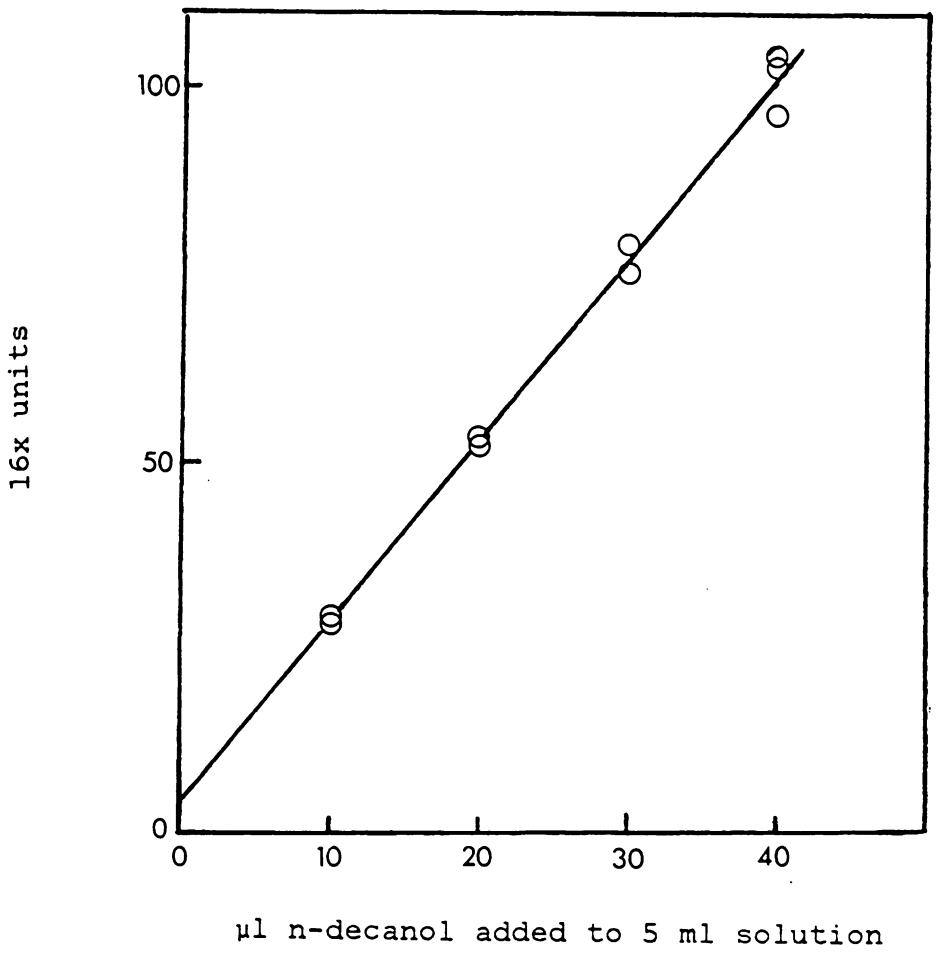

Figure 8: 10% n-decanol calibration plot

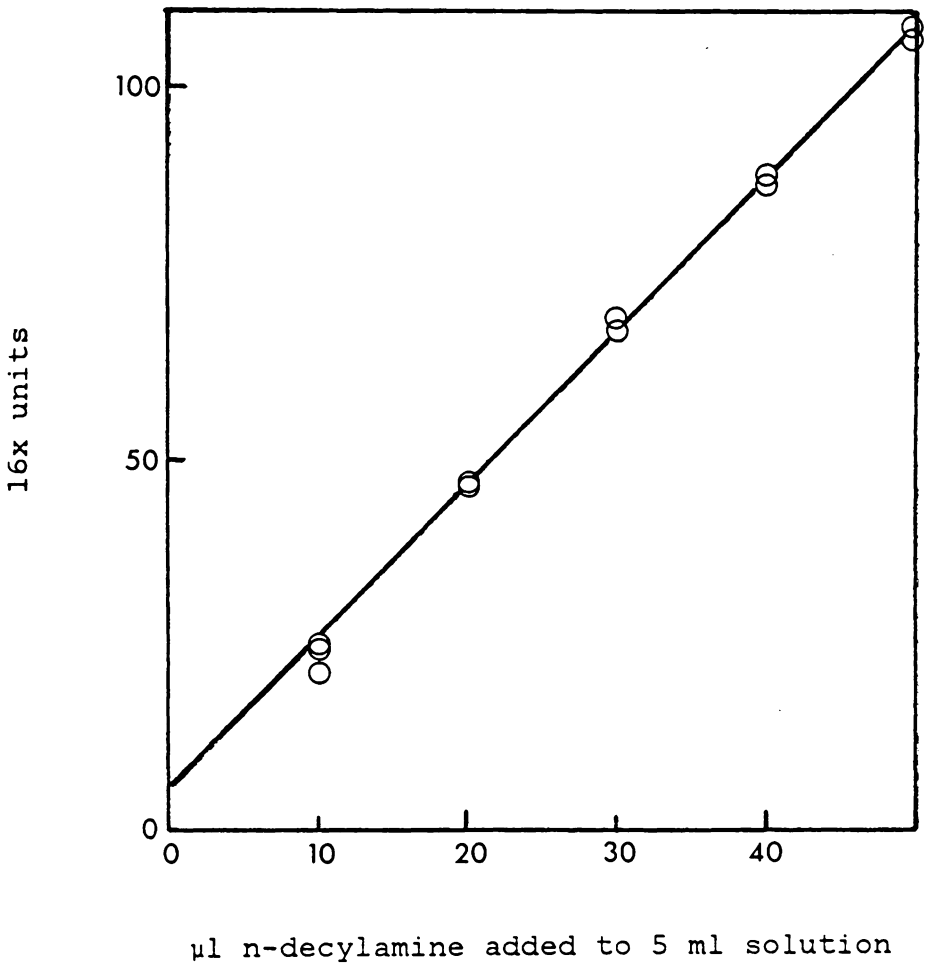

Figure 9: 10% n-decylamine calibration plot

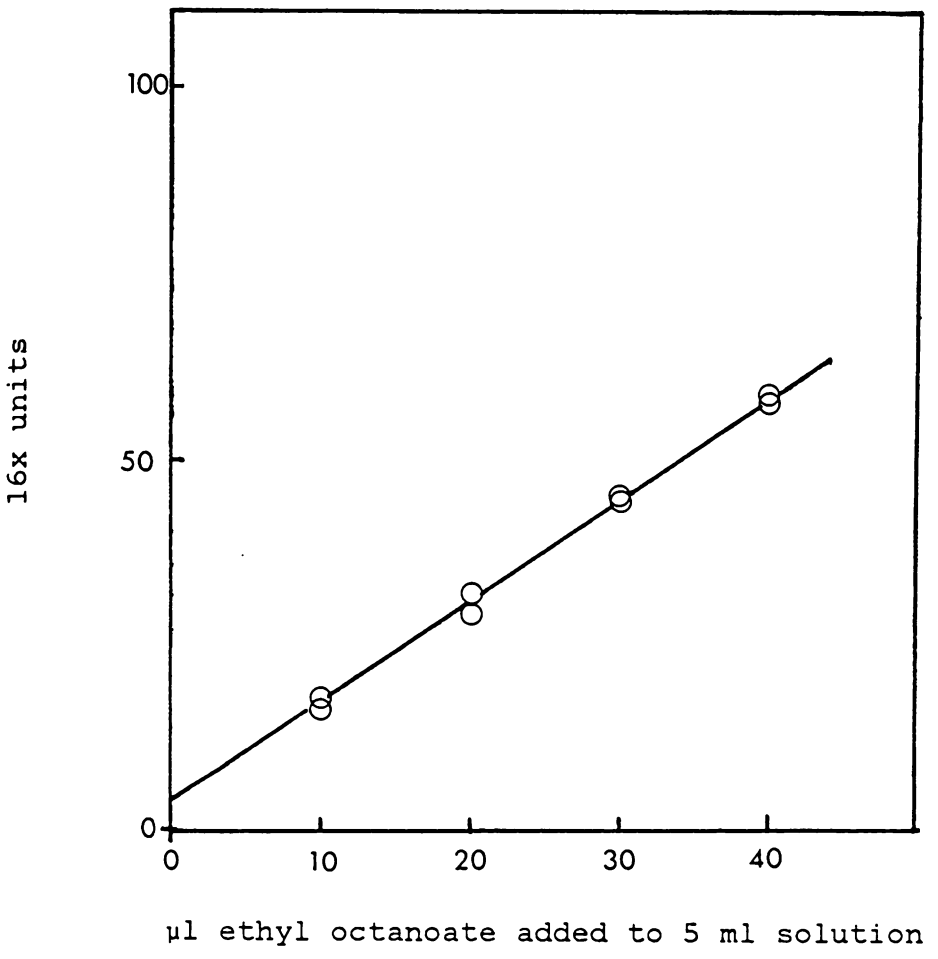

Figure 10: 10% ethyl octanoate calibration plot

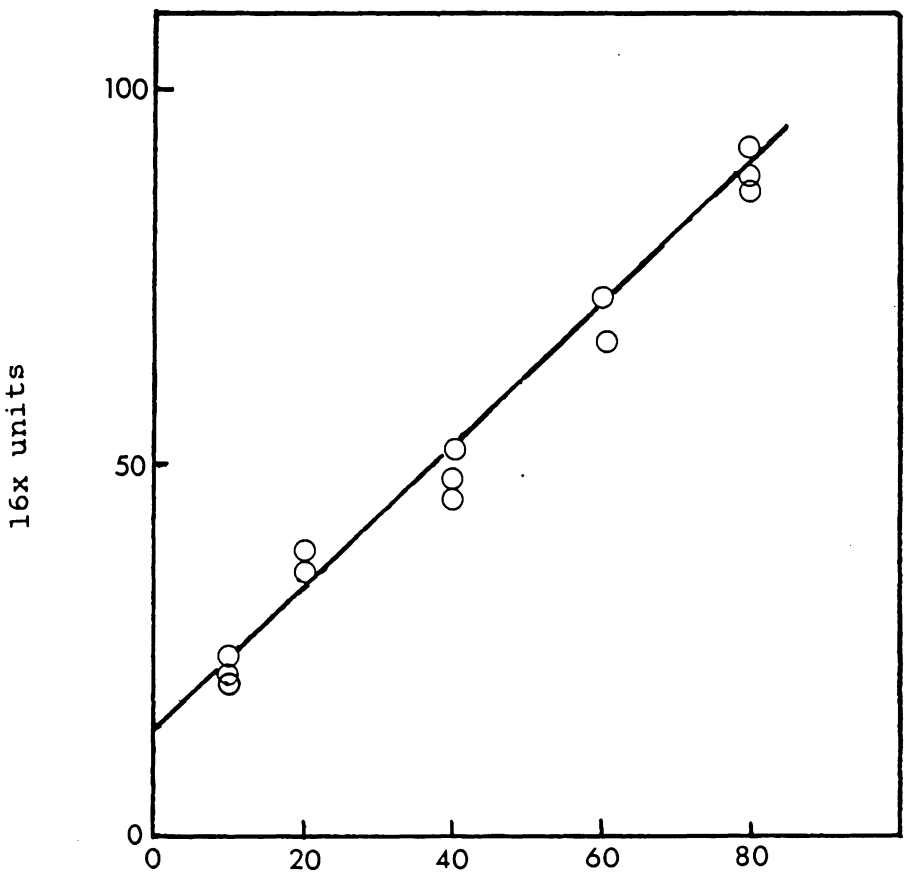

Figure 11: 10% n-decanoic acid calibration plot

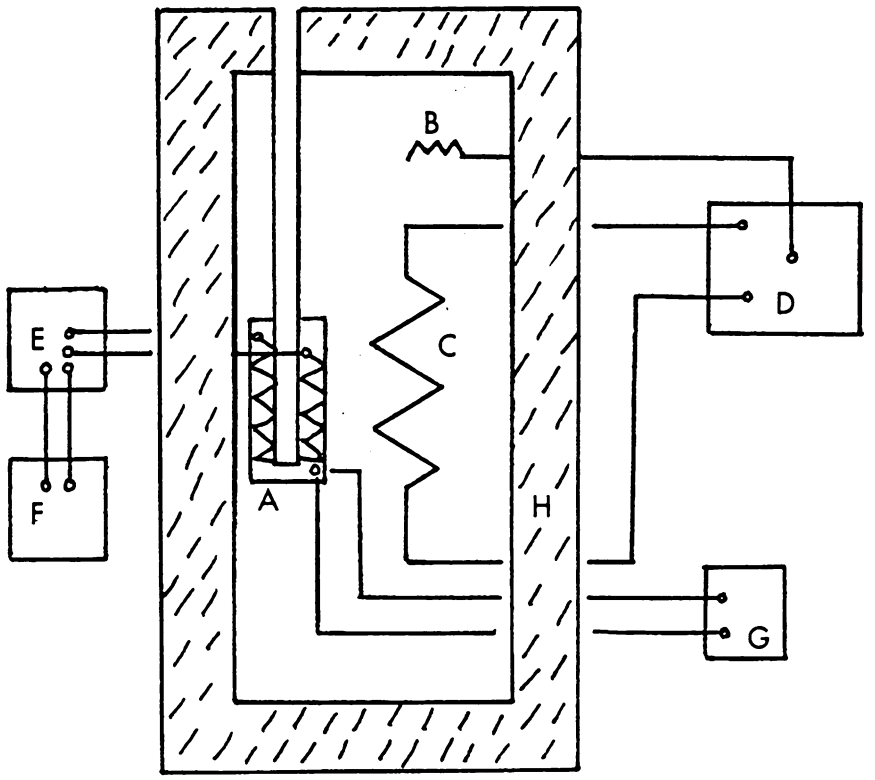

Figure 12: Schematic diagram of microcalorimeter

A: Microcalorimetric element (detector)
B: Temperature regulator probe
C: Temperature regulator heater
D: Temperature regulator
E: Amplifier
F: Integrator/counter
G: Platinum resistance thermometer
H: Insulation

reason measurements were not made for n-decylamine. The alumina was dried in the same way as for adsorption measurements, except the pellets were broken into small chunks. Solutions were prepared as previously described. For each experimental run, two 40 to 55 mg samples of dried and cooled alumina were weighed into custom-made Pyrex ampoules with breakable tips. The samples along with 2 empty ampoules for references were evacuated at $< 1x10^{-4}$ torr for 2 hours at $105 \pm 5^{o}C$ and sealed under vacuum. All ampoules were then sealed with Viton "o" rings to 15 ml stainless steel cylinders containing 5 ml of solution of known concentration. Each assembly, as shown schematically in Figure 13, was placed into the appropriate calorimeter cell and allowed to equilibrate for 2 to 12 hours. The bulb tip was broken and samples were allowed to reach steady state, defined as < 8 μJoules for 250 seconds. Typically steady state was established in 2 to 10 hours. The sensitivity of the calorimeter, S, was determined by electrical calibration and was calculated from the equation:

$$S = I^2Rt/C \quad \text{(Joules/g)} \qquad \text{<III-2>}$$

where I is the current passed through a standard resistance R for time t, and C is the number of counts obtained from the amplifier-integrator-counter. Counts are proportional to the area under the thermogram. Heats of immersion were calculated from the equation:

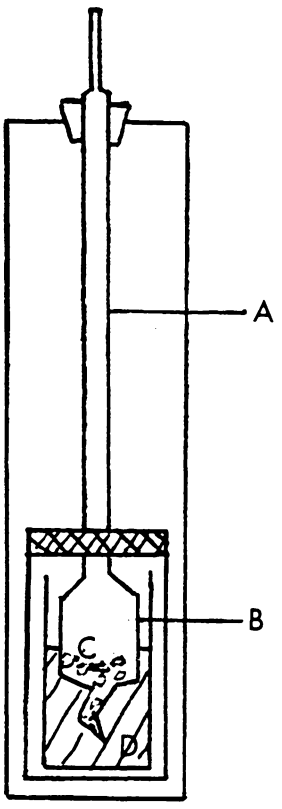

Figure 13: Sample cell assembly

A: Breaker rod
B: Glass ampoule
C: Alumina
D: Liquid

$$\Delta H_{imm} = S(C_s \pm C_b)1000/WA \quad (mJ/m^2) \qquad \text{<III-3>}$$

where C_s and C_b are the steady state sample and empty bulb counts, respectively, W is the sample weight in grams, and A is the specific surface area of the adsorbent in m^2/g. The counts C_s and C_b were subtracted in equation <III-3> if the empty bulb heat was exothermic and added if endothermic. All heats of immersion were exothermic. The numerical calorimetric data for each system are given in Appendix B.

Chapter IV

RESULTS AND DISCUSSION

4.1 ADSORPTION ISOTHERMS

Net adsorption isotherms for H151 alumina in heptane solutions of n-decanol, ethyl octanoate, n-decanoic acid, and n-decylamine are shown in Figures 14 - 17 . The specific surface excess, $n^{o}\Delta X_{A}/m$, is plotted in each case as a function of X_{A}. The total number of moles of both components in the solution is n^{o}, ΔX_{A} is the change in mole fraction of the polar component, A, upon equilibration with m grams of the adsorbent, and X_{A} is the equilibrium mole fraction of component A in the bulk solution. A sample calculation and the numerical results for each system can be found in Appendix C. The shape of the net isotherm in each case indicates preferential adsorption of the polar component over the concentration range investigated.

4.2 COMPONENT ISOTHERMS

The net adsorption isotherms were resolved into component isotherms using the Kipling-Elton method (3,4). Here the number of moles of heptane and the polar component in the surface layer, n_{H}^{s} and n_{A}^{s}, are calculated as a function of X_{A} using the following equations:

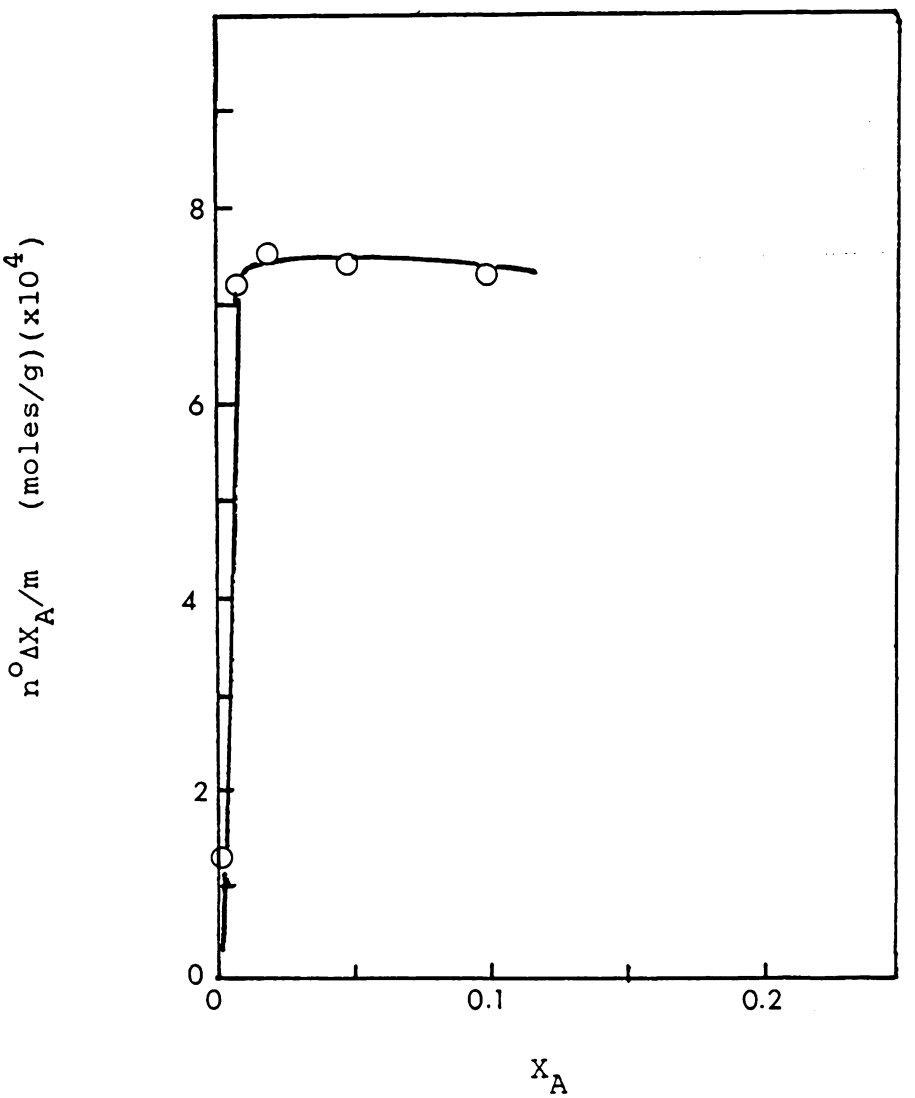

Figure 14: Net adsorption isotherm for n-decylamine/heptane/H151

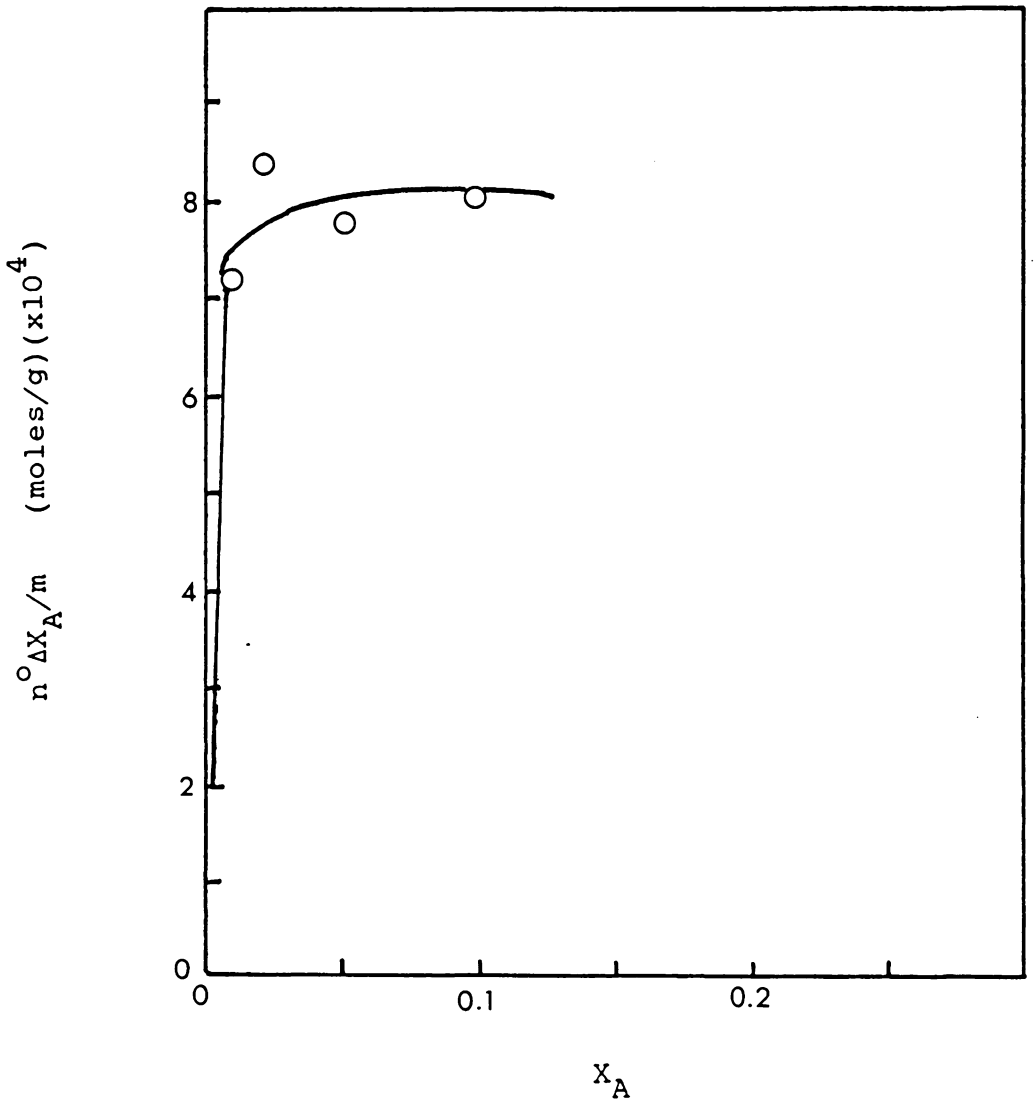

Figure 15: Net adsorption isotherm for n-decanol/heptane/H151

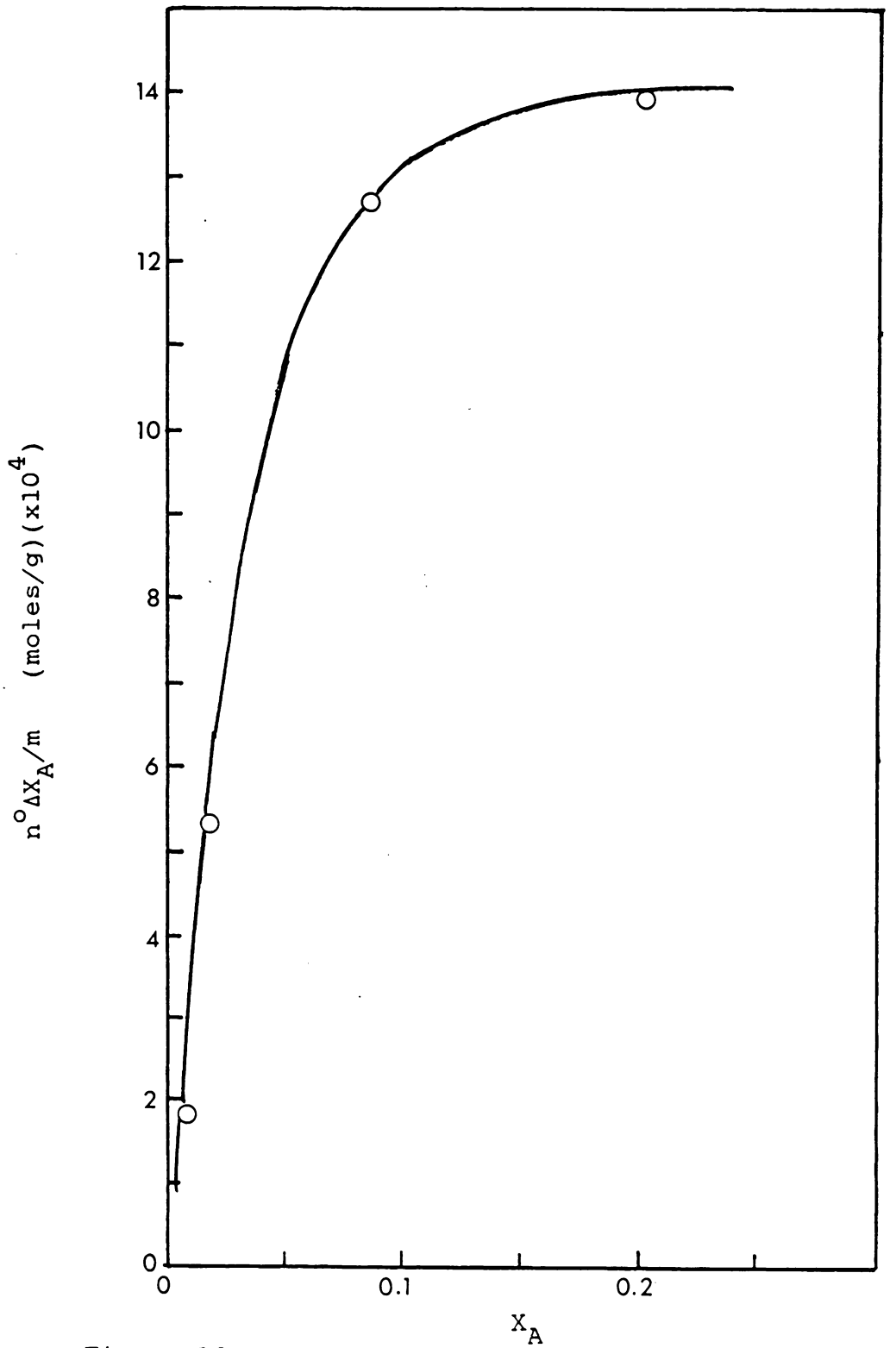

Figure 16: Net adsorption isotherm for n-decanoic acid/heptane/H151

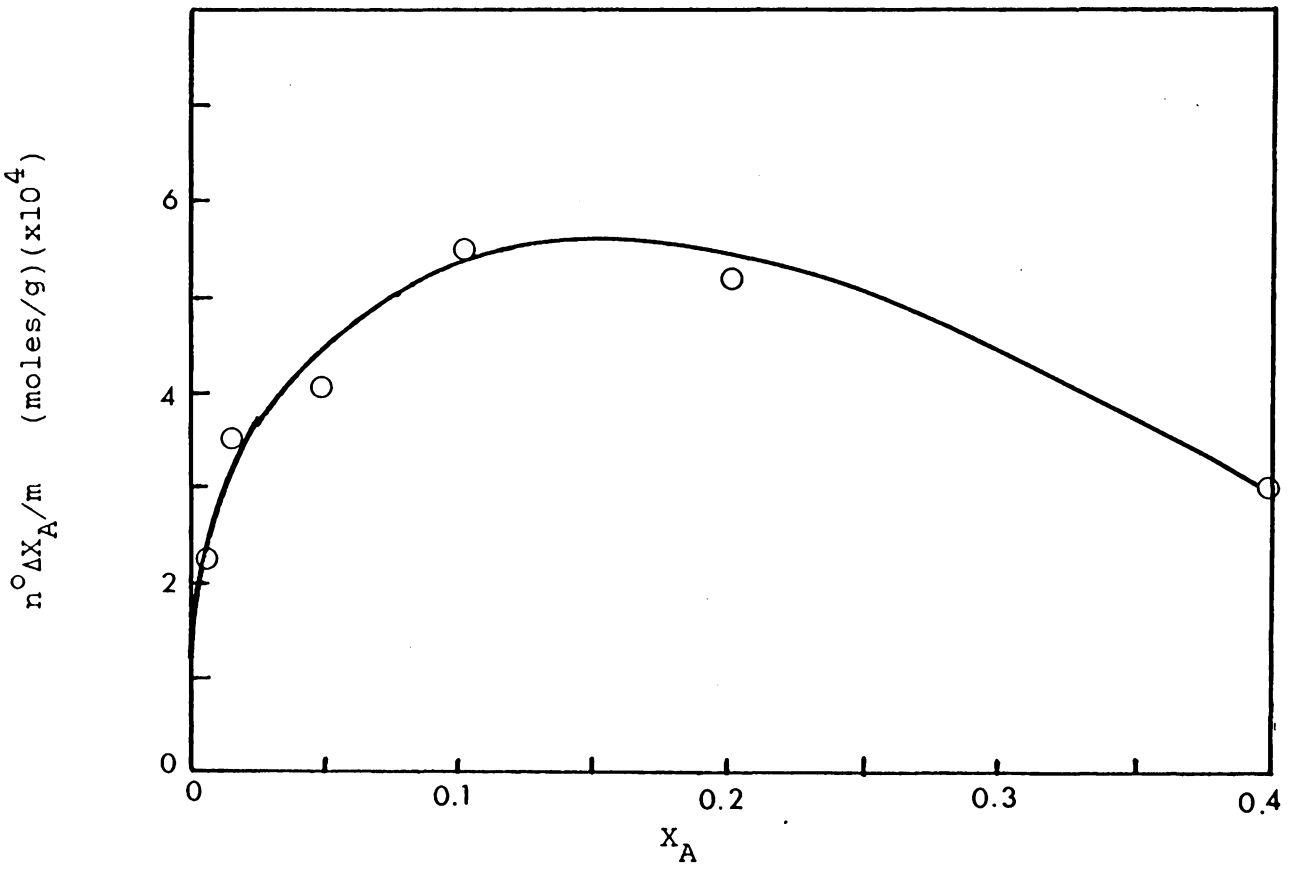

Figure 17: Net adsorption isotherm for ethyl octanoate/heptane/H151

$$n_A^s = (SX_A + n^o \Delta X_A s_H N)/\{(X_A s_A + X_H s_H)NS\} \qquad \text{<IV-1>}$$

$$n_H^s = (SX_H - n^o \Delta X_A s_A N)/\{(X_A s_A + X_H s_H)NS\} \qquad \text{<IV-2>}$$

where S is the specific surface area of the adsorbent, N is Avogadro's number, s_A and s_H are the cross-sectional molecular areas of the polar component and heptane, respectively, and $n^o \Delta X_A$ is the experimentally determined specific surface excess of component A. The values used for s_A and s_H depend on the surface orientation assumed for the molecules. Values of s corresponding to given surface orientations are listed in Table 2 . A perpendicularly oriented polar molecule is held to the surface by its polar group, with the hydrocarbon chain extending into the bulk solution. In a parallel orientation the molecule lies flat. The resolved isotherms based on the areas in Table 2 are shown in Figures 18 - 21 , and the numerical results are listed in Appendix D.

The orientation a molecule assumes upon adsorption depends on its interaction with both the solid surface and the bulk solution. For long-chain polar n-alkyl compounds in a nonpolar solvent both effects are significant. For example, at low concentrations of the polar component one would expect the polar groups to be attracted to the polar surface and the nonpolar hydrocarbon chain to prefer the

TABLE 2

Cross-sectional molecular areas

Molecule	s ($\AA^2$)	Surface Orientation	Ref.
heptane	63	parallel	(34)
n-decanol	20	perpendicular	(34)
ethyl octanoate	40	perpendicular	(34)
n-decanoic acid	22	perpendicular	(34)
n-decylamine	20	perpendicular	(34)

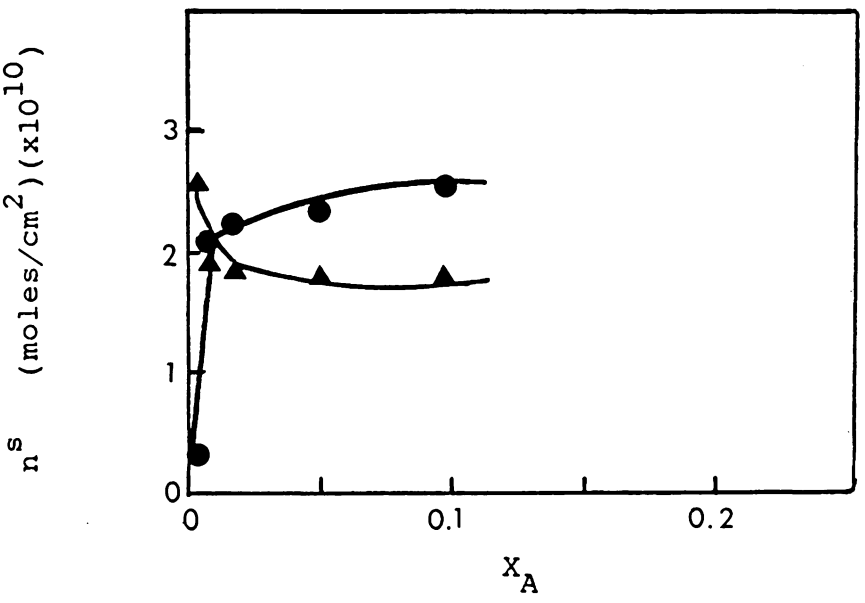

Figure 18: Resolved isotherms for n-decylamine/heptane/H151 (▲) heptane; (●) n-decylamine.

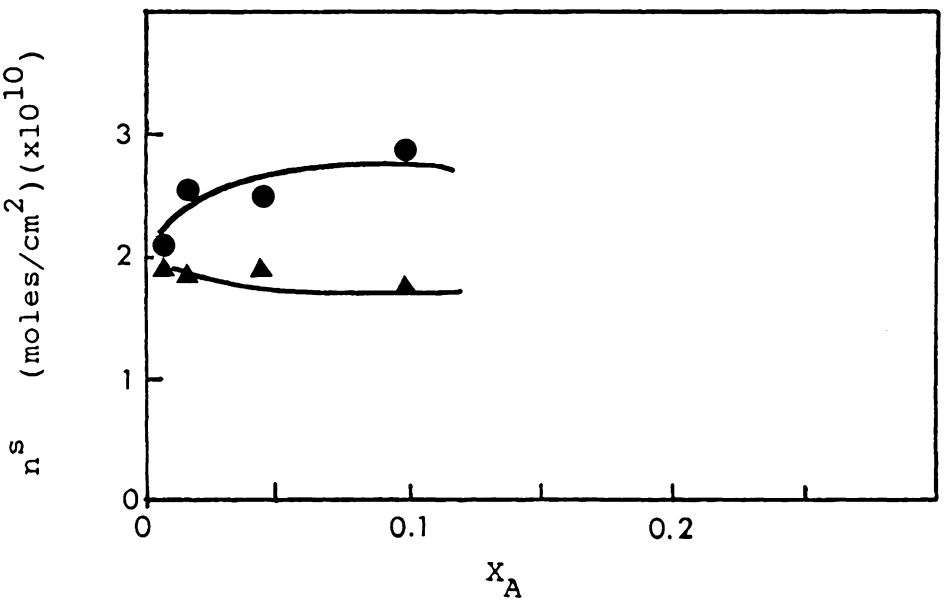

Figure 19: Resolved isotherms for n-decanol/heptane/H151 (▲) heptane; (●) n-decanol.

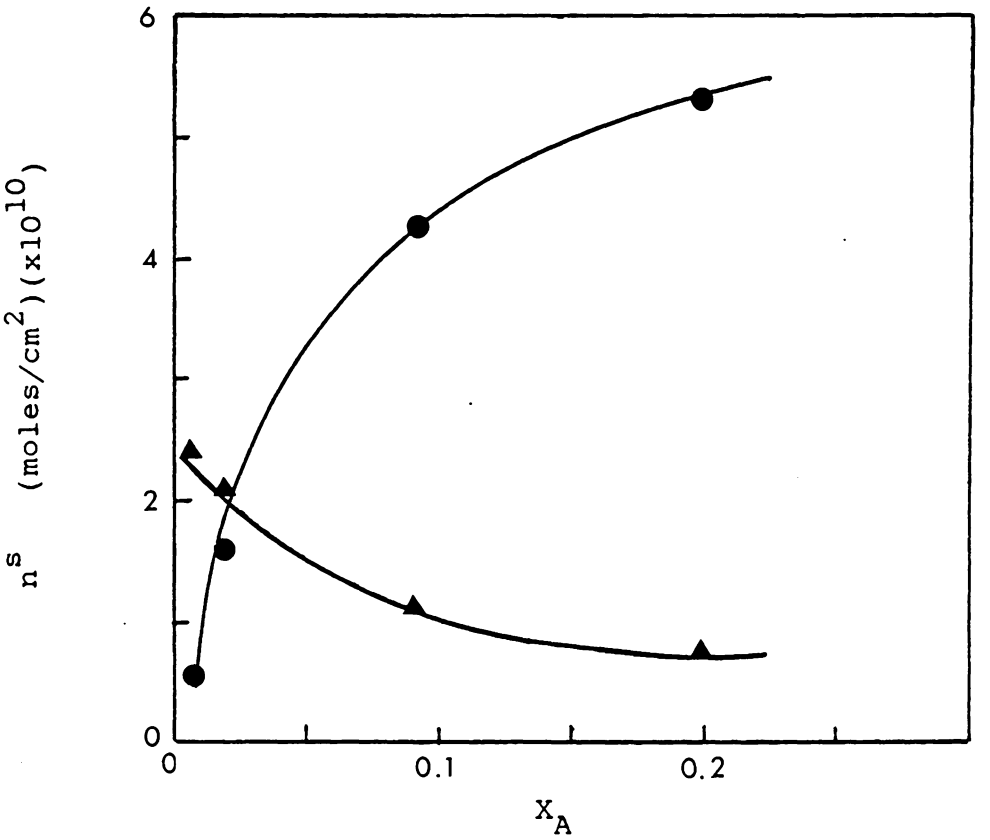

Figure 20: Resolved isotherms for n-decanoic acid/heptane/H151
(▲) heptane; (●) n-decanoic acid.

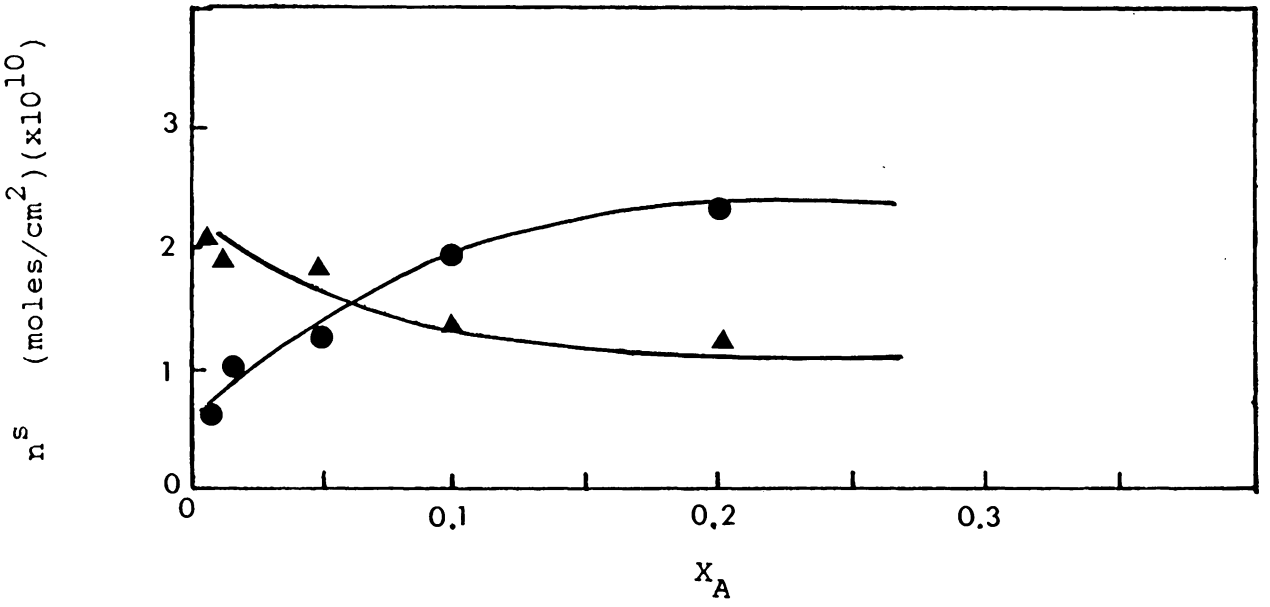

Figure 21: Resolved isotherms for ethyl octanoate/ heptane/H151
(▲) heptane; (●) ethyl octanoate.

relatively nonpolar bulk solution. Schay et al. (36) note that in fact the molecular orientation may change over the concentration range of the isotherm. Furthermore, the work of Rahman and Ghosh with stearic acid (31) indicates that adsorbed n-fatty acid molecules may not assume a simple orientation on the surface, with the adsorbed area per molecule intermediate between that for parallel and for perpendicular orientations.

Figures 22 - 25 illustrate the effect of different values of the assumed molecular area (s_A) on the resolved isotherms for each system studied. Heptane molecules are assumed to lie parallel to the surface with s_H=63 $\mathring{A}^2$. While the polar component is preferentially adsorbed in all cases, the assumed s_A value has a large effect on the n_H^s isotherm. As s_A increases, the n_H^s curve is lowered and the extent of preferential adsorption appears to increase. This is indicated by the increasing separation of the n_H^s and n_A^s isotherms. However, for the n-decanol, n-decylamine, and n-decanoic acid systems the n_A^s isotherm remains essentially the same as s_A is varied. Also, the intersection of the n_H^s and n_A^s curves is the same and very near X_A=0. This implies that s_A has no effect on the concentration range over which preferential adsorption occurs in these three systems. The value of ~20 $\mathring{A}^2$ for s_A corresponds to a perpendicular

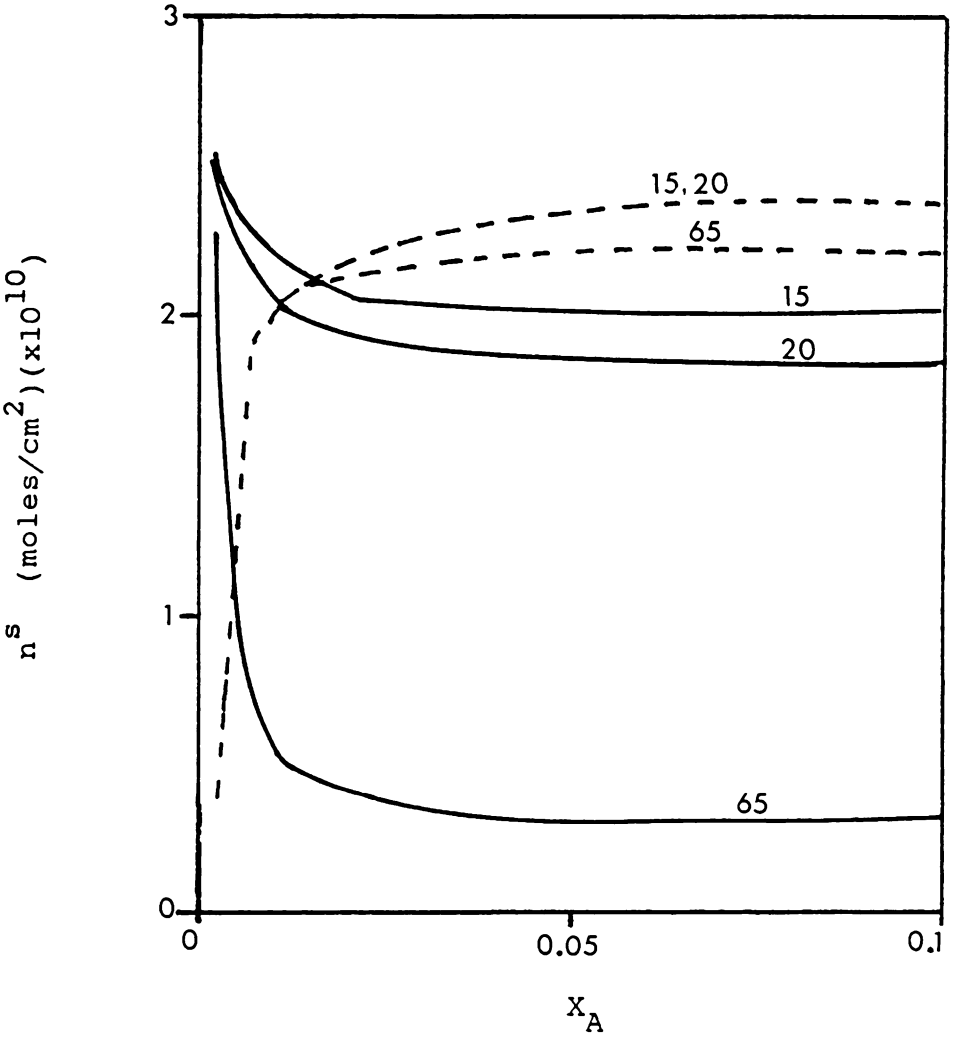

Figure 22: Effect of s_A on resolved isotherms for n-decylamine
(——) heptane; (- - -) n-decylamine. Numbers refer to s_A in $\mathring{A}^2$.

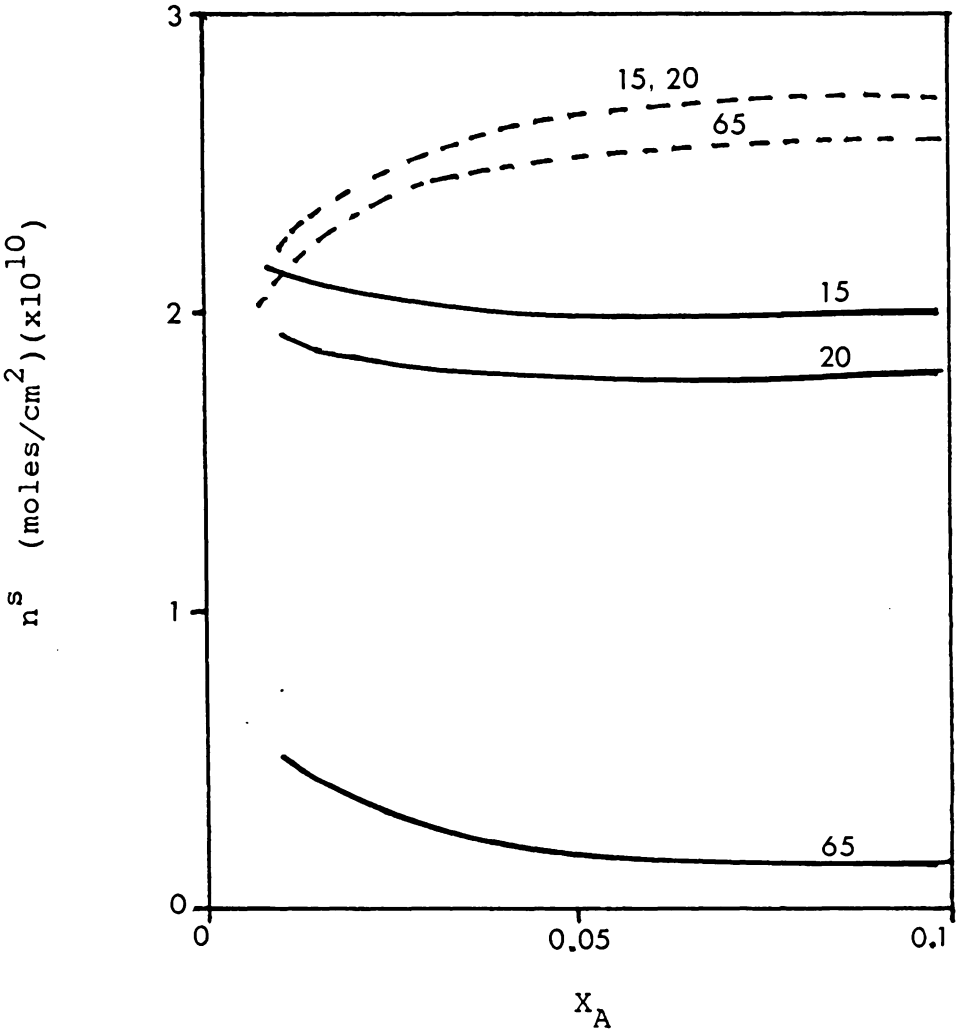

Figure 23: Effect of s_A on resolved isotherms for n-decanol (——) heptane; (- - -) n-decanol. Numbers refer to s_A in $\mathring{A}^2$.

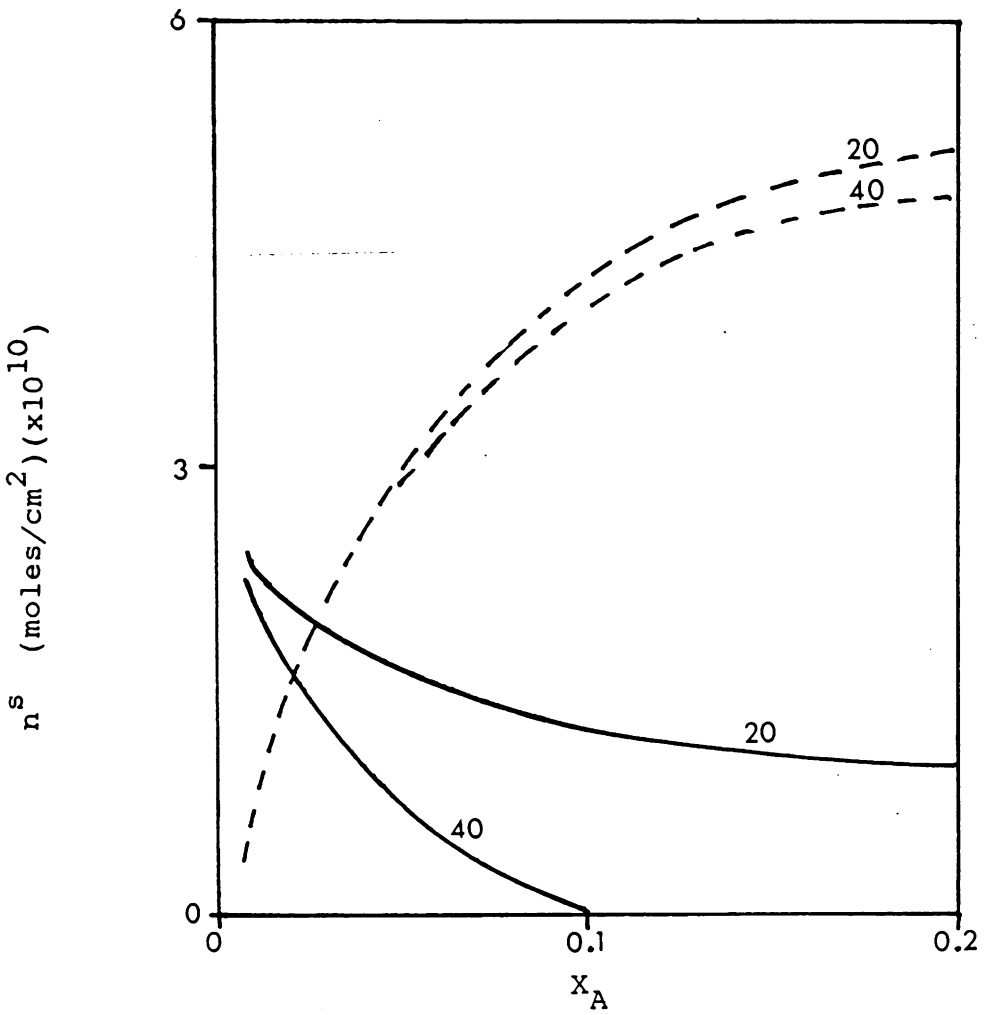

Figure 24: Effect of s_A on resolved isotherms for n-decanoic acid
(——) heptane; (- - -) n-decanoic acid. Numbers refer to s_A in $\mathring{A}^2$

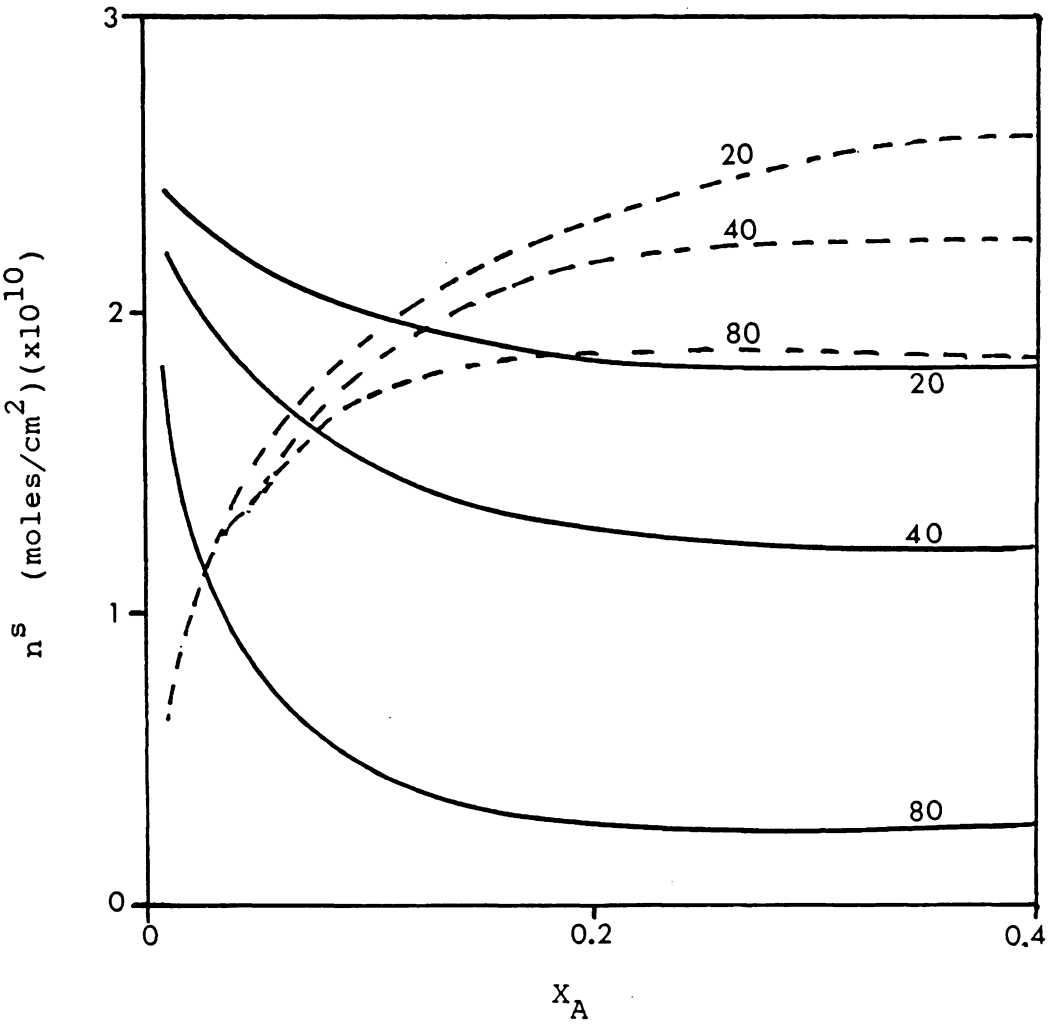

Figure 25: Effect of s_A on resolved isotherms for ethyl octanoate
(——) heptane; (– – –) ethyl octanoate. Numbers refer to s_A in $\mathring{A}^2$.

orientation whereas the higher values correspond to a partially parallel orientation. If as in these three systems the number of polar molecules on the surface remains constant as s_A is varied but the number of heptane molecules on the surface decreases, the implication is that the adsorption sites for the polar component are saturated. If the molecules are oriented partly parallel to the surface, a portion of the surface which would be occupied by heptane molecules is no longer available and n_H^s decreases. On the other hand, for the ethyl octanoate system the s_A value assumed does have a significant effect on the n_A^s isotherm and also affects the intersection of the two component isotherms. In this case, increasing s_A lowers the n_A^s curve and shifts the intersection to a lower concentration of the polar component. Thus for the ester system, the assumed molecular area significantly changes the concentration range over which preferential adsorption appears to occur. Increasing s_A lowers the number of ester molecules on the surface at each X_A (lowers the n_A^s isotherm). Therefore the results suggest that an ethyl octanoate molecule occupying >40 Å^2 blocks adsorption sites which would otherwise be available to both component molecules still in solution. These results again indicate that the orientation of an admolecule significantly affects the shape and

interpretation of the resolved isotherm. Thus care must be taken in assuming a given orientation.

4.3 HEAT OF IMMERSION

The heat of immersion, ΔH_{imm}, of H151 alumina in heptane solutions of n-decanol, ethyl octanoate, and n-decanoic acid is plotted as a function of X_A in Figures 26 - 28 . The numerical results can be found in Appendix B. For all systems, the de-mixing effect and the associated heat of dilution was assumed to be negligible with respect to ΔH_{imm}. This is a reasonable assumption based on the results of Noll and Burchfield for the n-butanol/toluene/silica system (37). In all cases the heat of immersion is independent of the concentration of the polar component for $X_A > 0.05$. Indeed, the heat of immersion in solution is equivalent to the heat of immersion in the pure polar component. These results suggest a large degree of preferential adsorption of the polar species. Heats of immersion in n-decanol and ethyl octanoate are identical. These results support the equivalency of the resolved n_A^s isotherms (Figures 19 and 21). Furthermore, the maximum heat of immersion in solutions of n-decanoic acid is greater than that in solutions of n-decanol and of ethyl octanoate, and the maximum of the n_A^s isotherm is also greater for n-decanoic

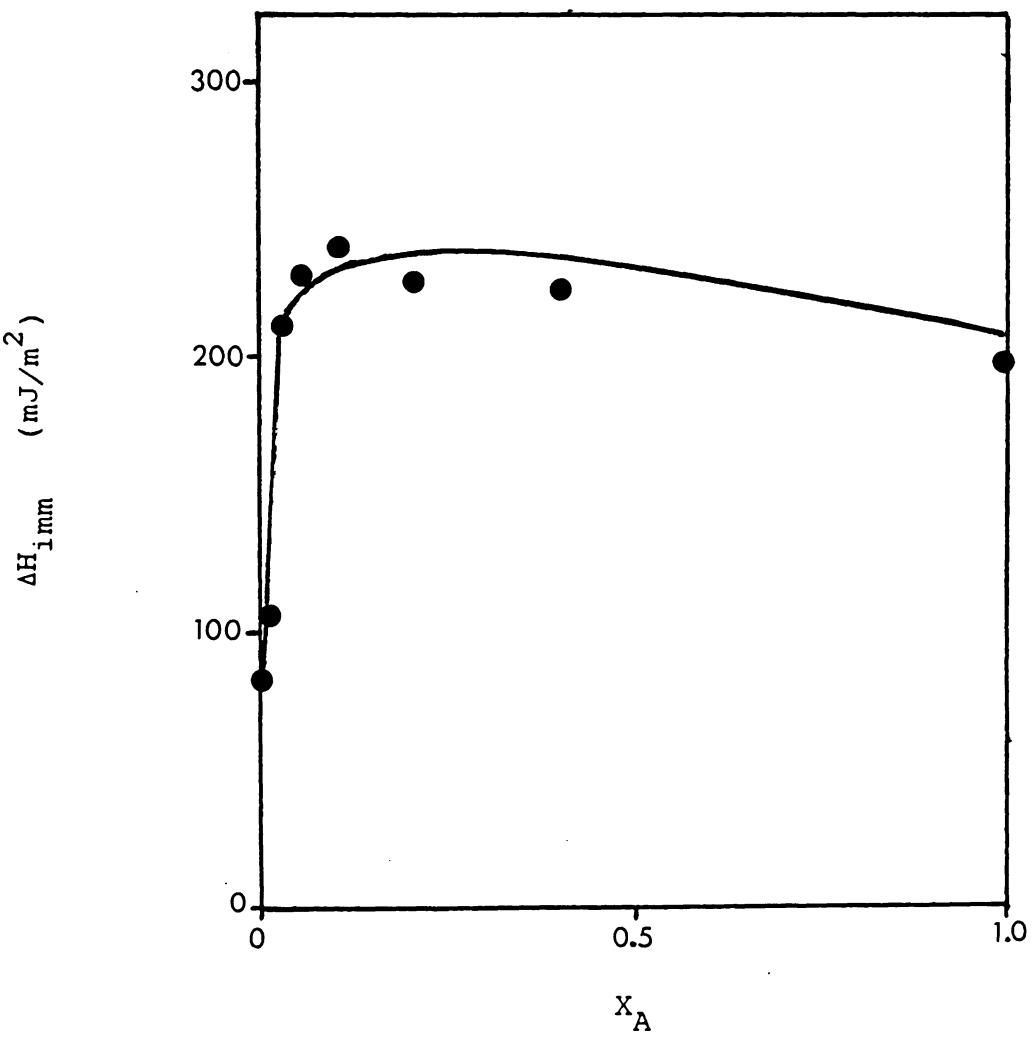

Figure 26: Heat of immersion of H151 in n-decanol+heptane

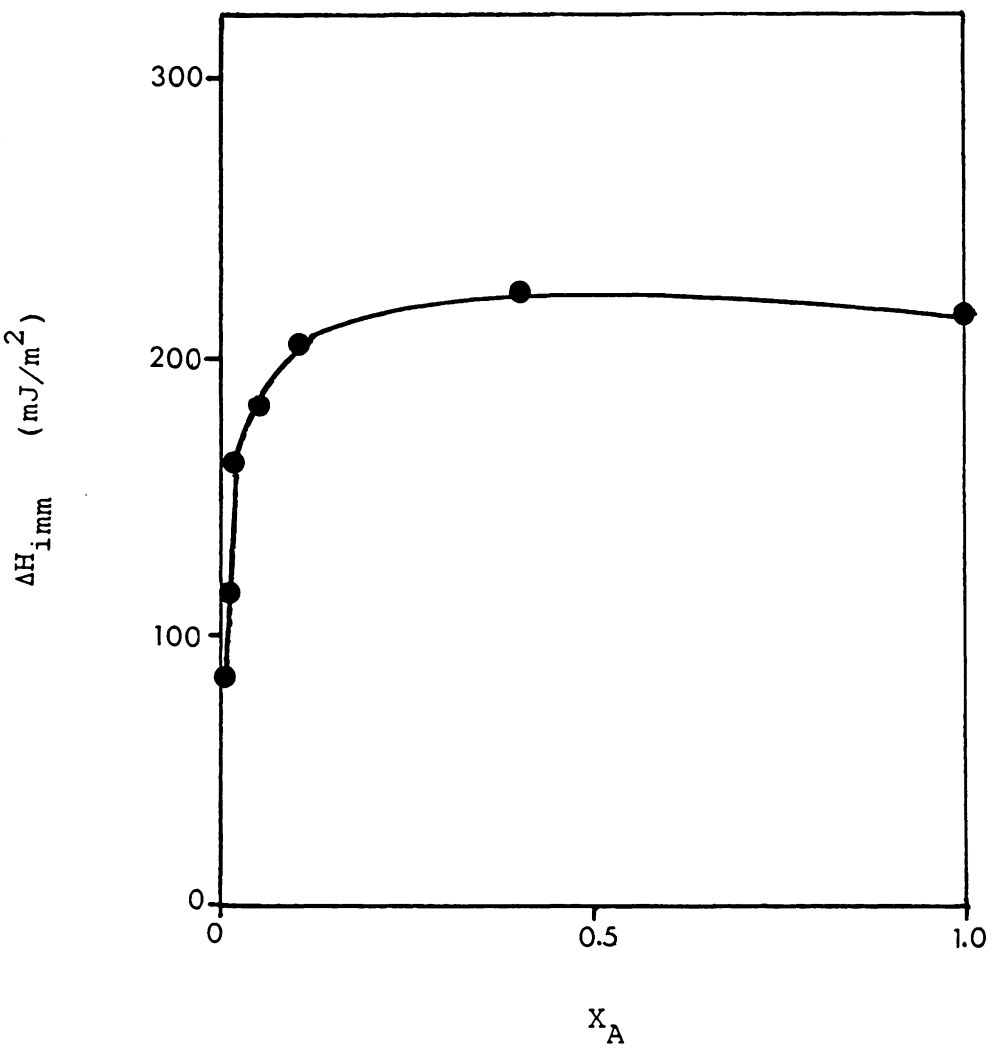

Figure 27: Heat of immersion of H151 in ethyl octanoate+heptane

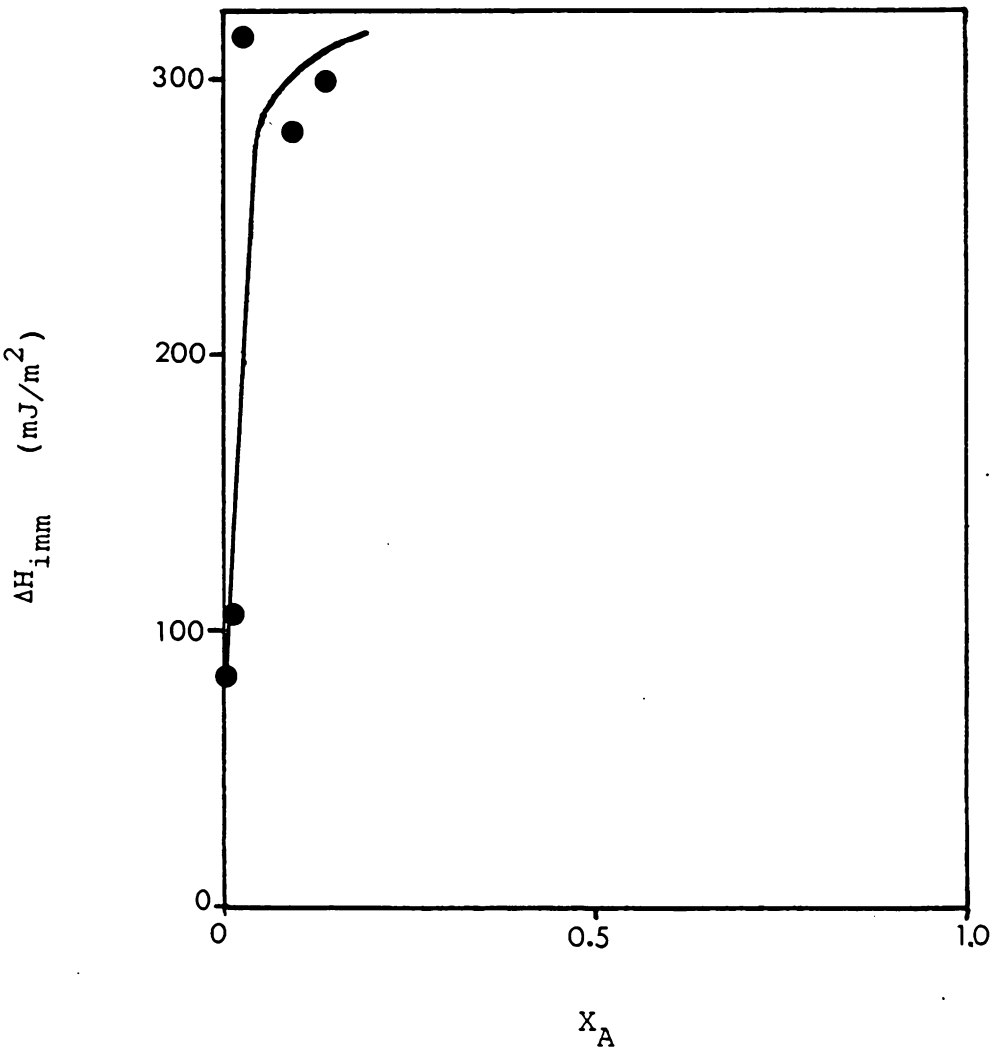

Figure 28: Heat of immersion of H151 in n-decanoic acid+heptane

acid (Fig. 20). Results in which the heat of immersion has been used to support the resolved isotherms have not been previously reported in the literature.

4.4 SURFACE HETEROGENEITY

The data for the solutions of n-decanol and ethyl octanoate in heptane were analyzed in terms of surface heterogeneity using the Rudzinski model (21). The heterogeneity parameter c was calculated, and then theoretical excess heats of immersion were calculated from the equation:

$$\Delta_w^T H = -cn^o\{(1-\phi_A^s)\ln(1-\phi_A^s)+\phi_A^s\ln\phi_A^s\} \qquad \text{<IV-3>}$$

(the last term in equation <II-13>) and correlated to experimental values for each case. An ideal solution was assumed. No literature references were found for the activity coefficients for the solutions studied. In practice the previously described method involves varying n^o and r in combination, each over a reasonable range of values (38). The monolayer capacity, n^o, was estimated from the surface excess isotherm by the method of Schay (2). The monolayer capacity was varied from 8×10^{-6} to 1×10^{-5} moles/m^2 for the n-decanol system and from 3×10^{-6} to 1.5×10^{-5} moles/m^2 for the ethyl octanoate system. The ratio s_A/s_H, defined as r, was varied from 0.2 to 2.0 for both solutions. Illustrative calculations and the results for the "best fit"

combinations of n^o and r are given in Appendix E. Figures 29 - 32 show the effect on the theoretical excess heat of immersion of varying n^o and r in both systems. The best fit of theory to experiment is shown for both cases in Figures 33 and 34 . The theoretical and experimental excess heats of immersion are plotted as a function of Φ_A^s along with the total experimental heat of immersion. The corresponding n^o, r, and c values, respectively, are $1x10^{-5}$ moles/m^2, 0.5, and $20x10^6$ mJ/mole for n-decanol, and $1.5x10^{-5}$ moles/m^2, 0.5, and $4.7x10^6$ mJ/mole for ethyl octanoate. Figures 35 and 36 show the plot of the linear regression of equation <II-12> used to obtain c for each system. Good linear correlations were obtained in both cases.

Several conclusions can be drawn from these results. First, the model seems to describe the n-decanol system better than the ethyl octanoate system. In each case the surface is the same. "Surface heterogeneity" refers to the variation in adsorption energy of both solution components from one adsorption site to another; these variations can result from crystallographic and/or chemical differences (21). Thus the interaction of the alcohol with the surface may be more "heterogeneous" than that of the ester. However, this does not seem likely since one would expect both molecules to interact similarly, through hydrogen

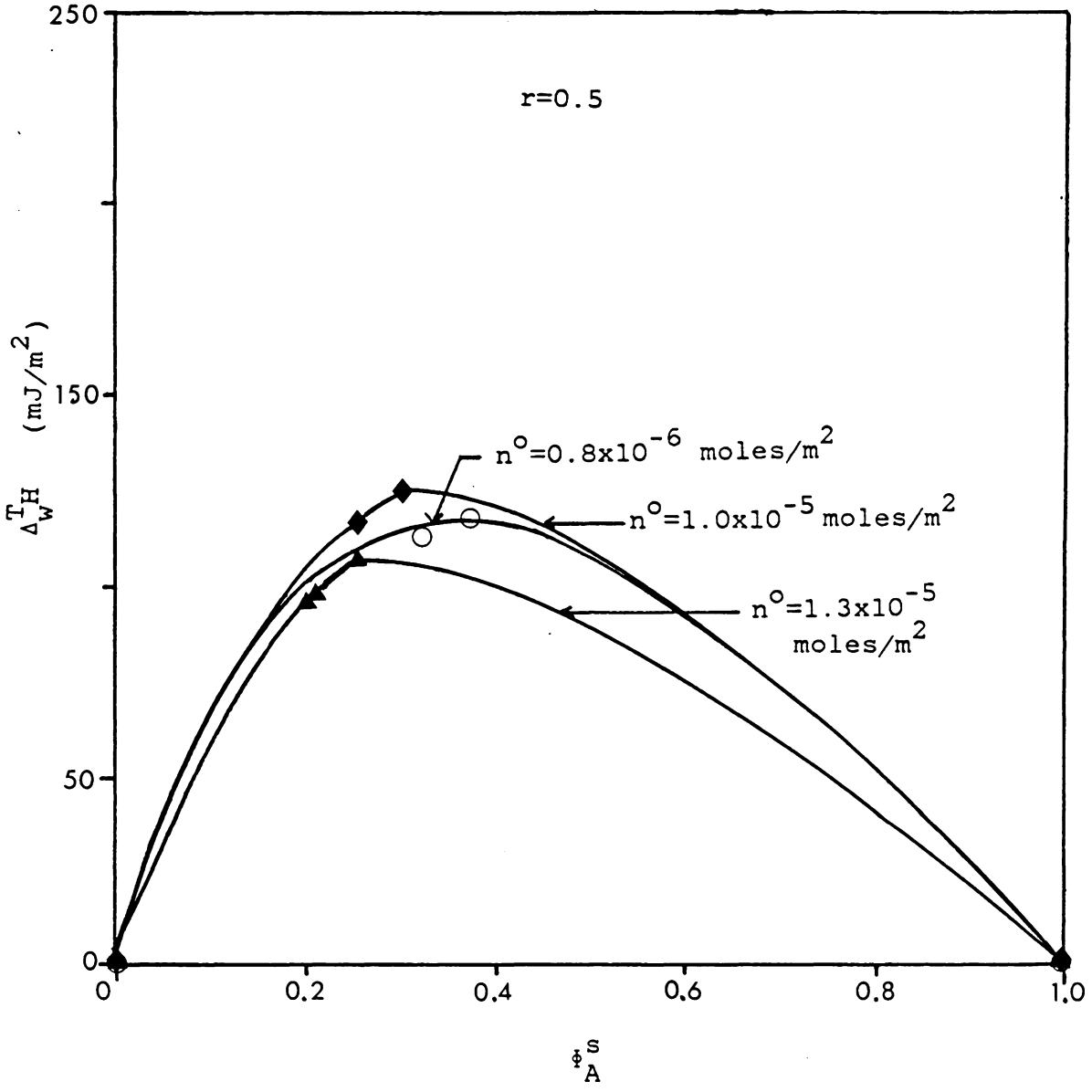

Figure 29: Effect of n^o on theoretical excess heat of immersion in n-decanol+heptane

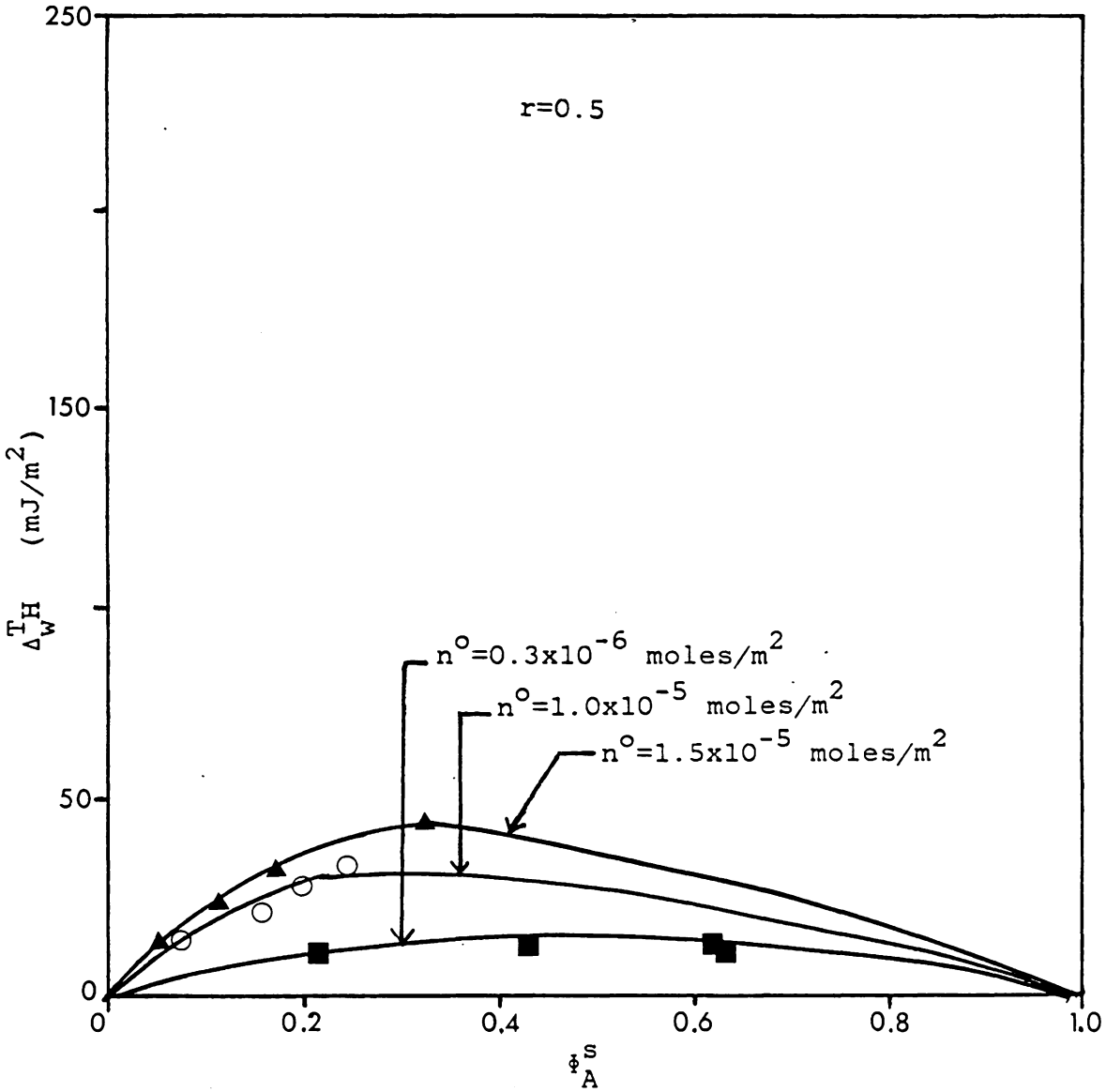

Figure 30: Effect of n^o on theoretical excess heat of immersion in ethyl octanoate+heptane

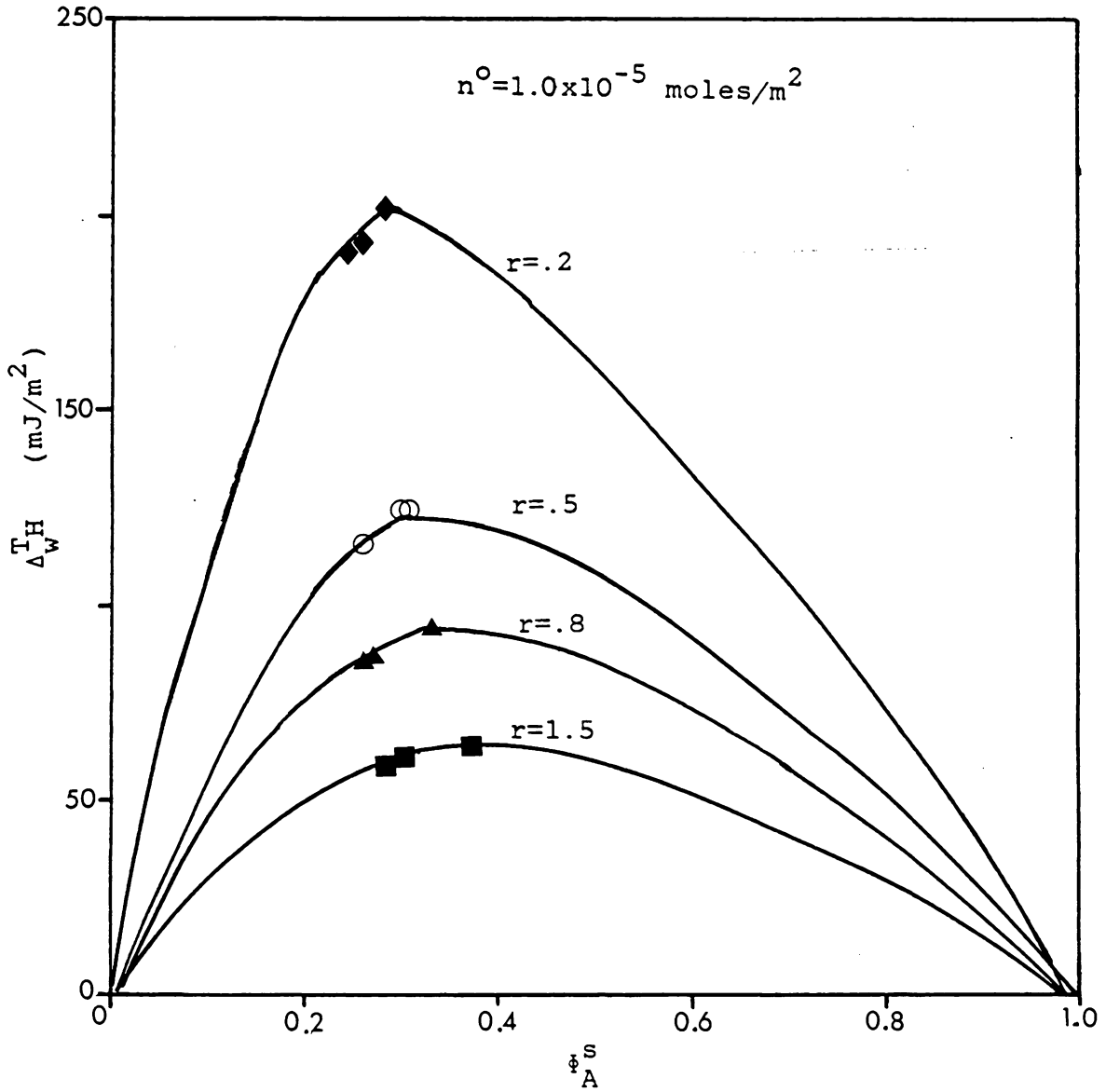

Figure 31: Effect of r on theoretical excess heat of immersion in n-decanol+heptane

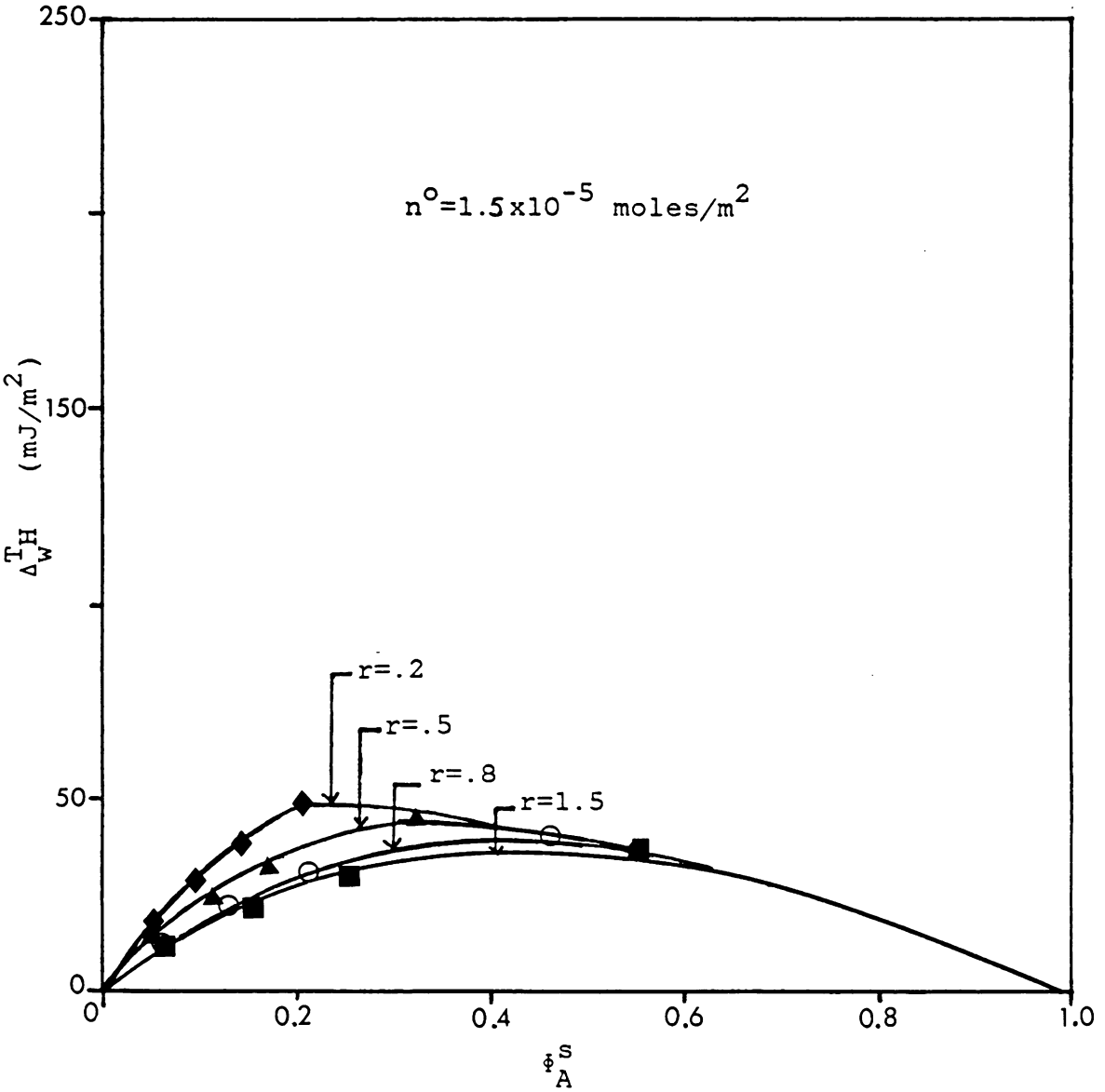

Figure 32: Effect of r on theoretical excess heat of immersion in ethyl octanoate+heptane

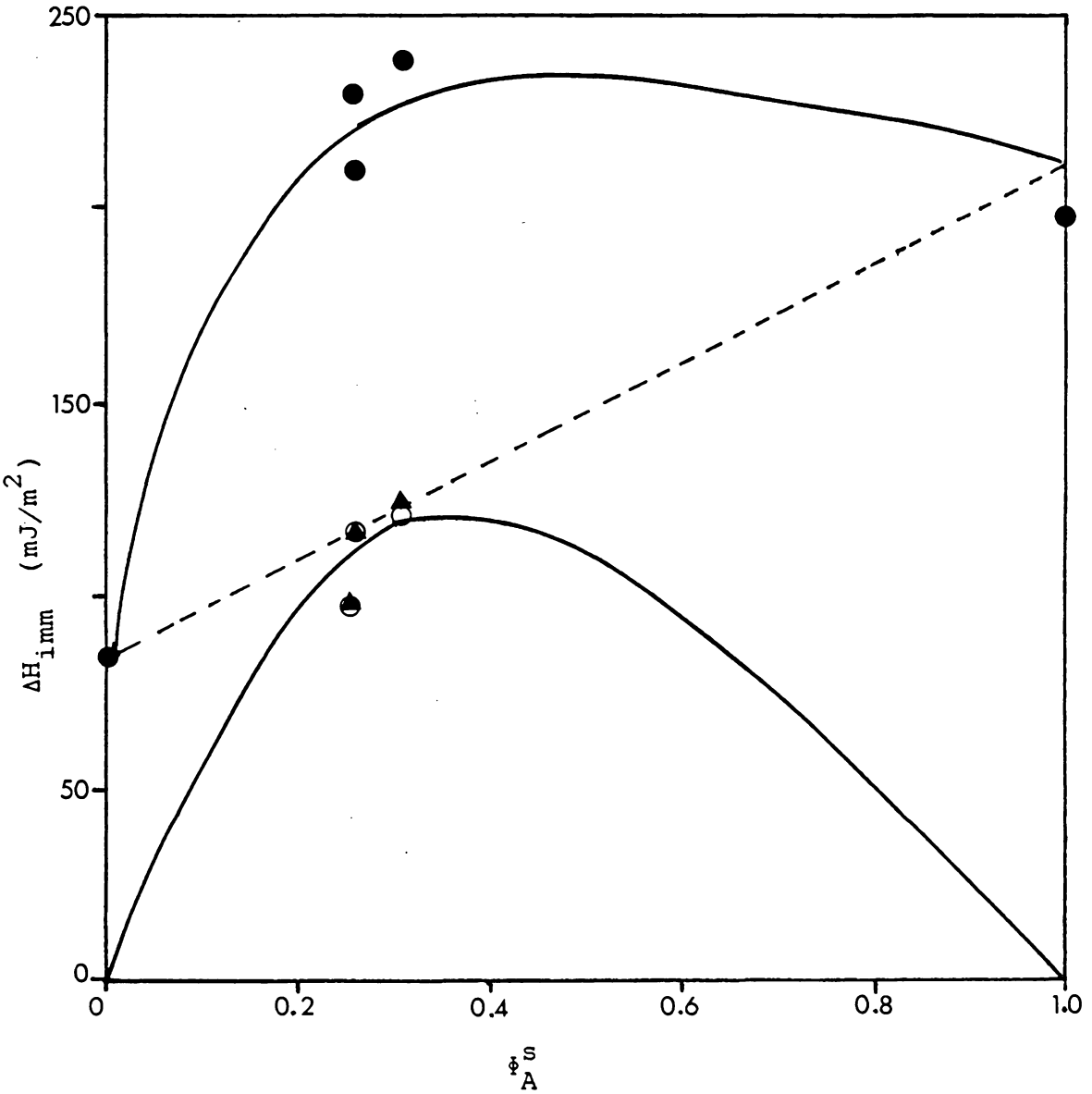

Figure 33: Best fit of Rudzinski model for n-decanol system ● experimental heat of immersion; ▲ theoretical excess; ○ experimental excess.

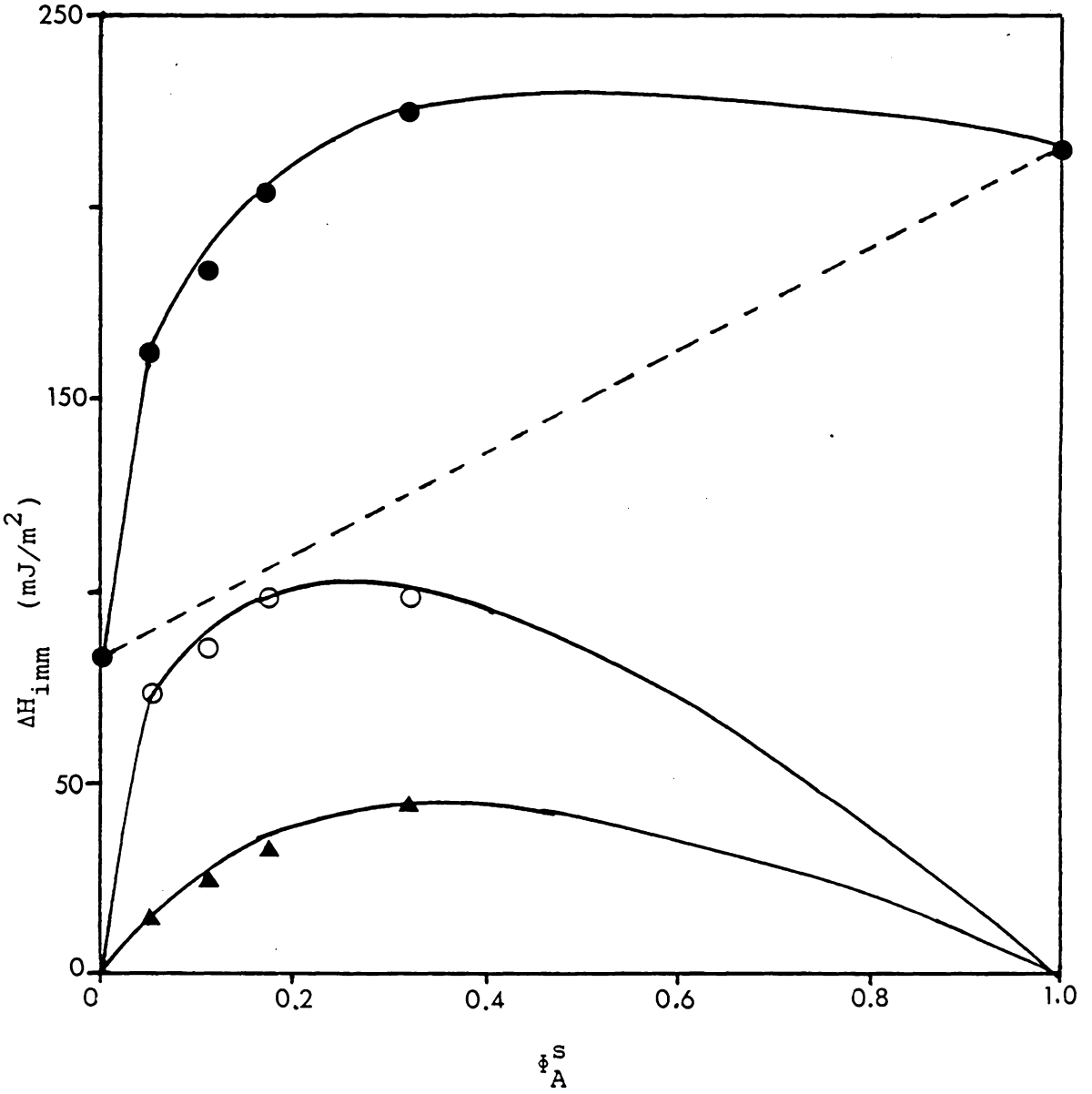

Figure 34: Best fit of Rudzinski model for ethyl octanoate system
● experimental heat of immersion; ▲ theoretical excess; ○ experimental excess.

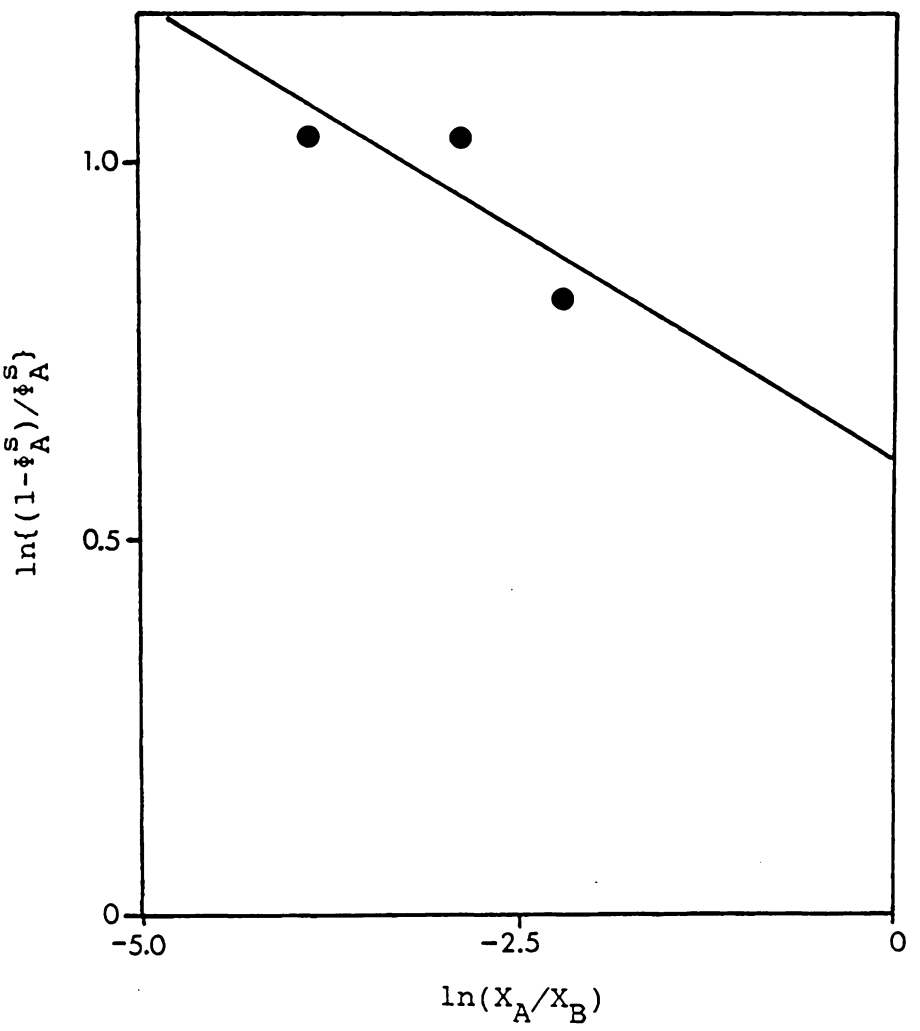

Figure 35: Linear regression to determine c for n-decanol system
Linear plot of equation <II-12>; slope=-RT/c; $n^o=1.0x10^{-5}$; r=.5.

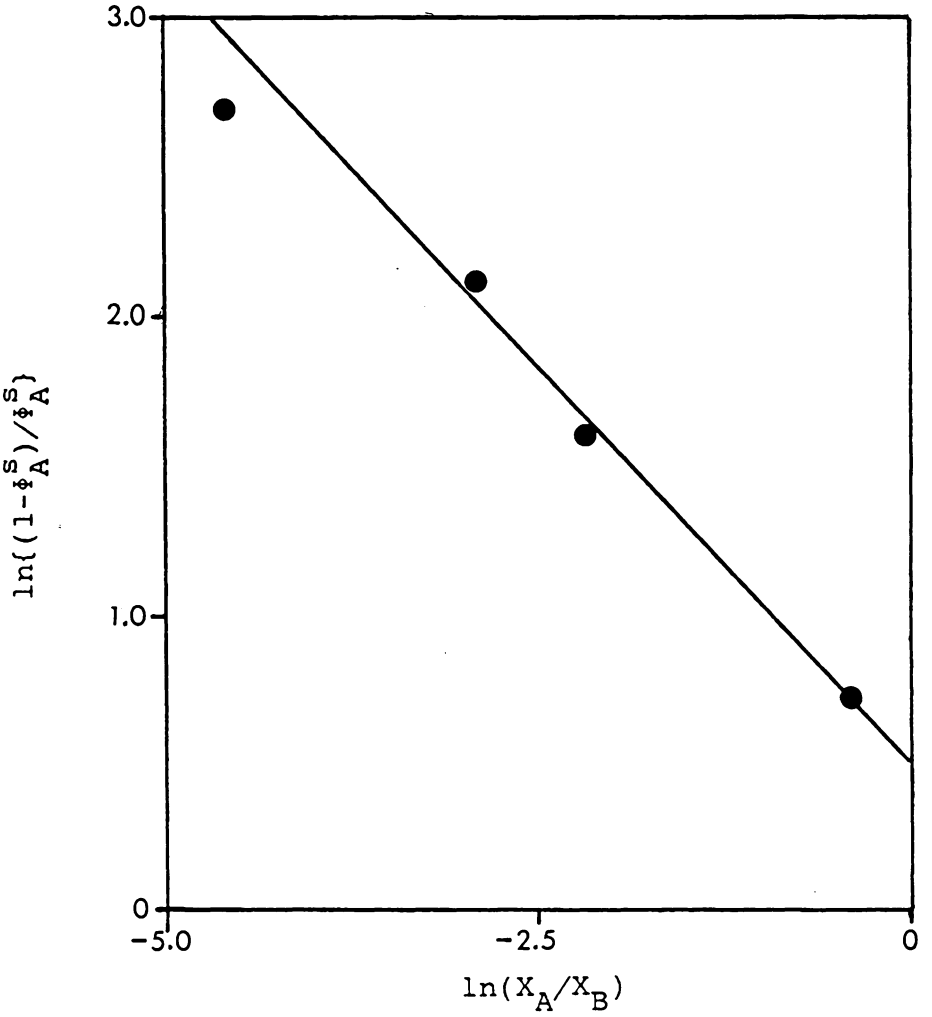

Figure 36: Linear regression to determine c for ethyl octanoate system
Linear plot of equation <II-12>; slope=-RT/c; $n^o=1.5x10^{-5}$; r=.5.

bonding, with the surface. The heat of immersion supports this conclusion, since its magnitude is identical for both solutions and is not sufficiently large to suggest chemical adsorption. Another possibility is that the assumptions of the model are appropriate for n-decanol but not for ethyl octanoate solutions. Specifically, both the bulk and surface phases were assumed to be ideal. Again, however, one would not expect significant differences between n-decanol and ethyl octanoate in this respect. Finally, it is possible that a right-hand widened energy distribution (see Figure 5 b) would better describe the ester system (38). In both cases though, the fit of the model is reasonable, given the necessary assumptions (38).

The selection of values of n^{o} and r is somewhat arbitrary. Since the surface excess isotherms from which n^{o} values were estimated do not extend over the entire concentration range, the curves were extrapolated to determine a feasible range for n^{o}. As is seen in Figures 29 and 30, a small change in the value of n^{o} has a minimal effect on the fit of the model in each case. For monolayer capacities less than the minimum value indicated for each system, negative values of ϕ_A^s resulted.

The effect of r is different for each system. In the case of n-decanol, increasing r (increasing s_A) lowers the

maximum of the theoretical excess heat of immersion plot but does not affect the range of ϕ_A^s. For ethyl octanoate increasing r increases the range of ϕ_A^s but has little effect on the maximum of the theoretical excess heat of immersion curve. Since ϕ_A^s refers to the areal fraction of the surface covered by the polar component, one would expect that increasing s_A would in fact increase ϕ_A^s. This effect is seen for ethyl octanoate but not for n-decanol. The influence of r on the magnitude of the theoretical excess heat of immersion in n-decanol solution is due to the fact that decreasing r increases the value of the heterogeneity parameter, c. Since ϕ_A^s is independent of the r value chosen, the additional excess heat of immersion calculated as r is decreased is due to the increase in the value of c. For ethyl octanoate it appears that the change in c as r is varied is compensated for by the concomitent change in ϕ_A^s when the excess heat of immersion is calculated at each concentration (X_A). Values of c calculated as r is varied are given for both systems in Table 3 .

TABLE 3

Variation of the heterogeneity parameter c as r is varied

r	c (mJ/mole) ethyl octanoate $n^o=1.5\times10^{-5}$ moles/m^2	c (mJ/mole) n-decanol $n^o=1.0\times10^{-5}$ moles/m^2
0.2	6×10^6	34×10^6
0.5	5×10^6	20×10^6
0.8	4×10^6	15×10^6
1.5	3.5×10^6	10×10^6

4.5 EQUILIBRIUM CONSTANTS AND SURFACE AREA DETERMINATION

The adsorption equilibrium constant, K, was calculated for all four systems using the Everett method (10). Equation <II-2> relates the surface excess to K. Plots of $X_A^{\ell}X_B^{\ell}/\{n^{o}\Delta X_A^{\ell}/m\}$ as a function of X_A are shown in Figures 37 - 40 . Although the model assumes bulk and surface phase ideality and equal-size solution components, good linear correlations were obtained in all cases. Everett and Brown (39) also cite good correlations for solutions with ratios of a_2/a_1 from 0.5 to 1.5. The resulting values of the monolayer capacity, n^{s}/m, and K are given in Table 4 . For all systems, K is greater than 1, indicating preferential adsorption of the polar component (7). The results suggest that the order of preference of the components adsorbed onto H151 alumina from heptane solutions is ethyl octanoate > n-decanol > n-decylamine > n-decanoic acid. These results do not support the resolved isotherms (Figs. 18 - 21) for which a perpendicular surface orientation was assumed for each polar molecule. In the resolved isotherms the order of preferential adsorption appears to be n-decanoic acid > n-decanol ≈ n-decylamine ≈ ethyl octanoate.

Adsorbent surface areas were calculated using the cross-sectional molecular areas for a perpendicular orientation of each polar component. The calculated values

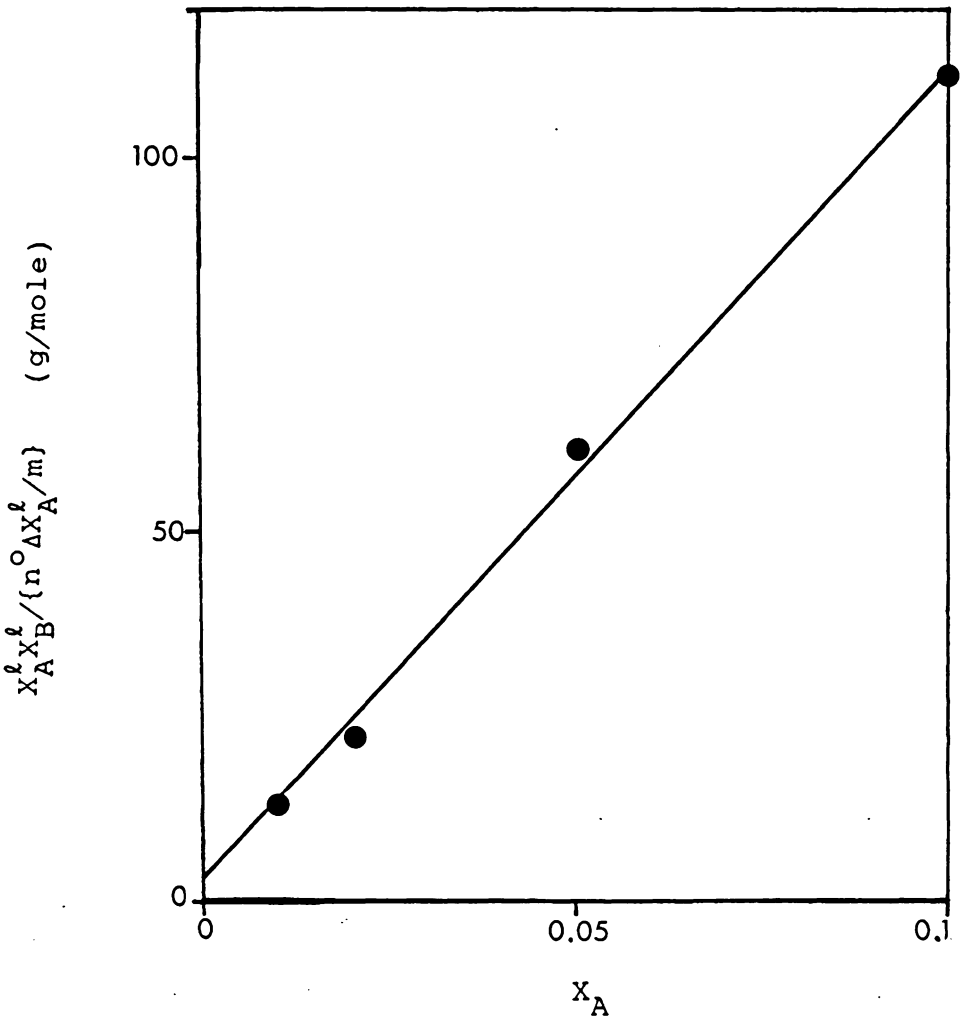

Figure 37: Plot to determine equilibrium constant for n-decanol/heptane/H151

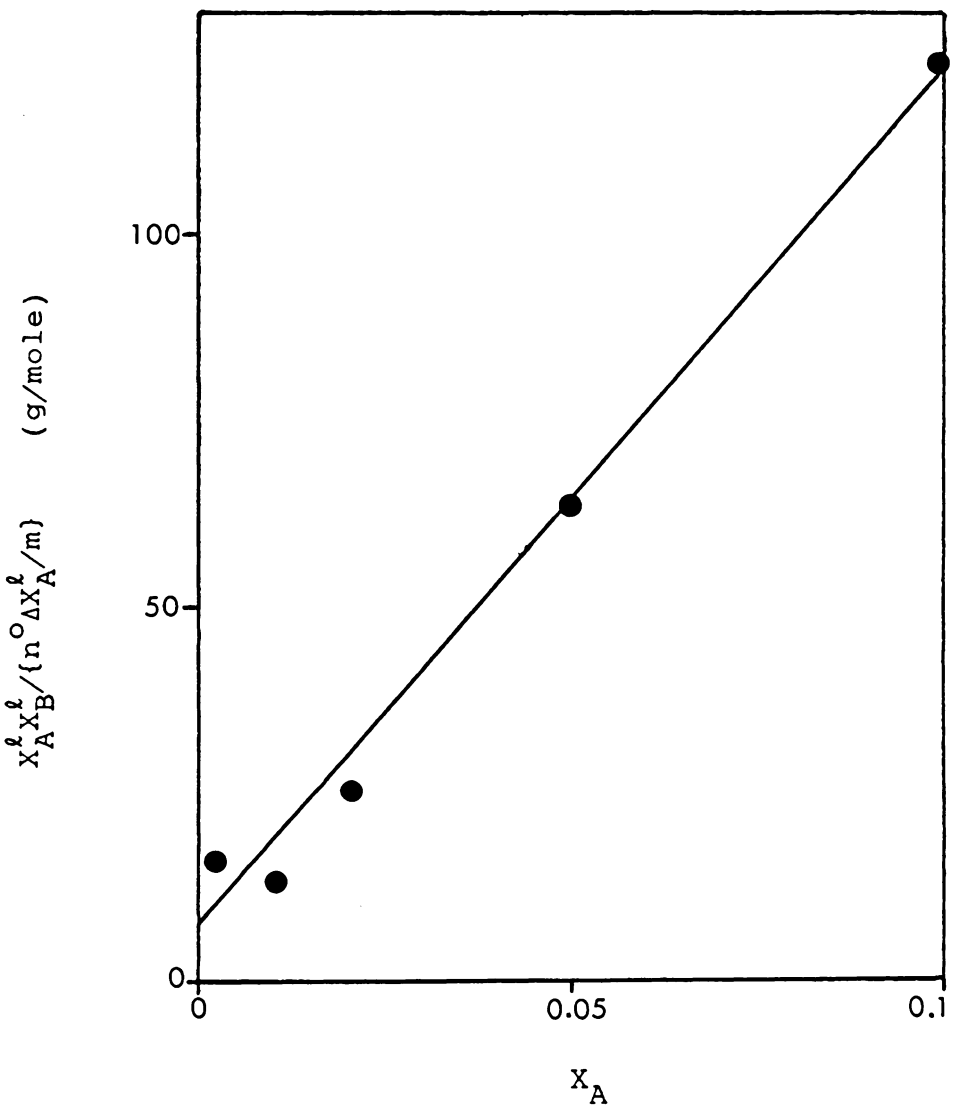

Figure 38: Plot to determine equilibrium constant for n-decylamine/heptane/H151

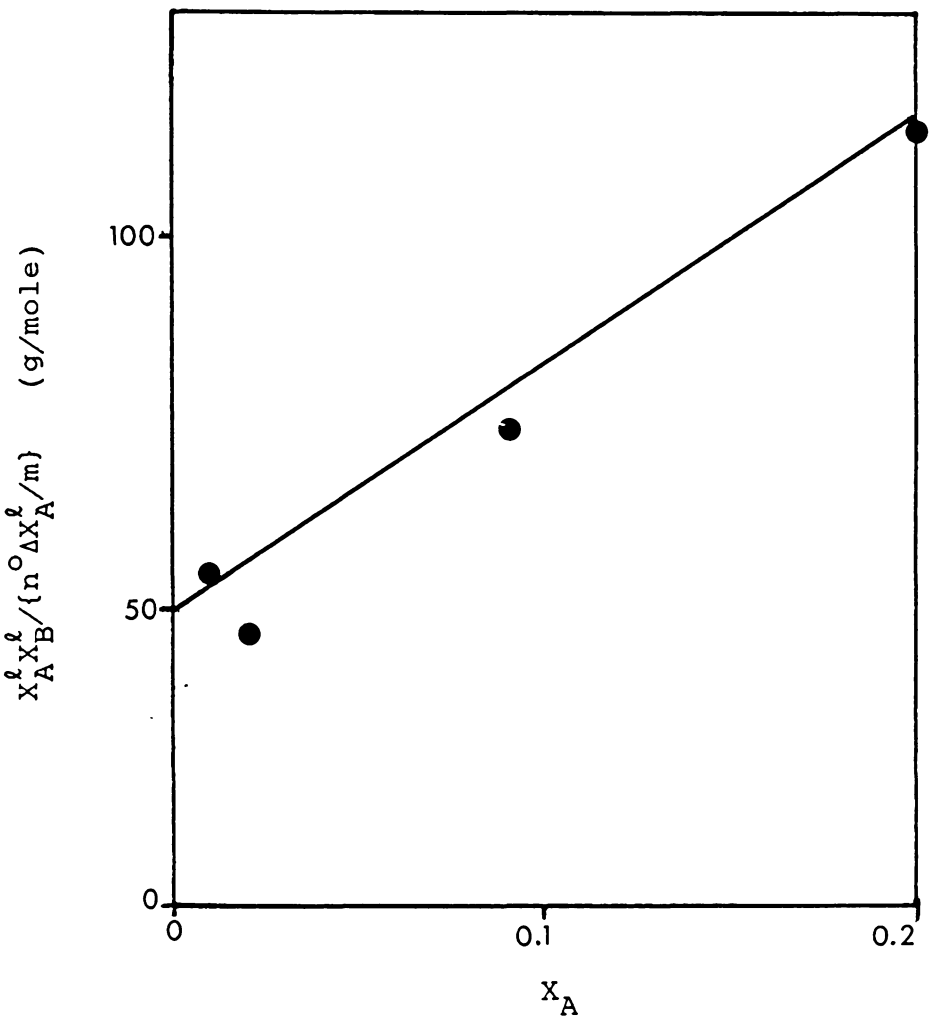

Figure 39: Plot to determine equilibrium constant for n-decanoic acid/heptane/H151

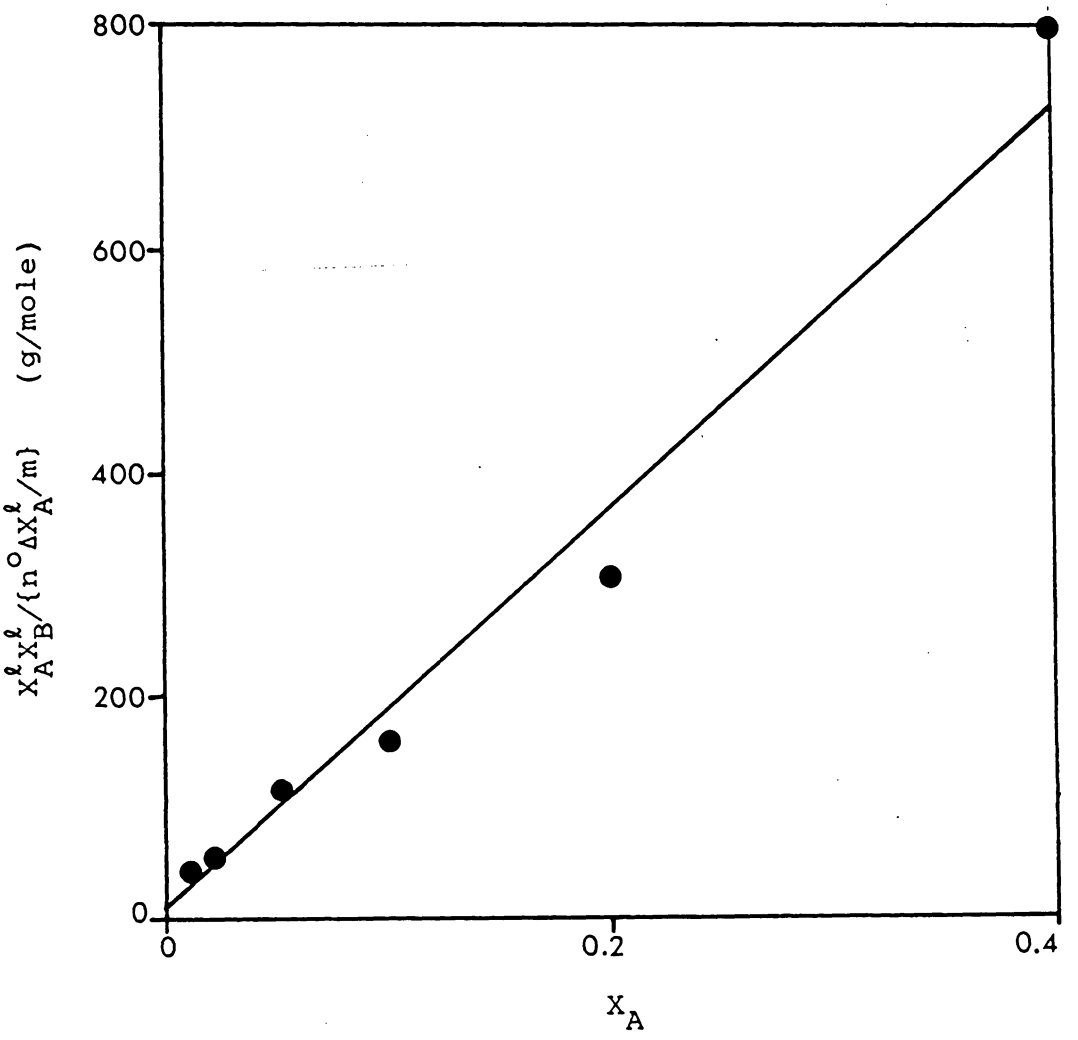

Figure 40: Plot to determine equilibrium constant for ethyl octanoate/heptane/H151

TABLE 4

Equilibrium constants and monolayer capacities *

Adsorbate	K	n^s/m (moles/g) ($\times 10^4$)	S (m^2/g) **
n-decanoic acid	10.3	27.8	368
n-decylamine	178	8.62	104
n-decanol	346	9.17	110
ethyl octanoate	1080	5.26	127

* Calculated by equation <II-2>

** Calculated assuming the following cross-sectional areas ($Å^2$/molecule): n-decanoic acid, 22; n-decylamine, 20; n-decanol, 20; ethyl octanoate, 40.

are also shown in Table 4 . The surface area calculated using n-decanoic acid agrees well with the reported BET nitrogen area of 338 m^2/g for H151 alumina. The following cross-sectional molecular areas would be required to yield a surface area of ~338 m^2/g: 65 $\mathring{A}^2$ for n-decylamine, 61 $\mathring{A}^2$ for n-decanol, and 107 $\mathring{A}^2$ for ethyl octanoate. These results suggest that the surface orientation of these molecules may not be entirely perpendicular.

The heat of immersion in n-decanol and ethyl octanoate solutions was also used to determine the adsorbent surface area by the Everett method (12). Figures 41 and 42 show the linear regression of equation <II-4> used to obtain $n_A^{s,o}$, the reciprocal of the slope. The plot for n-decanol covers the concentration range from X_A=0.01 to X_A=0.1; the plot for ethyl octanoate covers the concentration range from X_A=0.01 to X_A=0.4. The results are summarized in Table 5 . For ethyl octanoate, $n_A^{s,o}$ is equal to 15.4×10^{-4} moles/gram. If s_A is assumed to be 40 A^2 the surface area calculated is 368 m^2/g. Although this area agrees reasonably well with the BET value of 338 m^2/g, it is not equivalent to the 127 m^2/g obtained using equation <II-2> and 40 $\mathring{A}^2$ as the molecular area.

For n-decanol, a negative slope is obtained (Figure 41). Therefore the method cannot be used to estimate surface area

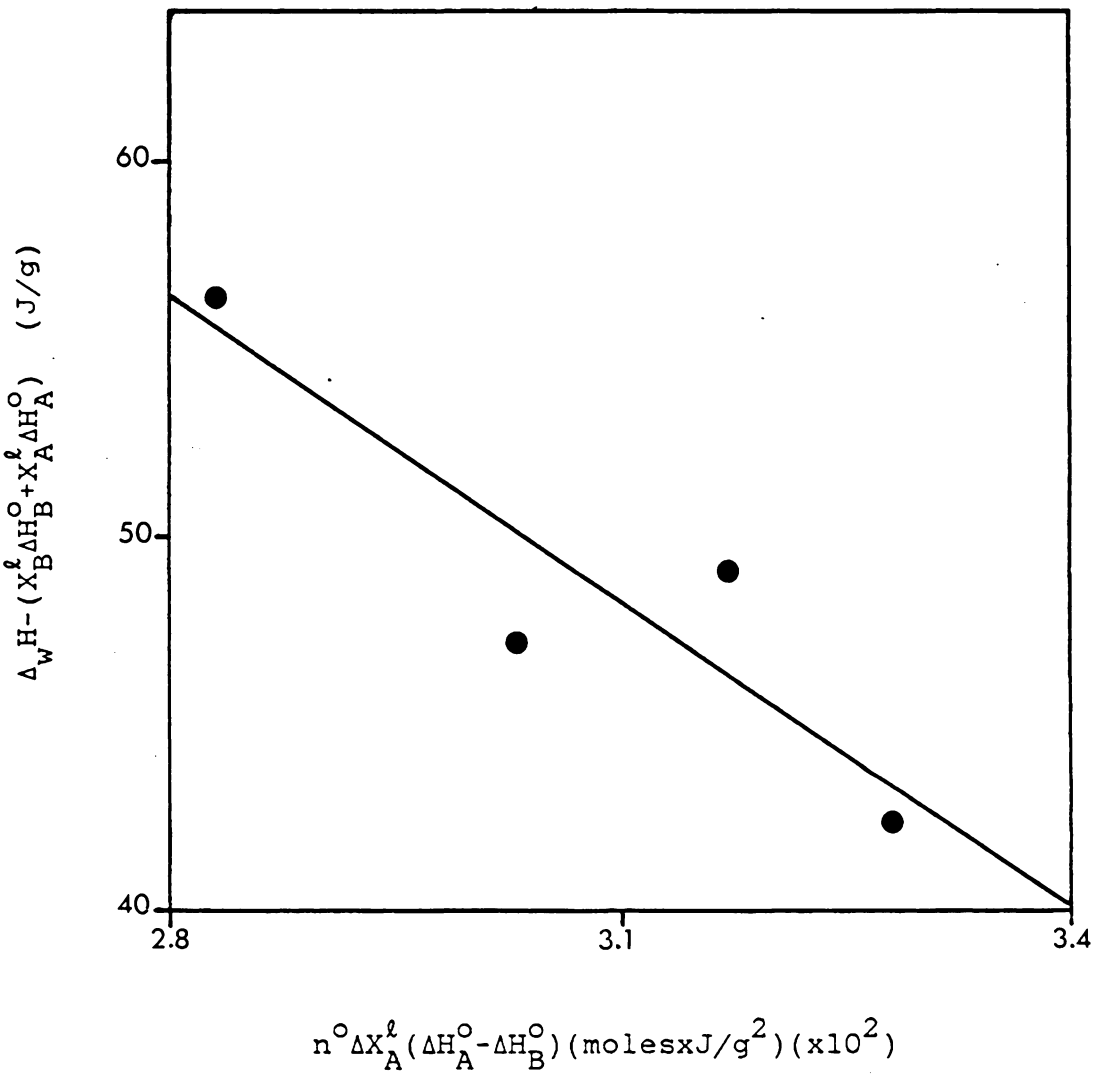

Figure 41: Plot to determine monolayer capacity by heat of immersion in n-decanol+heptane.

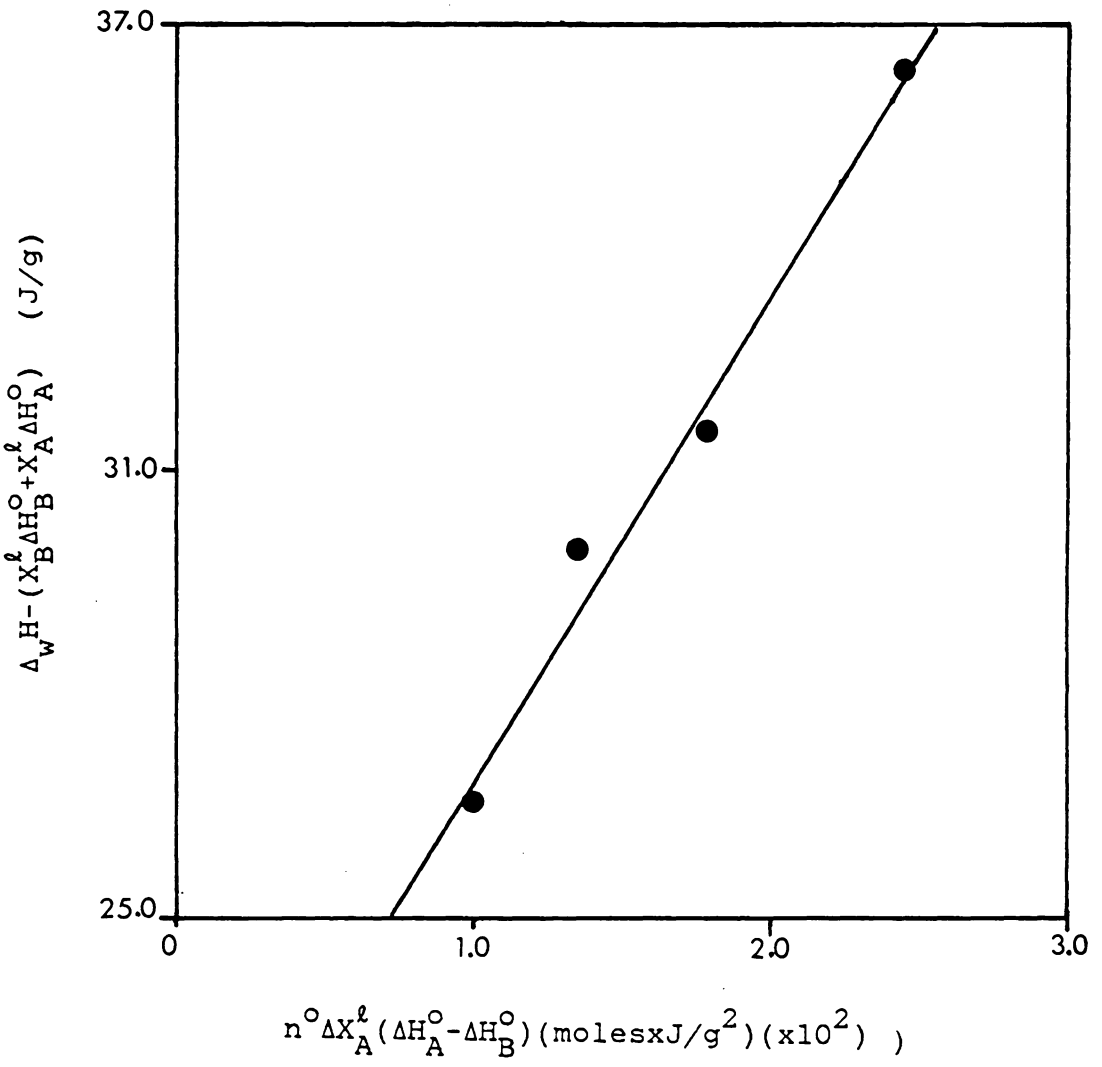

Figure 42: Plot to determine monolayer capacity by heat of immersion in ethyl octanoate+heptane.

TABLE 5

Surface area of H151 by heat of immersion*

Adsorbate	s_A ($\AA^2$)	$n_A^{s,o}$ (moles/g)($\times 10^4$)	S (m^2/g)
n-decanol	20	-5.5	-66
ethyl octanoate	40	15.3	368

*Calculated by equation <II-4>

in this case. Since only four points define the linear plot it is possible that experimental error causes the regression line to have a negative slope.

4.6 ELECTRON SPECTROSCOPY FOR CHEMICAL ANALYSIS (ESCA)

Appendix F summarizes the experimental method for ESCA and the results for H151 samples equilibrated with 10% solutions of n-decanol, n-decylamine, ethyl octanoate, and n-decanoic acid in heptane. It is difficult to draw any conclusions from the ESCA data as to the nature of the adsorptive interactions in solution. The samples were handled much differently than for adsorption and heat of immersion measurements; in fact for ESCA it was necessary to rinse the alumina with heptane and expose it to a vacuum after equilibration with the solutions. The absence of a nitrogen peak in the spectrum of the n-decylamine sample suggests that none of the amine remained on the surface after sample preparation.

Chapter V

SUMMARY

The adsorption of n-decanol, n-decylamine, n-decanoic acid, and ethyl octanoate from heptane solutions onto alumina was studied. Preferential adsorption of the polar component occurs to a greater extent at low concentrations for the alcohol and amine than for the acid and ester. If a perpendicular surface orientation is assumed for each polar compound, it appears that the acid reaches a much greater coverage than the other polar molecules at concentrations of $X_A > 0.2$. These conclusions are supported by both the net and resolved isotherms and heats of immersion. However, the selection of the cross-sectional area of the preferentially adsorbed component affects the shape and interpretation of the resolved isotherm.

The data for the n-decanol and ethyl octanoate systems were also analyzed using the Rudzinski model of surface heterogeneity. The model was found to fit both cases within the limits imposed by assuming an ideal solution and a Gaussian distribution of adsorption site energies in each case. This suggests that the surface is in fact heterogeneous. Again the significance of the values chosen as cross-sectional molecular areas was illustrated.

The Everett method was used to calculate equilibrium constants and the adsorbent surface area. The K values suggest that the order of preferential adsorption is ethyl octanoate > n-decanol > n-decylamine > n-decanoic acid. If cross-sectional molecular areas corresponding to perpendicular surface orientation of the acid molecules and to partially parallel surface orientation of the ester, alcohol, and amine molecules are assumed, the surface area calculated for the alumina agrees well with the reported BET nitrogen value in each case. However, although good linear correlations were obtained for plots to determine the equilibrium constants and monolayer capacities, the order of preferential adsorption indicated by the equilibrium constants does not agree with that suggested by the net and resolved isotherms.

If preferential adsorption in different systems is being compared, the calculated equilibrium constants should support the experimental adsorption isotherms and heats of immersion. If this is the case, then the K values can be used to quantify the extent of preferential adsorption. On the other hand, the discrepancy in the systems studied suggests that the assumptions of the Everett model are not appropriate in these cases; hence the equilibrium constants do not support the experimental results. Therefore, for the

systems studied it is concluded that the order of preferential adsorption is n-decanoic acid > n-decanol ≈ n-decylamine ≈ ethyl octanoate, as suggested by the experimentally determined net isotherms, the heats of immersion, and the resolved isotherms.

REFERENCES

1. D.H. Everett in Specialist Periodical Report, Colloid Sci., vol. 1, D.H. Everett, ed., Chem. Soc., London (1973).

2. G. Schay, L.G. Nagy, and T. Szekrenyesy, Period. Polytech., 4, 95 (1960).

3. J.J. Kipling and D.A. Tester, J. Chem. Soc., 4123 (1952).

4. G.A.H. Elton, J. Chem. Soc., 2958 (1951).

5. S.G. Ash, R. Bown, and D.H. Everett, J. Chem. Thermodyn., 5, 239 (1973).

6. J.J. Kipling, Adsorption from Solutions of Nonelectrolytes, Academic Press, London (1965).

7. D.H. Everett and C.E. Brown, in Specialist Periodical Report, Colloid Sci., vol. 2, ch. 2, D.H. Everett, ed., Chem. Soc., London (1975).

8. D.H. Everett and R.T. Podoll in Specialist Periodical Report, Colloid Sci., vol. 3, ch. 2, D.H. Everett, ed., Chem. Soc., London (1979).

9. D.H. Everett and J. Davis in Specialist Periodical Report, Colloid Sci., vol. 4, D.H. Everett, ed., Chem. Soc., London (1983).

10. D.H. Everett, Trans. Faraday Soc., 60, 1803 (1964).

11. D.F. Billet, D.H. Everett, and E.H.M. Wright, Proc. Chem. Soc., 216, (1964).

12. D.H. Everett, Trans. Faraday Soc., 61, 2478 (1965).

13. F.C. Tompkins, Trans. Faraday Soc., 46, 569 (1950).

14. T.L. Hill, J. Chem. Phys., 17, 762 (1949).

15. W.A. House in Specialist Periodical Report, Colloid Sci., vol. 4, ch. 1, D.H. Everett, ed., Chem. Soc., London (1983).

16. W. Rudzinski, J. Oscik, and A. Dabrowski, Chem. Phys. Lett., 20, 444 (1973).

17. J. Oscik, A. Dabrowski, and W. Rudzinski, Colloid Polym. Sci., 50, 255 (1977).

18. W. Rudzinski and S. Partyka, J. Chem. Soc., Faraday Trans. 1, 77, 2577 (1981).

19. M. Borowko, M. Jaroniec, and W. Rudzinski, Monatsh. Chem., 112, 59 (1981).

20. W. Rudzinski, J. Narkiewicz-Michalek, and S. Partyka, J. Chem. Soc., Faraday Trans. 1, 78, 2361 (1982).

21. W. Rudzinski, L. Lajtar, J. Zajac, E. Wolfram, and I. Paszli, J. Colloid Interface Sci., 96, 339 (1983).

22. S. Sircar and A.L. Meyers, J. Phys. Chem., 74, 2828 (1970).

23. J. Oscik, A. Dabrowski, M. Jaroniec, and W. Rudzinski, J. Colloid Interface Sci., 56, 403 (1976).

24. A. Dabrowski and M. Jaroniec, J. Colloid Interface Sci., 69, 287 (1979).

25. J. Jednacak-Biscan and V. Pravdic, J. Colloid Interface Sci., 75, 322 (1980).

26. J. Jednacak-Biscan and V. Pravdic, J. Colloid Interface Sci., 90, 44 (1982).

27. C.G. Armistead, A.J. Tyler, and J.A. Hockey, Trans. Faraday Soc., 67, 493 (1971).

28. C.G. Armistead, A.J. Tyler, and J.A. Hockey, Trans. Faraday Soc., 67, 500 (1971).

29. J.J. Kipling and E.H.M. Wright, J. Chem. Soc., 3535 (1964).

30. I. Ralston, Fatty Acids and Their Derivatives, John-Wiley, New York (1948).

31. M.A. Rahman and A.K. Ghosh, J. Appl. Chem. Biotechnol., 27, 529 (1977).

32. M. Borowko, J. Goworek, and M. Jaroniec, Monatsh. Chem., 113, 669 (1982).

33. M. Oscik, J. Goworek, and R. Kusak, J. Colloid Interface Sci., 79, 308 (1981).

34. A.L. McClellan and H.F. Harnsberger, J. Colloid Interface Sci., 23, 577 (1967).

35. J. Goworek, M. Jaroniec, and J. Czarniecki, Monatsh. Chem., 114, 559 (1983).

36. G. Schay, L.G. Nagy, and G. Foti, Acta. Chim. Acad. Sci. Hung., 100, 289 (1979).

37. L.A. Noll and T.E. Burchfield, U.S.D.O.E. Publication #DE82015392, June 1982.

38. W. Rudzinski, personal communication (1984).

39. C.E. Brown and D.H. Everett in Specialist Periodical Report, Colloid Sci., vol. 2, D.H. Everett, ed., Chem. Soc., London (1973), pp. 52-53.

40. P. Hiemenz, Principles of Colloid and Surface Chemistry, Marcel Dekker,Inc., New York (1977).

41. R.H. Ottewill, C.H. Rochester, and A.L. Smith, eds., Adsorption from Solution, Academic Press, New York (1983).

42. G.D. Parfitt and C.H. Rochester, eds., Adsorption from Solution at the Solid/Liquid Interface, Academic Press, New York (1983).

43. A.W. Adamson, Physical Chemistry of Surfaces, John-Wiley, New York (1967).

Appendix A

CALIBRATION DATA SET

n-Decylamine/Heptane
$X_A = .002$

µl A added to 5 ml solution	Attenuation	Units	16x units
10	16x	24.2	24.2
10	32x	14.3	28.6
10	32x	14.5	29.0
20	64x	13.4	53.6
20	64x	13.4	53.6
30	64x	19.8	79.2
30	64x	19.3	77.2
30	64x	19.2	76.8
40	64x	24.2	96.8
40	64x	24.1	96.4

Appendix B

MICROCALORIMETRY DATA AND RESULTS

Heat of Immersion - Results

A. n-Decanol/Heptane/H151:

X_A	ΔH_{imm} (mJ/m^2)	avg. ΔH_{imm} (mJ/m^2)
0.00	83.4	83.4
.001	89.5	
	120.1	104.8
0.02	219.6	
	203.1	211.4
0.05	224.2	
	235.2	229.7
0.10	228.2	
	252.5	240.4
0.20	216.5	
	234.9	225.7
0.40	206.0	
	243.6	224.8
1.00	194.2	
	203.9	199.1

B. n-Decanoic Acid/Heptane/H151:

X_A	ΔH_{imm} (mJ/m^2)	avg. ΔH_{imm} (mJ/m^2)
0.00	83.4	83.4
.001	66.9	
	128.7	97.8
0.02	287.3	
	303.0	295.2
0.06	239.1	
	286.7	262.9
0.13	260.4	
	294.7	277.6

C. Ethyl Octanoate/Heptane/H151:

X_A	ΔH_{imm} (mJ/m^2)	avg. ΔH_{imm} (mJ/m^2)
0.00	83.4	83.4
.001	123.3	
	106.6	114.9
0.01	162.8	
	162.8	162.8
0.05	178.9	
	187.6	183.3
0.10	217.0	
	192.0	204.5
0.40	228.4	
	221.4	224.9
1.00	221.4	
	209.2	215.3

Calorimetry Data for n-Decanol/Heptane/H151

Sensitivity = PS

cell 1 = .00207001 J/count cell 3 = .00208491 J/count
cell 2 = .00212292 J/count cell 4 = .00215464 J/count
reference heat: EN = endothermic, EX = exothermic

X_A	Sample Wt. (g)	Sample Cell	Sample Counts	Ref. Cell	Ref. Counts	Ref. Heat	Sample Equil. Time (min.)
0.00	.0495	3	536	4	129	EN	57
.001	.0505	1	727	2	15	EN	101
	.0488	3	873	4	75	EN	140
0.02	.0550	1	1958	2	14	EN	428
	.0518	3	1617	4	86	EN	319
0.05	.0468	1	1696	2	17	EN	222
	.0503	3	1822	4	93	EN	204
0.10	.0376	1	1404	2	3	EX	174
	.0399	3	1566	4	65	EN	137
0.20	.0471	1	1654	2	11	EN	108
	.0362	3	1320	4	56	EN	69
0.40	.0503	1	1702	2	10	EX	133
	.0514	3	1972	4	56	EN	304
1.00	.0543	1	1797	2	73	EX	85
	.0519	3	1729	4	13	EX	51

Calorimetry Data for n-Decanoic Acid/Heptane/H151

Sensitivity = PS

cell 1 = .00207001 J/count cell 3 = .00208491 J/count
cell 2 = .00212292 J/count cell 4 = .00215464 J/count
reference heat: EN = endothermic, EX = exothermic

X_A	Sample Wt. (g)	Sample Cell	Sample Counts	Ref. Cell	Ref. Counts	Ref. Heat	Sample Equil. Time (min.)
0.00	.0495	3	536	4	129	EN	57
.001	.0451	1	489	2	3	EN	122
	.0496	3	949	4	84	EN	328
0.02	.0531	1	2472	2	18	EN	625
	.0432	3	2043	4	76	EN	416
0.06	.0495	1	1916	2	15	EN	198
	.0469	3	2114	4	63	EN	196
0.13	.0530	1	2259	2	5	EX	222
	.0406	3	1867	4	70	EN	153

Calorimetry Data for Ethyl Octanoate/Heptane/H151

Sensitivity = PS

cell 1 = .00207001 J/count cell 3 = .00208491 J/count
cell 2 = .00212292 J/count cell 4 = .00215464 J/count
reference heat: EN = endothermic, EX = exothermic

X_A	Sample Wt. (g)	Sample Cell	Sample Counts	Ref. Cell	Ref. Counts	Ref. Heat	Sample Equil. Time (min.)
0.00	.0495	3	536	4	129	EN	57
.001	.0477	1	957	2	3	EN	278
	.0477	3	746	4	76	EN	194
0.01	.0493	1	1297	2	13	EN	240
	.0419	3	1021	4	82	EN	285
0.05	.0544	1	1587	2	5	EN	305
	.0564	3	1642	4	71	EN	208
0.10	.0465	1	1652	2	4	EX	347
	.0497	3	1477	4	68	EN	196
0.40	.0441	1	1659	2	14	EX	305
	.0430	3	1499	4	43	EN	253
1.00	.2014	3	6894	4	62	EX	512

Appendix C

SURFACE EXCESS CALCULATION, DATA, AND RESULTS

Calculation of specific surface excess for n-decanol, n-decylamine, and ethyl octanoate:

Definition of terms:

n^o = total number of moles of heptane and polar component (A) initially in solution

ΔX_A = change in mole fraction of component A upon equilibration with solid

X_A^i = initial mole fraction A

X_A^f = final mole fraction A

n_A^i = initial number of moles A

n_A^f = final number of moles A

$\Delta\mu l_A$ = microliters of A adsorbed, calculated from change in solution concentration, measured by refractive index

d_A = density of A

M_A = molecular weight A

m = mass of solid in grams

Calculation of specific surface excess, $n^o\Delta X_A/m$:

$$n^o\Delta X_A = n^o(X_A^i - X_A^f) = n^o\{(n_A^i/n^o) - (n_A^f/n^o)\}$$
$$= n_A^i - n_A^f$$

$$n_A^f = n_A^i - (\Delta\mu l_A d_A / M_A \times 10^3)$$

$$n^{\circ}\Delta X_A/m = n_A^i - \{n_A^i - (\Delta\mu l_A d_A/M_A x 10^3)\}/m$$
$$= \Delta\mu l_A d_A/M_A x 10^3 m$$

Calculation of specific surface excess for n-decanoic acid:

Definition of terms:

$W_{H,s}$ = weight heptane in concentrated calibration solution

$W_{A,s}$ = weight n-decanoic acid in concentrated calibration solution

W_{ads} = weight acid adsorbed

$\Delta\mu l_A$ = microliters read from calibration curve of 16x units vs µl concentrated calibration solution added to 5 ml solution

$W_{\mu l}$ = weight of µl quantity of calibration solution

$W_{A,\mu l}$ = weight of n-decanoic acid in µl quantity of calibration solution

$$W_{A,\mu l} = W_{A,s} W_{\mu l}/(W_{A,s}+W_{H,s})$$

$W_{A,\mu l}$ for 20 µl, $W_{A,20}$, was calculated and used to calculate W_{ads} for samples:

$$W_{ads} = W_{A,20}\Delta\mu l_A/20\mu l$$

Then the specific surface excess is calculated as before, substituting W_{ads} for $\Delta\mu l_A d_A$ in the previous equation:

$$n^{\circ}\Delta X_A/m = W_{ads}/M_A x 10^3 m$$

Surface Excess Data and Results

A. n-Decanol/Heptane/H151:

X_A	$\Delta[A]$ (μl)	m (g)	$n^o\Delta X_A/m$ (moles/g)($\times 10^4$)	avg. $n^o\Delta X_A/m$ (moles/g)($\times 10^4$)
.01	30.4	.195	8.18	
	30.9	.183	8.82	
	44.9	.369	6.37	
	47.1	.442	5.58	7.24
.02	19.8	.127	8.17	
	21.4	.130	8.63	
	50.1	.328	8.00	
	46.9	.277	8.86	8.41
.05	24.8	.166	7.80	
	30.9	.184	8.80	
	56.9	.394	7.56	7.74
.10	60.9	.469	6.80	
	38.4	.239	8.42	
	37.3	.211	9.23	
	56.9	.381	7.82	
	62.8	.479	6.87	8.09

B. n-Decylamine/Heptane/H151:

X_A	$\Delta[A]$ (μl)	m (g)	$n^o\Delta X_A/m$ (moles/g)($\times 10^4$)	avg. $n^o\Delta X_A/m$ (moles/g)($\times 10^4$)
.002	3.7	.201	.919	
	5.3	.215	1.23	
	5.3	.198	1.34	
	10.7	.384	1.39	
	11.4	.431	1.32	1.24
.01	29.8	.219	6.82	
	28.6	.186	7.71	
	23.2	.128	9.08	
	43.8	.347	6.32	
	46.7	.370	6.32	7.25
.02	32.7	.215	7.61	
	33.1	.200	8.26	
	31.4	.192	8.17	
	52.4	.372	7.04	
	55.5	.419	6.63	7.54
.05	34.5	.228	7.57	
	32.6	.207	7.89	
	54.8	.408	6.73	7.40
.10	25.2	.172	7.15	
	29.0	.186	7.78	
	34.4	.203	8.48	
	52.8	.405	6.53	7.30

C. n-Decanoic acid/Heptane/H151:

X_A	$\Delta[A]$ (mg)	m (g)	$n^o\Delta X_A/m$ (moles/g)($\times 10^4$)	avg. $n^o\Delta X_A/m$ (moles/g)($\times 10^4$)
.01	.0049	.209	1.36	
	.0053	.135	2.28	
	.013	.439	1.72	
	.012	.384	1.82	1.80
.02	.018	.200	5.23	
	.019	.220	5.01	
	.036	.414	5.04	
	.033	.330	5.81	5.30
.05	.010	.219	2.54	
	.014	.231	3.51	
	.019	.411	2.68	
	.020	.437	2.66	2.85
.09	.051	.238	12.44	
	.044	.184	13.92	
	.059	.284	12.07	
	.058	.270	12.46	12.70
.20	.044	.182	14.07	
	.051	.194	15.27	
	.086	.377	13.24	
	.089	.390	13.24	14.00

D. Ethyl Octanoate/Heptane/H151:

X	Δ[A] (μl)	m (g)	$n^{o}\Delta X_A/m$ (moles/g)(x10^4)	avg. $n^{o}\Delta X_A/m$ (moles/g)(x10^4)
.01	7.5	.199	1.90	
	3.7	.173	1.08	
	24.1	.428	2.84	
	26.5	.418	3.20	2.25
.02	10.0	.213	2.37	
	14.6	.228	3.23	
	15.0	.207	3.66	
	36.7	.460	4.03	
	35.6	.417	4.31	3.50
.05	12.1	.192	3.19	
	11.2	.158	3.58	
	36.2	.393	4.65	4.00
.10	38.2	.364	5.30	
	28.1	.249	5.69	5.50
.20	17.0	.189	4.53	
	17.2	.193	4.49	
	22.5	.200	5.69	
	42.0	.381	5.57	
	34.3	.293	5.91	5.20
.40	8.0	.216	1.87	
	9.4	.241	1.97	
	35.1	.432	4.10	
	25.2	.326	3.90	3.00

Appendix D

NET AND RESOLVED ISOTHERM RESULTS

Solute	X_A	$n^o \Delta X_A/m$ (moles/g) ($\times 10^4$)	n_A^s (moles/cm^2)	n_H^s ($\times 10^{10}$)
n-Decanol (s_A=20 Å^2)	.01	7.25	2.19	1.94
	.02	8.40	2.57	1.82
	.05	7.75	2.51	1.84
	.10	8.10	2.86	1.73
Ethyl octanoate (s_A=40 Å^2)	.01	2.25	.69	2.20
	.02	3.50	1.10	1.94
	.05	4.00	1.34	1.79
	.10	5.50	1.96	1.39
	.20	5.20	2.23	1.22
	.40	3.00	2.28	1.19
n-Decanoic acid (s_A=22 Å^2)	.01	1.80	.56	2.24
	.02	5.30	1.64	2.06
	.09	12.70	4.27	1.15
	.20	14.00	5.36	.76
n-Decylamine (s_A=20 Å^2)	.002	1.24	.35	2.53
	.01	7.25	2.05	1.98
	.02	7.54	2.18	1.95
	.05	7.40	2.26	1.92
	.10	7.30	2.46	1.86

Appendix E

SURFACE HETEROGENEITY CALCULATIONS

Sample Calculations

Solution: Ethyl Octanoate/Heptane
Adsorbent: H151 alumina
$n^o = 1.5 \times 10^{-5}$ moles/m^2
r = 0.5

1) Experimental surface excess and heat of wetting data:

X_A	n_A^e (moles/m^2)(x10^6)	$\Delta_w H$ (mJ/m^2)
0.00	---	83.4
0.01	0.67	162.8
0.05	1.18	183.3
0.10	1.63	204.5
0.40	0.89	224.9
1.00	---	215.3

2) Calculation of Φ_A^s :

$$\Phi_A^s = \frac{n_A^e + n^o X_A r}{n^o(1 - X_A + rX_A)} \qquad \text{<II-11>}$$

X_A	Φ_A^s
0.00	0.00
0.01	.050
0.05	.106
0.10	.167
0.40	.324
1.00	1.00

3) Linear regression for calculation of c:

$$\ln\left[\frac{1-\Phi_A^S}{\Phi_A^S}\right] = \frac{RT\ln(2^{r-1})-\varepsilon_o}{c} - \frac{RT}{c}\ln\left[\frac{X_A}{X_B}\right] \qquad \text{<II-12>}$$

X_A	X_B	Φ_A^S	$\ln\{(1-\Phi_A^S)/\Phi_A^S\}$	$\ln(X_A/X_B)$
0.01	0.99	.050	2.94	-4.6
0.05	0.95	.106	2.13	-2.9
0.10	0.90	.167	1.61	-2.2
0.40	0.60	.324	.735	-.41

Plot $\ln\{(1-\Phi_A^S)/\Phi_A^S\}$ as a function of $\ln(X_A/X_B)$. See Figure 36.

Slope = -0.532 = -RT/c
$c = -(8314)(302)/-0.532 = 4.7 \times 10^6$ mJ/mole

4) Calculation of theoretical excess heat of wetting, $\Delta_w^T H$ and experimental excess heat of wetting, $\Delta_w^E H$:

$$\Delta_w^T H = -cn^o\{(1-\Phi_A^S)\ln(1-\Phi_A^S)+\Phi_A^S\ln\Phi_A^S\} \qquad \text{<II-13>}$$

$$\Delta_w^E H = \Delta_w H-\{(\Delta_w H_A-\Delta_w H_B)+\Delta_w H_B\}$$

Φ_A^S	$\Delta_w^T H$ (mJ/m^2)	$\Delta_w^E H$ (mJ/m^2)
0.00	0.00	0.00
.050	14.0	72.8
.106	23.9	85.9
.167	31.9	99.1
.324	44.5	98.7
1.00	0.00	0.00

5) Plot of $\Delta_w^T H$ and $\Delta_w^E H$ as a function of Φ_A^S. See Figure 34.

Results for n-Decanol "Best Fit"

Solution: n-Decanol/Heptane
Absorbent: H151 alumina

$n^o = 1.0 \times 10^{-5}$ moles/m^2
$r = 0.5$

X_A	n_A^e (moles/m^2) (x 10^6)	$\Delta_w H$ (mJ/m^2)	Φ_A^s	$\ln\{(1-\Phi_A^s)/\Phi_A^s\}$	$\ln(X_A/X_B)$	$\Delta_w^T H$ (mJ/m^2)	$\Delta_w^E H$ (mJ/m^2)
0.00	----	83.4	0.00	----	----	0.000	0.000
0.02	2.48	211.4	.261	1.04	-3.9	116.2	97.8
0.05	2.29	229.7	.260	1.05	-2.9	116.1	116.2
0.10	2.40	240.4	.305	0.82	-2.2	124.6	121.7
1.00	----	199.1	1.00	----	----	0.000	0.000

$c = 2.1 \times 10^7$ mJ/mole

Appendix F

ESCA (ELECTRON SPECTROSCOPY FOR CHEMICAL ANALYSIS)

Experimental

H151 alumina pellets were dried in a glass vial in a 110°C oven for at least two hours. The vial was removed from the oven and capped immediately, then allowed to cool to room temperature. The pellets were then pulverized to a fine powder using a clean mortar and pestle. The powder was dried at 110°C for at least 2 more hours in a glass vial, then cooled to room temperature as described above before use. Solutions of 10 mole percent n-decanol, n-decylamine, n-decanoic acid, and ethyl octanoate in heptane were prepared as previously described in the experimental section for adsorption measurements. Equilibration of the adsorbent with the solutions was done as for the adsorption measurements, except approximately 0.6 grams of alumina and 10 ml solution were used. After equilibration all samples were filtered as follows. A small porcelain Hirsch funnel was cleaned, dried, pre-rinsed with heptane, and fitted with filter paper. The sample (adsorbent + supernatant) was poured into the filter under suction, then rinsed 2 or 3

times with approximately 10 ml of heptane. The alumina was air dried by suction for about 3 minutes, then transferred to a glass vial and capped. Between samples, the funnel was rinsed with ethanol, then acetone, then copiously with heptane. A new piece of filter paper was used for each sample. One sample consisted of untreated H151 powder to be used as a control.

Samples were analyzed with a Kratos X-SAM instrument using a 1253.6 eV Mg electron source and a hemispherical analyzer. A wide scan was done for each sample; narrow scans were done for the C1s, O1s, and Al2p peaks. A trace sodium peak was visible in the spectrum for pure H151.

Results

The wide scan spectra for all samples are shown in Figures 43 - 47 The narrow scan spectra for pure H151 alumina are shown in Figure 48 . Curve fits of the C1s peak for each sample are shown in Figures 49 - 53 . All binding energies (BE) were corrected to C1s=285.0 eV. The relative atomic fraction (RAF) of each element was calculated from the area of the photopeak using the equation:

$$RAF = (Area)/\{(S)(KE)(XSMFP)\} \qquad \text{<F-1>}$$

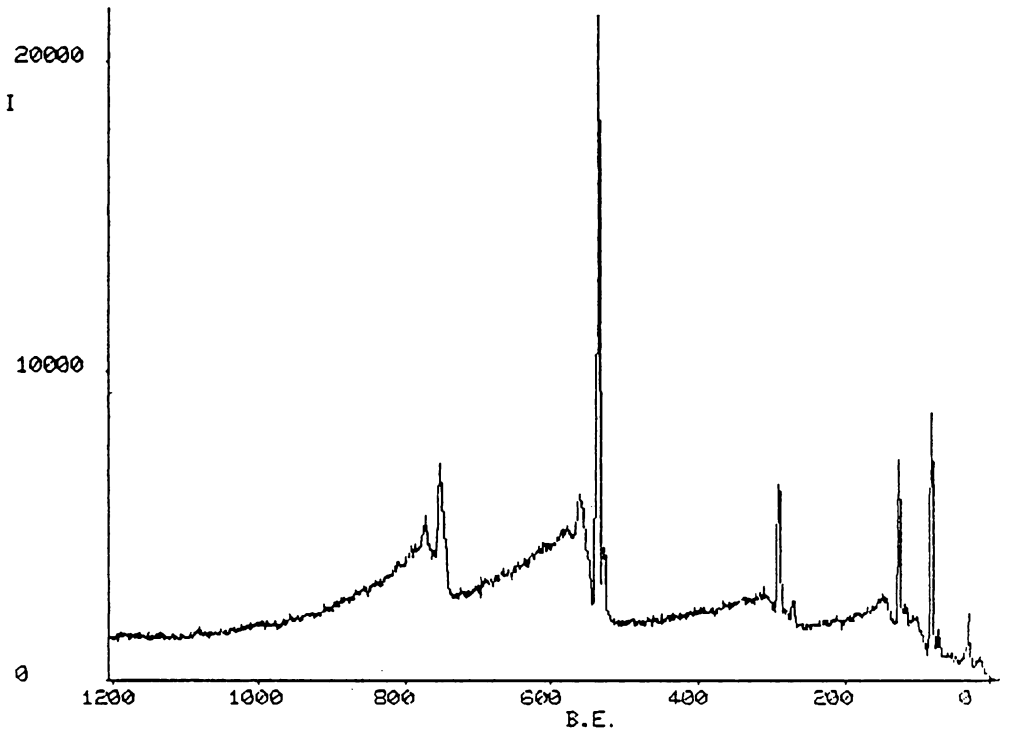

Figure 43: Wide scan ESCA spectrum of H151 sample

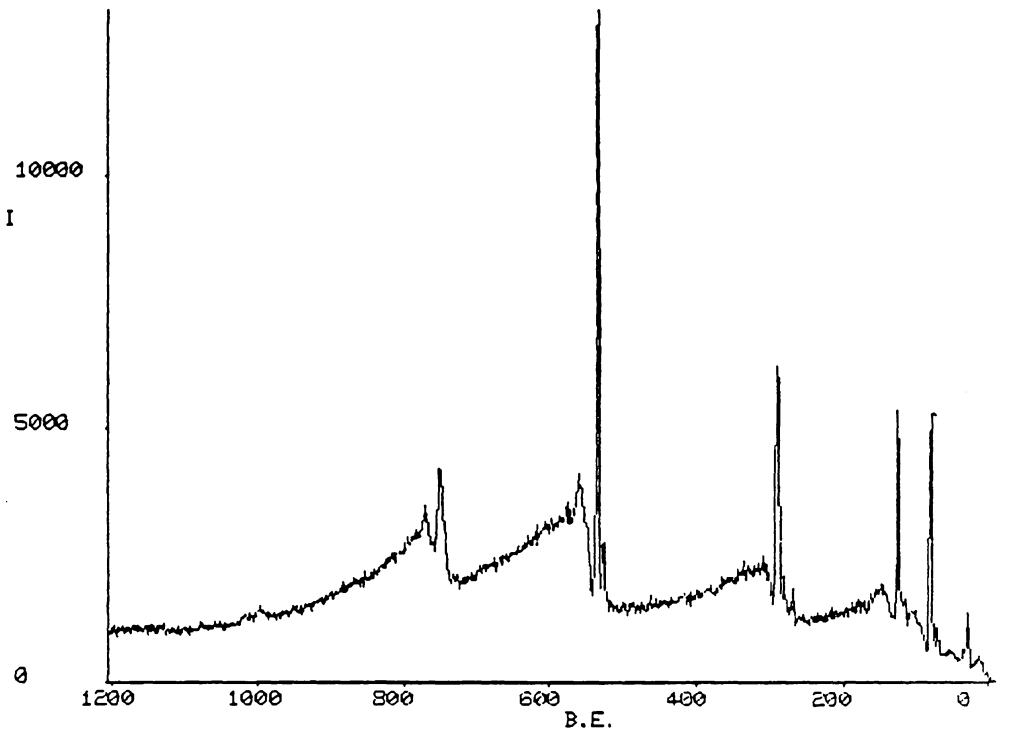

Figure 44: Wide scan ESCA spectrum of 10% n-decanol sample

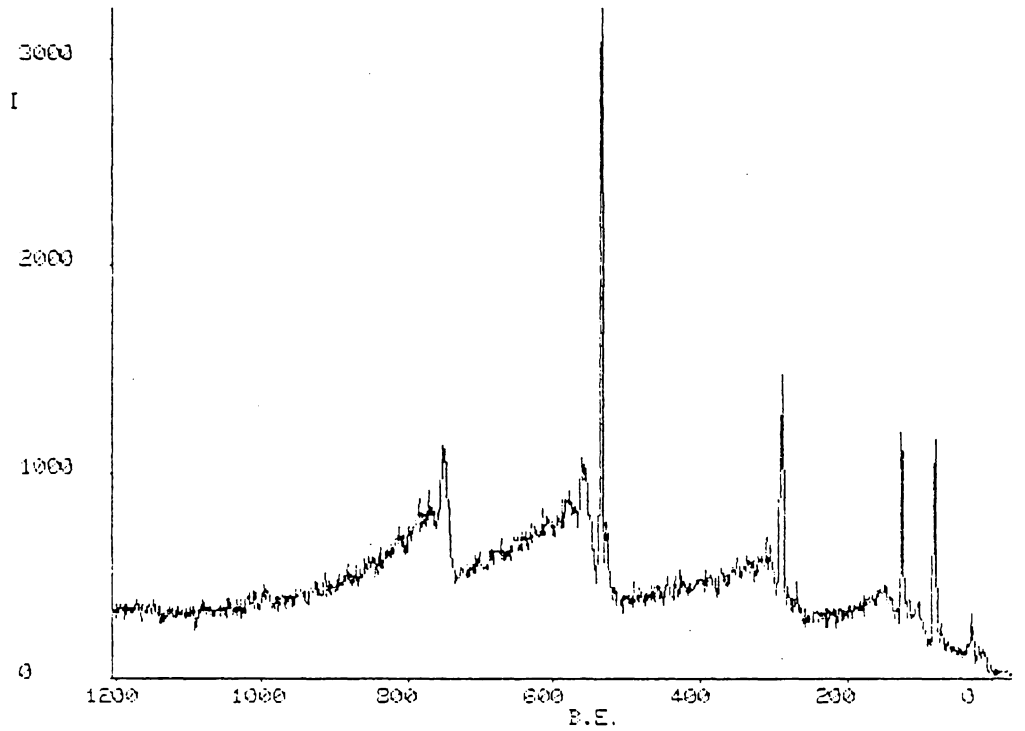

Figure 45: Wide scan ESCA spectrum of 10% ethyl octanoate sample

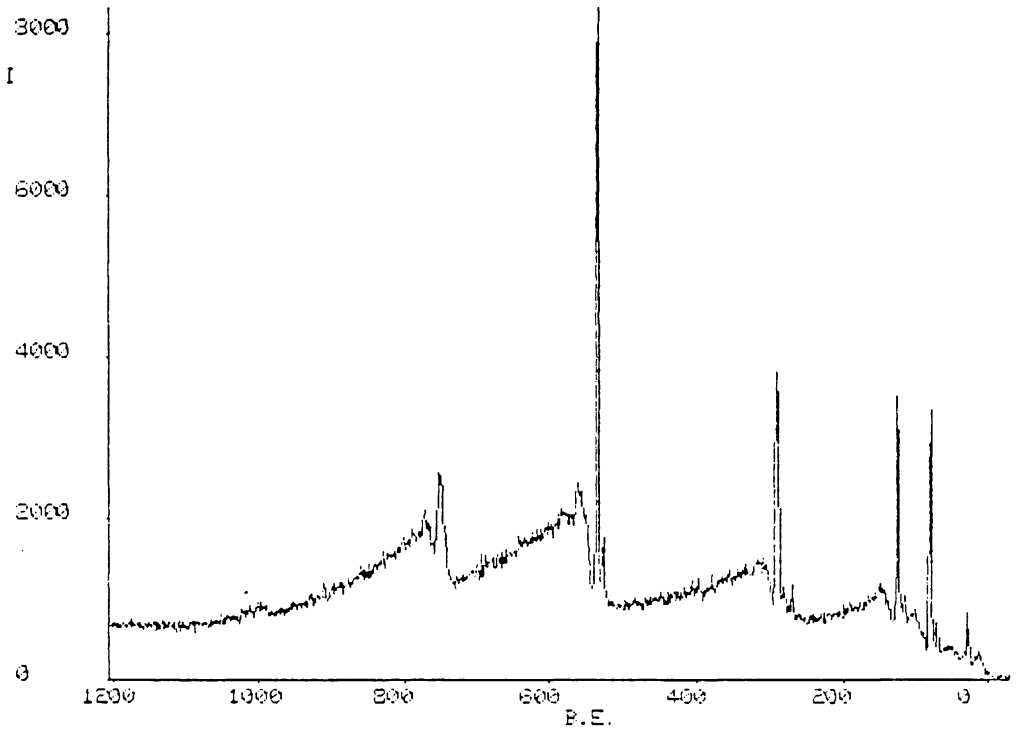

Figure 46: Wide scan ESCA spectrum of 10% n-decylamine sample

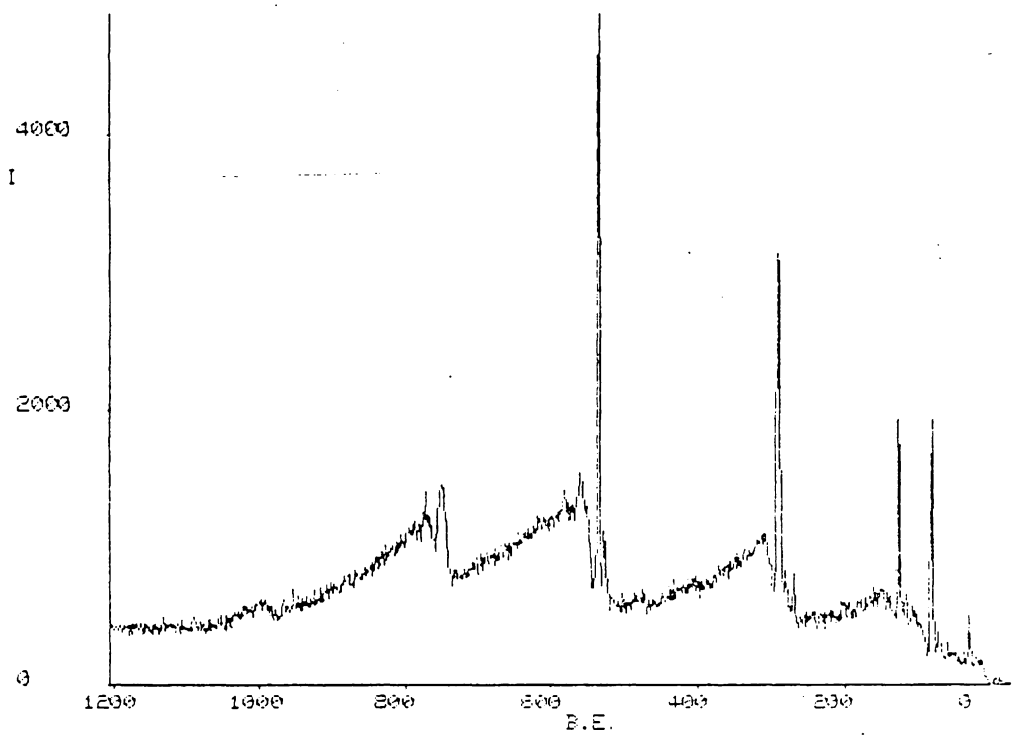

Figure 47: Wide scan ESCA spectrum of 10% n-decanoic acid sample

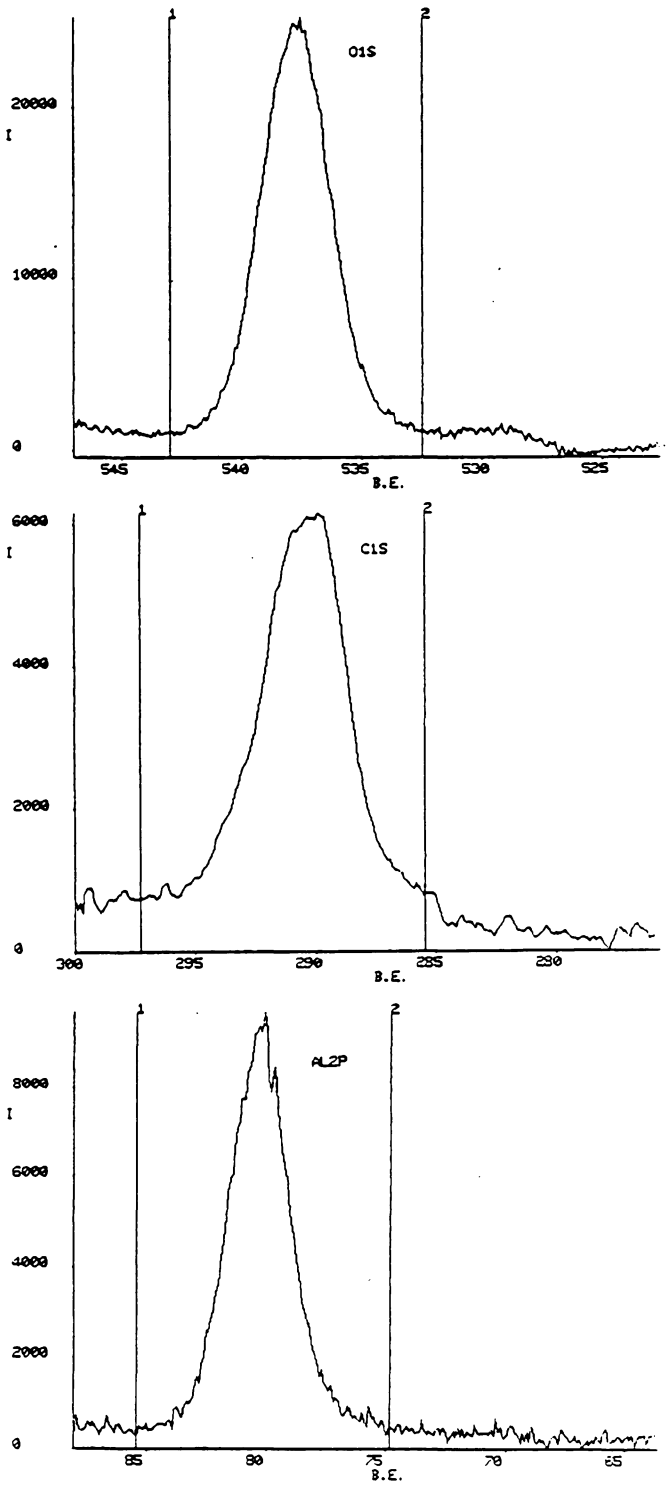

Figure 48: Narrow scan ESCA spectra for H151 sample

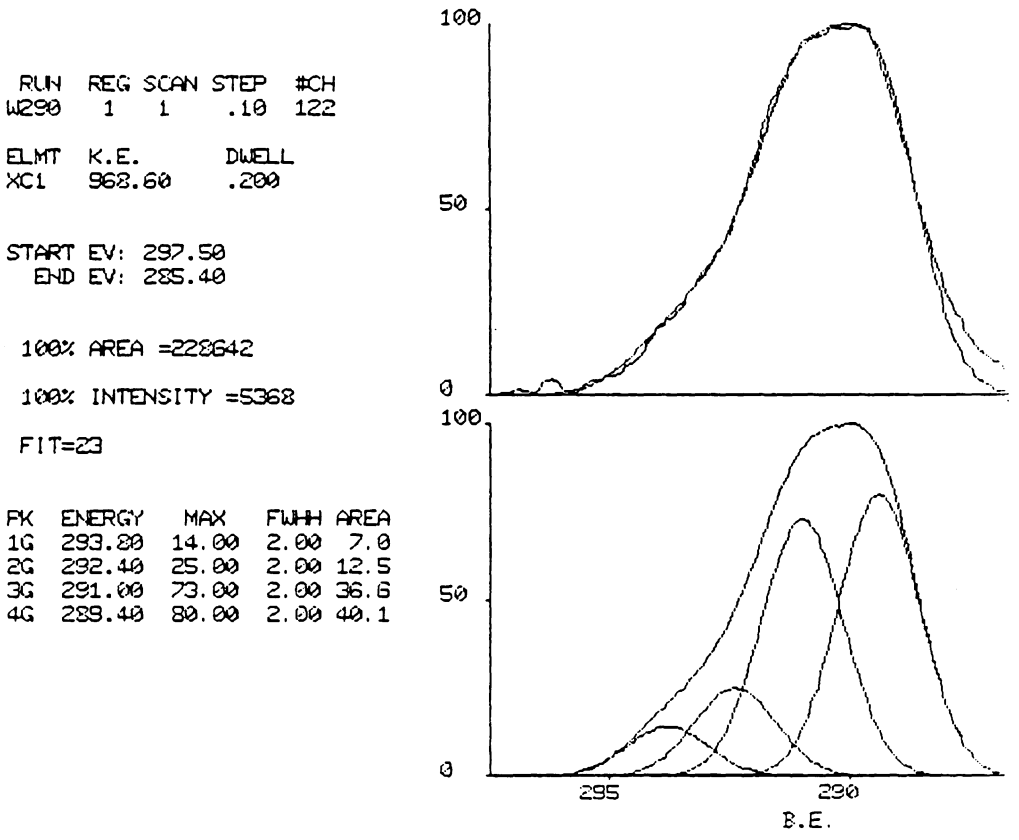

Figure 49: Curve fit of Cls peak of H151 sample

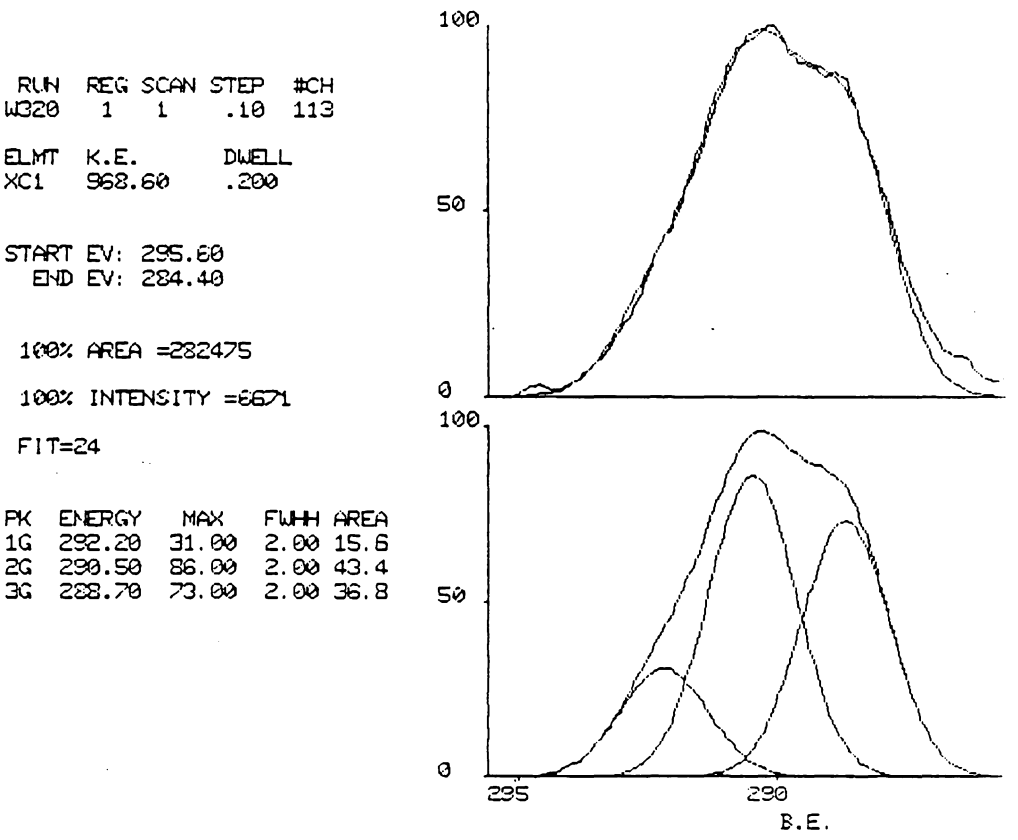

Figure 50: Curve fit of C1s peak of 10% n-decanol sample

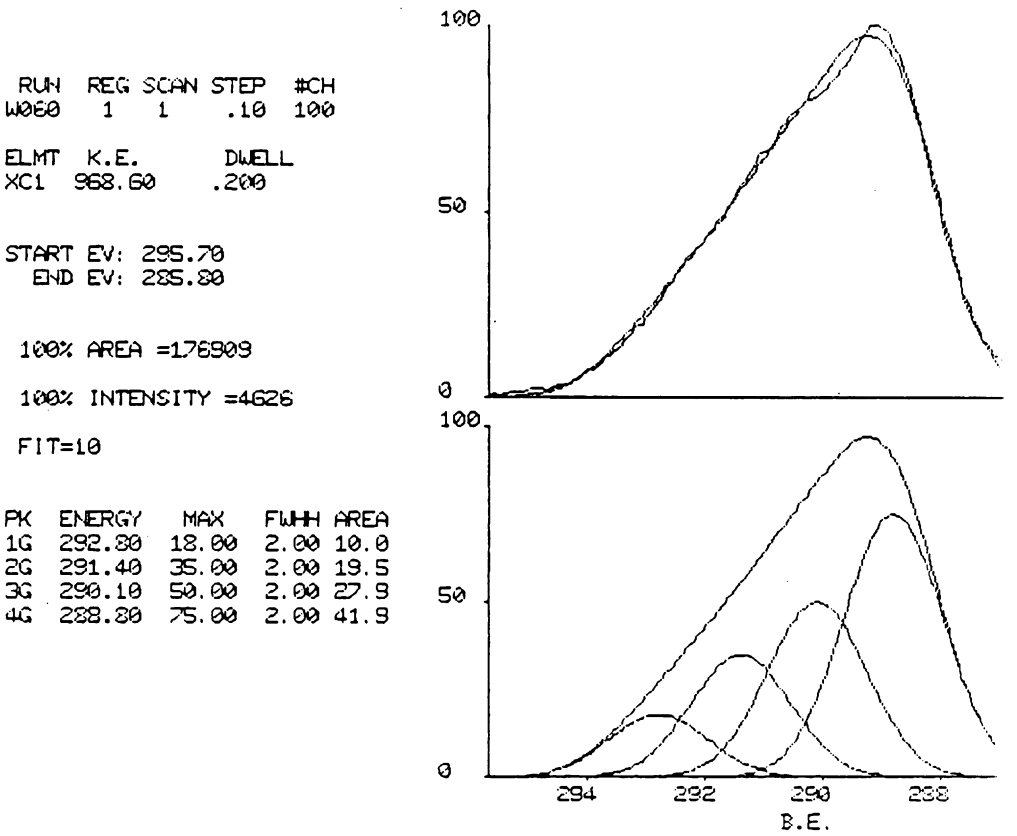

Figure 51: Curve fit of Cls peak of 10% ethyl octanoate sample

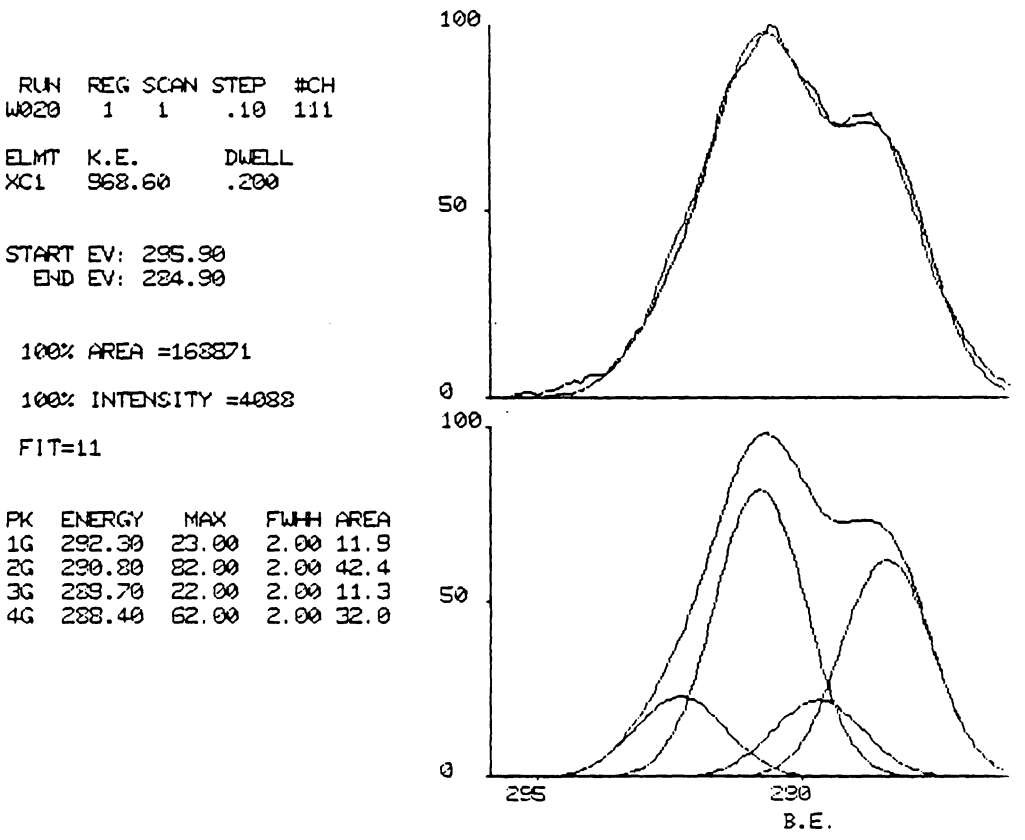

Figure 52: Curve fit of C1s peak of 10% n-decylamine sample

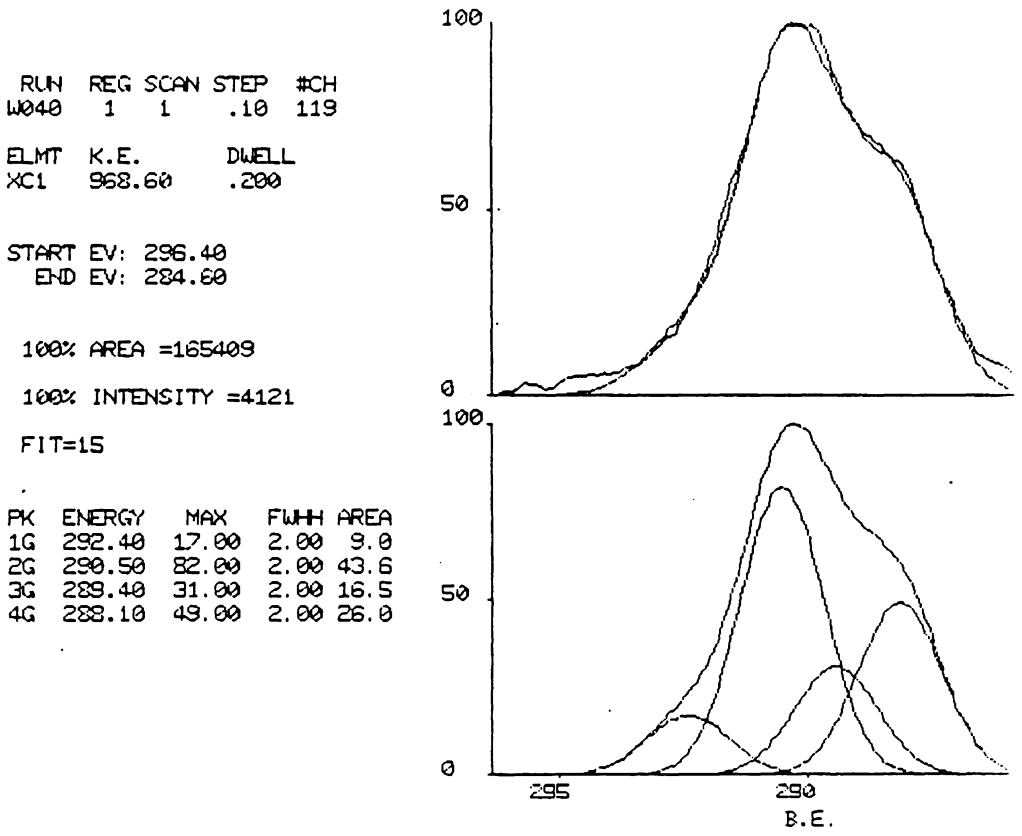

Figure 53: Curve fit of Cls peak of 10% n-decanoic acid sample

where S refers to the number of sweeps for the spectrum, XSMFP is the photoelectron cross-section times mean free path for the electron, and KE is the corrected kinetic energy:

$$KE = 1253.6 - BE \quad eV \qquad \text{<F-2>}$$

The cross-section times mean free path values used are given in Table 6 . Atomic percents (AP) were calculated from the relative atomic fractions. In each case, the atomic percent of each element was ratioed to that of carbon in the same sample. The ESCA results are summarized in Table 7 .

TABLE 6

Photoelectron cross section x mean free path values

Electron	XSMFP
C1s	403.419
O1s	924.359
Al2p	268.631

*Reference: J.H. Scofield, J. Electron Spectroscopy and Related Phenomena, 8, 129 (1976).

TABLE 7

ESCA Results

	Peak								
	C1s			O1s			Al2p		
Adsorbate	BE	AP	AP/%C	BE	AP	AP/%C	BE	AP	AP/%C
None	285.0	21.5	1.00	532.9	46.5	2.16	75.4	32.1	1.49
n-decanol	285.0	35.7	1.00	531.7	38.0	1.06	74.5	26.3	0.74
ethyl octanoate	285.0	32.3	1.00	533.2	40.5	1.25	76.0	27.2	0.84
n-decanoic acid	285.0	43.6	1.00	531.7	32.2	0.74	74.6	24.3	0.56
n-decylamine	285.0	37.4	1.00	531.1	35.9	0.96	74.0	26.7	0.71

The two page vita has been removed from the scanned document. Page 1 of 2

The two page vita has been removed from the scanned document. Page 2 of 2